İSTANBUL TECHNICAL UNIVERSITY ★ INFORMATICS INSTITUTE

A COMPUTATIONAL STUDY ON INACTIVATION MECHANISMS OF GABA – AT

M.Sc. Thesis by
Hatice GÖKCAN

Department : Computational Science and Engineering

Programme : Computational Science and Engineering

Thesis Supervisor: Assist. Prof. Dr. F. Aylin KONUKLAR

AUGUST 2010

İSTANBUL TECHNICAL UNIVERSITY ★ INFORMATICS INSTITUTE

A COMPUTATIONAL STUDY ON INACTIVATION MECHANISMS OF GABA – AT

M.Sc. Thesis by
Hatice GÖKCAN

702071017

Date of submission :   **19 August 2010**
Date of defence examination: **07 June 2010**

Supervisor (Chairman) :   **Assist. Prof. Dr. F. Aylin KONUKLAR**
Members of the Examining Committee :   **Prof. Dr. Dilek ÇALGAN (BU)**
   Assist. Prof. Dr. Adem TEKİN
   (ITU)

AUGUST 2010

İSTANBUL TEKNİK ÜNİVERSİTESİ ★ BİLİŞİM ENSTİTÜSÜ

GABA – AT İNAKTİVASYONU MEKANİZMALARI ÜZERİNE HESAPSAL BİR ÇALIŞMA

YÜKSEK LİSANS TEZİ
Hatice GÖKCAN

702071017

Tezin Enstitüye Verildiği Tarih : 19 Ağustos 2010
Tezin Savunulduğu Tarih : 07 Haziran 2010

Tez Danışmanı : Yrd. Doç. Dr. F. Aylin KONUKLAR(İTÜ)
Diğer Jüri Üyeleri : Prof. Dr. Dilek ÇALGAN (BÜ)
Yrd. Doç. Dr. Adem Tekin (İTÜ)

AĞUSTOS 2010

ACKNOWLEDGEMENTS

May 2010   Hatice Gökcan

                                                              Computational Science and Engineering

TABLE OF CONTENTS

ABBREVIATIONS

Å	: Angstron
ψ	: Wave function
$\hbar$	: Planck's constant
V	: Potential energy
G	: Gibbs free energy
m	: Mass
∇^2	: Laplacian
Z	: Atomic number
ε_0	: Permititivity constant
r	: Distance
H_{tot}	: Totla Hamiltonian
T_n	: Kinetic energy of nuclei
T_c	: Kinetic energy of electrons
V_{nc}	: Potential energy of nuclear – electron attraction
V_{ee}	: Potential energy of electron – electron repulsion
H_e	: Electronic Hamiltonian operator
E_e	: Electronic energy
H_n	: Nuclear Hamiltonian operator
ε_i	: One electron energy eigenvalues
χ_i	: Spin orbital
H^{core}	: Core Hamiltonian
ζ	: Coulomb operator
ξ	: Exchange oprator
f_i	: Fock operator
n	: Quantum number
l	: Quantum number
m_l	: Quantum number
N	: Normalization constant
Y_{lm_l}	: Spherical harmonic
n_{eff}	: Effective principal quantum number
Z_{eff}	: Effective atomic number
ϕ	: Atomic orbital
P_{tu}	: Density matrix elements
H_{rs}^{core}	: Core integral
F_{rs}	: Fock matrix element
S	: Unit matrix
E_j	: Coulomb repulsion beteen electrons
E_{XC}	: Exchange – correlation energy
E_X	: Exchange energy
E_C	: Correlation energy

ε_X	: Exchange energy per partice
ε_c	: Correlation energy per particle
E_X^{Becke}	: Becke's exchange functional
λ	: Coupling parameter
U_{XC}^{λ}	: Exchange – correlation energy according to coupling parameter
u_{xc}	: Exchange correlation potential density
E_{XC}^{LSDA}	: Exchange correlation energy from LSDA
E_{XC}^{B3LYP}	: Exchange correlation energy from B3LYP
E^{HF}	: Hartree – Fock energy
E_C^{VWN}	: Vosko, Wilk, Nusair function
E_C^{LYP}	: LYP correlation functional
ϕ_s	: Basis function
c_{si}	: Coefficient of sth basis function according to i^{th} MO
d_{si}	: Coefficient of primitive Gaussian function
E_{EN}	: Distortion energy
G_{ENP}	: Electrostatic component of solvation
$G_{cavitiy}$	: Thermal free energy in cavitiy
$G_{dispersion}$	: Thermal free energy of dispersion
$G_{electrostatic}$	: Electrostatic thermal free energy
q	: Charge
ε	: Dielectric constant
γ_k	: Reduced density matrix of order k
R	: Gas constant
T	: Temprature
K	: Boltzman function
kcal	: Kilocalory
PLP	: Pyridoxal 5 – phosphate
PMP	: Pyridoxamine 5 – phosphate
GABA	: Gamma-aminobutyric acid
GABA-AT	: Gamma-aminobutyric acid aminotransferase
GEG	: Gamma ethynyl GABA
Dilantin	: Diphenylhydantoin
Vigabatrin	: Gamma vinyl GABA
R-KG	: R – ketoglutarate
PHE	: Phenylalanine
ARG	: Arginine
ILE	: Isoleucine
GLU	: Glutamate
THR	: Threonine
HF	: Hartree – Fock
STO	: Slater – type orbital
GTO	: Gaussian – type orbital
AO	: Atomic orbital
MO	: Molecular orbital
SCF	: Self consistent field
ZDO	: Zero differential overlap
PM3	: Parametrized Model 3
NDDO	: Neglect of diatomic differential overlap
AM1	: Austin Model 1

DFT	**:**	Density functional theory
LDA	**:**	Local density approximation
LSDA	**:**	Local spin density approximation
B3LYP	**:**	Becke three-parameter Lee – Yang – Parr
KS	**:**	Kohn – Sham
PES	**:**	Potential energy surface
PCM	**:**	Polarized continuum model
NBO	**:**	Natural bond orbital
NAO	**:**	Natural atomic orbital
BO	**:**	Born Oppenheimer
IEFPCM	**:**	Integral Equation Formalism PCM
UFF	**:**	Universal Force Field
SCRF	**:**	Self Consistent Reaction Field
G03	**:**	Gaussian 03
IRC	**:**	Intrinsic reaction coordinate
TS	**:**	Transition structure

LIST OF FIGURES

A COMPUTATIONAL STUDY ON INACTIVATION MECHANISMS OF GABA – AT

SUMMARY

γ-aminobutyric acid (GABA) is one of the inhibitory neurotransmitter in the mammalian central nervous system which is degraded to succinic semialdehyde via transamination with R-ketoglutarate by catalysis of pyridoxal 5-phosphate (PLP)-dependent enzyme GABA aminotransferase (GABA-AT) [17]. Reduction of GABA concentration in brain causes convolution besides several neurological diseases such as epilepsy, Parkinson's disease, Huntington's chorea, and Alzheimer's disease [14, 23]. Thus, increasing the concentration of GABA in brain will lead therapeutic applications. Due to the ineffectiveness of GABA to cross blood-brain barrier, several inactivators were reported to control the level of GABA in brain by inactivation of GABA-AT.

Silverman and co-workers have reported some fluorine containing conformationally restricted analogues of GABA as potential mechanism based inactivators [18]. One of them is 5-amino-2-fluorocyclohex-3-enecarboxylic acid. This compound could go through enzyme-catalyzed elimination that inactivates GABA-AT either by Michael addition that yields a covalently modified active site residue or an aromatization mechanism, which produces a modified coenzyme. According to the experimental results, it was observed that fluorine elimination occurs thus it is not probable to inactivate the GABA-AT via an enamine mechanism, where the fluorine elimination does not occur [18].

The ultimate aim of this study is to identify the more plausible inactivation mechanism of GABA-AT with 5-amino-2-fluorocyclohex-3-enecarboxylic acid in conjunction with experimental results. The stationary structures throughout the experimentally proposed pathways have been optimized at the B3LYP/6-31+G(d,p) level of theory. The solvent effect is also take into consideration.

GABA – AT İNAKTİVASYONU MEKANİZMALARI ÜZERİNE HESAPSAL BİR ÇALIŞMA

ÖZET

γ-aminobutirik asit (GABA), memeli merkezi sinir sisteminde engelleyici sinir inhibitörlerinden olup, piridoksal 5-fosfat (PLP) bağımlı GABA aminotransferaz enziminin katalizörlüğünde R-ketoglutarat ile transaminasyonu sonucunda süksinik semialdehite degrede olur [17]. Beyindeki GABA konsantrasyonunun düşüşü konvolüsyonun yanı sıra Parkinson hastalığı, Huntington koresi ve Alzheimer gibi çeşitli nörolojik hastalıklara neden olmaktadır [14, 23]. Bu nedenden ötürü, beyindeki GABA konsantrasyonunun artırılması terapatik uygulamalar sağlayacaktır. GABA'nın kan beyin bariyerini geçememesi nedeni ile, GABA-AT inaktivasyonu aracılığıyla GABA seviyesinin kontrolüne yönelik çeşitli inaktivatörler rapor edilmiştir.

Silverman ve çalışma arkadaşları bazı florin içeren konformasyonel olarak sınırlandırılmış bazı GABA analoglarını mekanizma bazlı inaktivatörler olarak rapor etmiştir [18]. Bunlardan birisi de 5-amino-2-florosikloheks-3-enekarboksilik asittir. Bu bileşen enzim katalizli eliminasyon ile kovalent olarak modifiye edilmiş aktif bölge oluşmasını sağlayan Michael eklenmesi veya modifiye koenzim üreten aromatizasyon mejanizması aracılığı ile GABA-AT'yi inaktive etmektedir. Deneysel verilere göre, flor eliminasyonu görülmektedir, bu yüzden GABA-AT'nin flor çıkışının gerçekleşmediği enamin mekanizması ile inaktivasyonu mümkün değildir [18].

Bu çalışmanın ana amacı, deneysel sonuçlar ışığında 5-amino-2-florosikloheks-3-enekarboksilik asit ile GABA-AT inaktivasyonunda gerçekleşmesi en mümkün mekanizmanın belirlenmesidir. Deneysel olarak öne sürülmüş olunan mekanizmalarda yer alan sabit yapılar B3LYP/6-31+G(d,p) teori seviyesinde optimize edilmiştir. Ayrıca çözücü etkisi de göz önünde alınmıştır.

1. INTRODUCTION

1.1 Enzymes

Enzymes are specialized proteins that lower the activation energy of a reaction [1]. The catalysis performed by reducing the transition state energies and by increasing the ground state energies [2]. On the other hand, they do not change the free energy difference (ΔG) between the reactants and products [3].

1.1.1 Active Site

In enzymes there are specific side chains that determine the catalytic activity and the specificity of that enzyme. The place that side chains form is called active site [3] which has a unique shape, such as a groove or a pocket that is specific for a particular substrate [1].

An enzyme has to be bound to its specific target which could be a small molecule or a macromolecule, to perform its task [3]. Therefore the first step in an enzyme catalyzed reaction is always the formation of the enzyme-substrate complex [1, 2]. The formation of the complex is facilitated by noncovalent interactions between the substrate and the amino acids in the active site such as ionic, ion-dipole, dipole-dipole or van der Waals interactions [2].

In an active site, there are two important regions for catalytic power, one of them binds the substrate (substrate binding region) while the other catalyzes the reaction (catalytic region). In some enzymes the substrate binding region involves the catalytic region [3].

1.1.2 Coenzymes

Some enzymes need another chemical component, which is called cofactor that situated in the active site and is required for the catalysis by those enzymes [2, 4].

A cofactor could be either an inorganic ion such as Fe^{2+}, Zn^{2+}, or an organic complex which is specifically called coenzyme [4, 5]. Moreover some enzymes may need both a coenzyme and an inorganic ion [4]. Coenzymes are a kind of transition carriers that are usually derived from vitamins [4, 5].

1.1.2.1 Pyridoxal Phosphate (PLP)

PLP, the phosphorylated and the oxidized form of vitamin B6 [6], is an organic cofactor in which it forms an imine with ε-amino group of a lysine residue of PLP-dependent enzymes [7]. Furthermore the formation of imine could be referred as Schiff base formation [8] which takes place in lots of different chemical reactions that leads different products based on the enzyme [6]. There is a particular interest about the PLP-dependent enzymes due to the diversity of chemical reactions such as decarboxylation, β-elimination, aldol cleavage, transimination and transamination [6, 9, 10].

The computational studies concentrate on the formation of PLP-Schiff base [11, 12]. According to those studies, if PLP is bound to lysine residue with an imine bond and bound to the enzyme covalently, it is called an internal aldimine [6, 11]. Moreover, a new imine bond is formed due to the reaction of the substrate with the Schiff base that produces external aldimine from Michaelis complex [11, 12, 13] This reaction is called transimination or transaldimization which is symmetrical [11]. It is also known that [12, 13] in most PLP dependent enzymes the nitrogen of pyridine ring is protonated and this protonation stabilizes the interactions in enzymatic residues [14]. This stabilization is achieved due to the electron-sink effect [12, 14].

3

1.1.3 GABA and GABA-AT

GABA aminotransferase (GABA-AT, E.C. 2.6.1.19), a member of subfamily II of α-family of pyridoxal 5-phosphate (PLP) dependent enzymes, is a homodimer in which all subunits contains an active site PLP that is covalently bound to Lys-329 via a Schiff base. Deduction of primary sequence of GABA-AT was established from cDNA of pig brain and peptide fragments of the enzyme from pig liver [15]. The x-ray structure of GABA-AT from pig liver was reported at 3.0-Å resolution in 1999 by Storici and co-workers that clarifies the geometry of active-site (Figure-1) [16].

γ-aminobutyric acid (GABA) is one of the inhibitory neurotransmitters in the mammalian central nervous system which is degraded to succinic semialdehyde via GABA-AT catalyzed reaction [17]. In addition to the production of succinic semialdehyde, the neurotransmitter L-glutamate is generated via transamination of PLP, which is restored from pyrdoxamine 5-phosphate (PMP), with R-ketoglutarate (R-KG) [17].
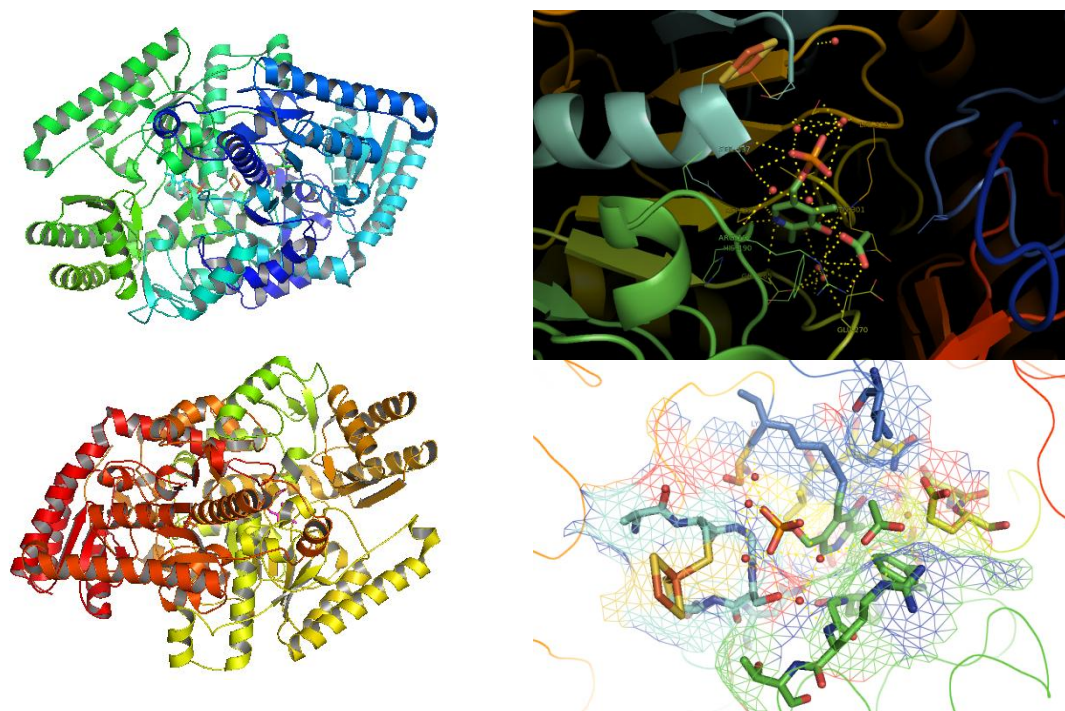
Figure 1.1 : GABA-AT from pig liver. **a)** X-ray diffraction. **b)** Ligand site at Chain A. **c)** Ligand site at Chain A with mesh type surface
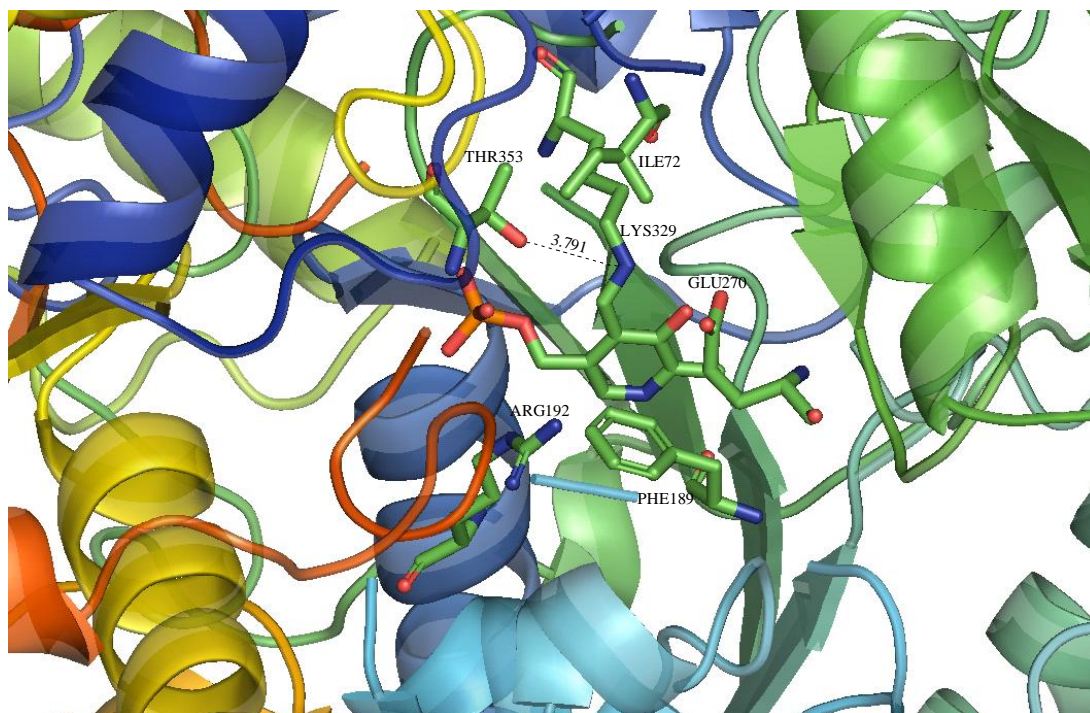
Figure 1.2 : Active site of GABA – AT that involves the amino acids; Lys329, Thr353, Phe189, Arg192, Ile72 and Glu270.

Active site of GABA-AT (**Figure 1.2**) involves PHE-189 which was observed that it changed its location according to the native form [15]. ARG-192 at the active site forms a salt bridge with the carboxylate group of the inhibitor in the cases of vigabatrin and GEG [15]. Moreover, it was observed that the distance between ILE-72 and branching methyl group is short ranging [15]. In the case of 3-F-GABA as an inhibitor van der Waals interaction occurs between the GLU-270 and the carboxylic acid [18]. Furthermore, THR353 in the other monomer of the homodimer was suggested for deprotonation of the ammonium ion of 3-F-GABA [18].

1.2. Enzyme Inhibition and Drugs

Lots of enzymes could be inhibited by certain chemicals. Computational chemists have a particular interest in drug designing to investigate the interactions between potential drugs and biomolecules [19]. The interactions with a drug and its target, such as enzymes, could be not only the non-bonded forces but also covalent [20].

Almost all drugs have therapeutic effect by binding to the active site of an enzyme to unable the substrate to displace it and bind to the active site. As a result of this obstacle the specific biochemical pathway of the enzyme and its substrate is blocked [21].

Blocking a certain pathway by inhibition of an enzyme could be reversible or irreversible. In reversible inhibition, the chemical agent inhibits the enzyme by weak chemical bonds [22]. On the other hand, the irreversible inhibition occurs when the chemical agent inactivates the enzyme permanently [22].

The irreversible inhibition could be competitive, in which the inhibitor competes to bind the active site with the substrate of the related enzyme, and noncompetitive where the inhibitor binds a location at the enzyme other than the active site [22].

1.2.1 Inhibition of GABA-AT

Reduction of GABA concentration in brain causes convolution, besides several neurological diseases such as epilepsy, Parkinson's disease, Huntington's chorea, and Alzheimer's disease [14, 23]. Increasing the concentration of GABA in brain has an anticonvulsant effect in brain [24, 25]. Nevertheless, GABA could not cross the blood-brain barrier so controlling the GABA directly could not be performed effectively [25, 26]. Several inhibitors were used and test for controlling the level of GABA in brain by either inhibition or inactivation of GABA-AT [26, 27, 28, 29].

Diphenylhydantoin (Dilantin) was introduced as an anticonvulsant drug over 65 years ago and it is widely used, but in general it is not appropriate. As a matter of fact the ratio of epileptic patients who do not respond any anticonvulsant drug in market is about 25% of all patients. As a result, the necessity of new anticonvulsant drugs is huge [15].

One strategy to inhibit or inactivate GABA-AT is using its analog. 4-amino-5-hexynoic acid, λ-ethynyl GABA or GEG, is one of the earliest analog, however it did not become a clinical candidate [15].

λ-vinyl GABA (vigabatrin) is another analog which is the most effective mechanism-based inactivator has a high potency for treatment of epilepsy, also is used in over 60 countries [15, 30, 31]. Nonetheless for effectiveness, vigabatrin should be taken daily about 0.5 g. Besides, it has some side effects, mostly a visual field defect [15]. There are three different inactivation mechanisms that have been suggested. Storici et. al. found and proposed the Michael Addition mechanism [15]. The data that have been obtained from carbon 14 labeling experiments support the Michael Addition via Enamine mechanism [15]. The last one of the suggested mechanisms is an enamine

6

mechanism which deprotonates the λ-carbon but followed a tautomerization through the vinyl double bond [30, 31].

The natural product gabaculine, which is a mechanism based inactivator of GABA-AT, is a kind of neurotoxin that was firstly isolated from *Streptomyces toyocaenis.* [11]. It was shown that gabaculine is a highly potent irreversible inactivator of GABA-AT and belongs a class of highly specific irreversible enzyme inhibitors which requires catalytic inactivation by target before inactivation step [11, 12]. Rando et. al. showed that it inactivates GABA-AT by an aromatization mechanism that modifies PLP [12]. According to the experiments, inactivation of brain GABA-AT was established by administration of gabaculine to animals and this leads an increase in level of GABA by 15-20 folds which is a proof of crossing the blood brain barrier of gabaculine [11, 13]. However, gabaculine was found toxic for theurepatic applications due to possibility of its high reactivity with some other enzymes [12, 15].

Silverman and co-workers have reported some fluorine containing conformationally restricted analogues of GABA as potential mechanism based inactivators [14, 18]. One of them is 5-amino-2-fluorocyclohex-3-enecarboxylic acid. 5-amino-2 fluorocyclohex-3-enecarboxylic acid is an composite structure which has the form of cyclohexene analogue of (1*R*,4*S*)-(+)-4-amino-2-cyclopentene-1-carboxylic acid but with an added fluorine atom [14]. This compound could go through enzyme-catalyzed elimination that inactivates GABA − AT either by Michael addition that leads to a covalently modified active site residue **(Mechanism 1)** or an aromatization mechanism which produces a modified coenzyme **(Mechanism 2)** (**Figure 1.3**). The double bond and fluorine in the structure is important for inhibition. It was also suggested that it could go through an enamine mechanism for inactivation, just like in vigabatrin, in which fluorine elimination does not occur unlike in aromatization and Michael addition mechanisms [14]. According to the experiments, it was observed that fluorine elimination, which is suggested as in **Mechanism 1** and **Mechanism 2** (**Figure 1.3**), occurs so it is not probable to inactivate the GABA-AT via an enamine mechanism [16].
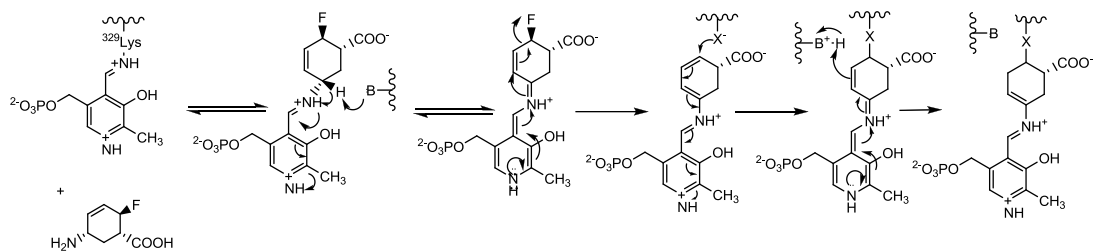
Mechanism 1
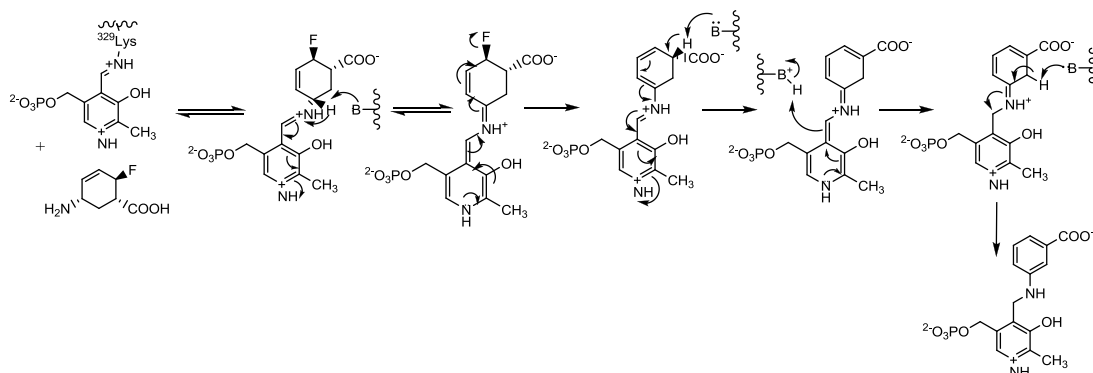
Mechanism 2

Figure 1.3 : Proposed mechanisms of inactivation of GABA-AT with 5-amino-2 fluorocyclohex-3-enecarboxylic acid. **Mechanism 1.** Inactivation via Michael addition mechanism. **Mechanism 2.** Inactivation via aromatization mechanism

1.2.1.1 Michael Addition

The β carbon of an α-β unsaturated carbonyl compounds is electrophilic due to the sharing partial positive charge of carbonyl carbon through resonance [32]. Due to this electrophilicity, a nucleophile could attack to the carbonyl group from β position (**Figure 1.4**) [32].
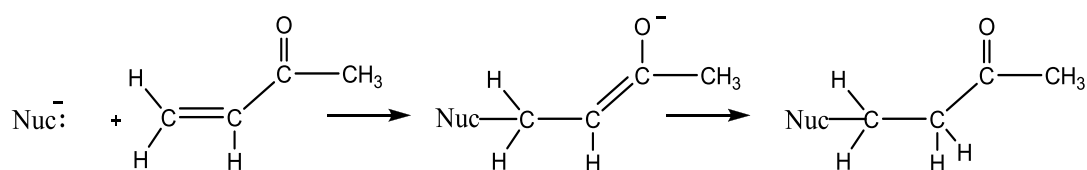
Figure 1.4 : Nucleophilic addition to β carbon. Formation of keto after protonation of enolate and tautomerization.

Michael addition is a kind of carbon-carbon and carbon-heteroatom bond forming reactions where an enolate ion is added to the double bond at an α-β unsaturated carbonyl compound [32, 33]. The Michael acceptor is the electrophile that accepts

the electron pair, while the Michael donor is the attacking nucleophile [32]. Bond formation between carbon and nitrogen via Michael addition is highly interested due to the formation of some important compounds such as β amino esters and derivatives [33].

Michael addition mechanisms are not only have significant roles on organic synthesis but also props in lots of enzymatic reactions [34, 35, 36]. Nucleophilic additions of DNA with prevalent Michael acceptors was studied by Pardo et. al. by examining the ammonia additions to Michael acceptors [37]. Moreover, to identify the stereochemistry of proton addition to enolate, quantum mechanical calculations were performed lots of Michael addition intermediates [38, 39]. Thomas and Kollman were also studied the Michael addition mechanism by examining the addition of sulfur nucleophiles to carbonyl compounds which are important in enzymatic processes of cysteine proteases [40].

In literature, the inactivation mechanism of GABA-AT via any of the substrate analogues has not been studied by means of computational tools. In this study 5-amino-2-fluorocyclohex-3-enecarboxylic acid is preferred in modeling the reaction mechanism. The ultimate aim of this study is to elucidate the inactivation mechanism of GABA-AT with 5-amino-2 fluorocyclohex-3-enecarboxylic acid in conjunction with experimental results. The elucidation of the inactivation reaction mechanism will make it possible to perform tailor-made synthesis for inhibitors and make great contribution to drug chemistry.

2. METHODOLOGY

2.1 The Schrödinger Equation

Erwin Schrödinger introduced a differential equation in 1926 where the wave function $\Psi(r_1, r_2, ..., t)$ evolves in time according to the equation

$$\hbar \frac{\partial \Psi(x,t)}{\partial t} = -\frac{\hbar^2}{2m} \frac{\partial^2 \Psi}{\partial x^2} + V(x)\Psi(x,t) \qquad (2.1)$$

In this equation, which is called time dependent Schrödinger equation, Ψ is the wave function, $\hbar$ is Planck's constant, m is mass of particle and V is the potential field. [41] The first step to solve the Schrödinger equation is expressing the wave function $\Psi(x,t)$ as the product of two functions [42]

$$\Psi(x,t) = \psi(x)\chi(t) \qquad (2.2)$$

Where the $\psi(x)$ depends only the distance x and $\chi(t)$ depends only the time t. If these function are substituted on the equation (2.1) and the partial derivatives are taken, it gives

$$i\hbar\psi(x) \frac{d\chi(t)}{dt} = -\frac{\hbar^2}{2m} \chi(t) \frac{d^2\psi(x)}{dx^2} + V(x)\psi(x)\chi(t) \qquad (2.3)$$

If the both sides are divided by $\psi(x)\chi(t)$ it gives

$$i\hbar \frac{1}{\chi(t)} \frac{d\chi(t)}{dt} = -\frac{\hbar^2}{2m} \frac{1}{\psi(x)} \frac{d^2\psi(x)}{dx^2} V(x) \qquad (2.4)$$

In equation (2.3) the left hand side depends only time while the right hand side depends only distance. Therefore when x changes only the right hand side changes. However the right hand side is equals to the left hand side, thus the right hand side of

the equation (2.4) must equal to a constant value. Due to the dimension of a constant are those of energy, the separation constant is determined as E, which is assumed that it is a real number [41, 42]. In consequence the equation could be separated into two parts, one time dependent and one spatial dependent. The time dependent part is shown by the equation

$$i\hbar \frac{d\chi(t)}{dt} = E\chi(t) \tag{2.5}$$

which has a solution of

$$\chi(t) = e^{-iEt/\hbar} \tag{2.6}$$

Therefore the substitution of equation (2.6) to the equation (2.2), the complete wave function has the form

$$\Psi(x,t) = e^{-iEt/\hbar} \psi(x) \tag{2.7}$$

The spatial dependent equation is given by

$$-\frac{\hbar^2}{2m} \frac{d^2\psi(x)}{dx^2} + V(x)\psi(x) = E\psi(x) \tag{2.8}$$

In this equation if the left hand side is written with the parenthesis in which whole part has the same multiplier $\psi(x)$ it gives

$$\left[-\frac{\hbar^2}{2m} \frac{d^2}{dx^2} + V(x) \right] \psi(x) = E\, \psi(x) \tag{2.9}$$

where the part in the paranthesis is referred as the Hamiltonian operator ($\hat{H}$).

The Hamiltonian operator expresses the total energy in term of position and momentum [42].

$$\hat{H} = \left[-\frac{\hbar^2}{2m} \frac{d^2}{dx^2} + V(x) \right] \tag{2.10}$$

Therefore, the time independent Schrödinger equation finally has the form of

$$\hat{H}\,\psi(x) = E\,\psi(x) \tag{2.11}$$

According to the equation (2.10) Hamiltonian is made up of both the kinetic energy and the potential energy

$$\hat{H} = T + V \tag{2.12}$$

where T is the kinetic energy operator which is related to linear momentum and V is the potential energy operator. In one dimension a particle with mass m has a kinetic energy as

$$T = -\frac{\hbar^2}{2m}\frac{d^2}{dx^2} \tag{2.13}$$

In three dimension the operator in the position representation is

$$T = -\frac{\hbar^2}{2m}\left\{\frac{\partial^2}{\partial x^2} + \frac{\partial^2}{\partial y^2} + \frac{\partial^2}{\partial z^2}\right\} = -\frac{\hbar^2}{2m}\nabla^2 \tag{2.14}$$

where ∇^2 (del, squared) is called the Laplacian. For an n particle system kinetic energy will have the form of

$$T = -\frac{\hbar^2}{2m}\sum_{i=1}^{n}\nabla_i^2 \tag{2.15}$$

Potential energy term in Hamiltonian is the Coulomb potential energy of an electron in the field of a nucleus which has an atomic number of Z

$$V = -\frac{Ze^2}{4\pi\varepsilon_0 r} \tag{2.16}$$

where ε_0 is the permititivity constant and r is the distance from the nucleus to electron.

Therefore the potential energy term would be given

$$V = \frac{1}{4\pi\varepsilon_0}\left[-\sum_i^{electrons}\sum_j^{nuclei}\left(\frac{Z_i e^2}{\Delta r_{ij}}\right) + \sum_i^{electrons}\sum_{j<i}^{electrons}\left(\frac{e^2}{\Delta r_{ij}}\right) \right.$$
$$\left. + \sum_i^{nuclei}\sum_{j<i}^{nuclei}\left(\frac{Z_I Z_j e^2}{\Delta R_{ij}}\right)\right]$$

(2.17)

where the electron-nuclear attraction is represented with the first term, electron-electron repulsion is represented with the second term and the nuclear-nuclear repulsion is represented with the last term.

2.2 The Born Oppenheimer Approximation

Schrödinger equation can not be solved analytically due to the number of particles in systems, even there are three particles in the simplest molecule H_2^+ [41]. Born-Oppenheimer approximation takes into account the great differences in masses of electrons and nuclei to overcome the difficulty of Schrödinger equations for many particle systems. Due to the great differences between the masses of electrons and nuclei, electrons respond to the displacements of nuclei immediately. For this reason taking the position of nuclei fixed could be useful to solve Schrödinger equation [41].

The nucleus is much slower than electrons due to the differences in masses. Therefore seperation of Schrödinger equation into two parts could be a good approximation, which is called Born-Oppenheimer approximation. In seperated form, one part describes the electronic wave function for a fixed nuclear geometry while the other part, where wave function plays the role of potential energy, describes the nuclear wave function. According to the approximation, the electronic wave function depends only on the nuclear position not their momenta.

The total Hamiltonian is then written as

$$H_{tot} = T_n + T_c + V_{nc} + V_{ee} + V_{nn}$$

(2.18)

where the kinetic energy of nuclei and electrons are represented as T_n and T_c respectively, and the potential energies of nuclear-electron attraction as V_{nc}, electron-

electron repulsion as V_{ee} and nuclear-nuclear repulsion as V_{nn}. Thus, is the Hamiltonian operator is transformed to a centre of mass system it gives

$$H_{tot} = T_n + H_e \tag{2.19}$$

where H_e is the electronic Hamiltonian operator which depends only on the nuclear position and could be written as

$$H_e = T_{en} + V_{ne} + V_{ee} + V_{nn} \tag{2.20}$$

If this Hamiltonian is used in electronic Schrödinger equation

$$H_e \psi_e (R,r) = E_e(R)\psi_e(R,r) \tag{2.21}$$

$$H_n \psi_n (R) = E_{tot}\psi_n(R) \tag{2.22}$$

$$(T_n + E_e(R)) \psi_n (R) = E_{tot}\psi_n(R) \tag{2.23}$$

where R and n denote nuclear coordinates while r and e denote electronic coordinates.

The nuclear Hamiltonian H_n, describes the vibrational, rotational and translational states of nuclei. Moreover the solution of the equation (2.23) allows to lay out the molecular potential energy curve, and generally to construct potential energy surface of a polyatomic system [41].

2.3 The Hartree-Fock Equations

Hartree-Fock (HF) calculations are the simplest ab initio method. The problem that has been focused on is the infeasibility of the solution of Schrödinger equation for many particle systems [19].

The total wave function of an atom could be approximated as a combination of the wave function for different energy levels. Hartree's guess was depends on this fact and the method writes an approximate wave function for an atom as the product of one-electron wave function

$$\Psi_0 = \psi_0(1)\psi_0(2)\psi_0(3) \dots \psi_0(n) \tag{2.24}$$

The equation 2.24 is called the Hartree product where Ψ_0 is a function of the coordinates of all electrons and $\Psi_0(1)$ is the function of coordinate of electron 1 and so on. The one electron wavefunctions are called atomic orbital if the dealed system is an ato [19]. In the case of a molecule Ψ_0 is called molecular orbital. [19] The zeroth approximation to the total wavefunction is Ψ_0.

The eigenvalue of Ψ_0 could be found by the equation

$$H\Psi_0 = H \, \psi_0(1)\psi_0(2)\psi_0(3) \, ... \, \psi_0(n)$$

$$H\Psi_0 = \left(\sum_{i=1}^{N} \varepsilon_i \right) \Psi_0 \tag{2.25}$$

which proves the energy eigenvalue of a many-electron wave function is the sum of one-electron energy eigenvalue [21].

An electron on the spin orbital χ_i, which is in the field of the nuclei and other electrons, has a Hamiltonian operator which contains three different contributions to the energy. Those contributions are the core Hamiltonian operator, Coulomb operator and the exchange operato [20]. Thus the Hamiltonian could be written as

$$H^{core}(1)\chi_i + \sum_{j \neq i}^{N} \zeta_j(1)\chi_i(1) - \sum_{j \neq i}^{N} \xi_j(1)\chi_i(1) = \sum_j \varepsilon_{ij}\chi_j(1) \tag{2.26}$$

where $H^{core}(1)$ is the core Hamiltonian, $\zeta_j(1)$ is Coulomb and $\xi_j(1)$ exchange operators. If the equation is simplified according to the $\{\zeta_i(1) - \xi_i(1)\}\chi_i(1) = 0$

$$f_i\chi_i = \sum_j \varepsilon_{ij}\chi_j \tag{2.27}$$

where f_i is called the Fock operator

$$f_i(1) = H^{core}(1) + \sum_{j=1}^{N}\{\zeta_i(1) - \xi_i(1)\} \tag{2.28}$$

while for a closed shell system it has the following form

$$f_i(1) = H^{core}(1) + \sum_{j=1}^{N/2}\{2\zeta_i(1) - \xi_i(1)\} \tag{2.29}$$

2.4 Slater-type Orbitals (STOs) and Gaussian-type Orbitals (GTOs)

The orbital of an atom of atomic number Z is written as

$$\phi_{nlm_l}(r,\theta,\phi) = Nr^{n_{eff}-1}e^{-Z_{eff}\rho/n_{eff}}Y_{lm_l}(\theta,\phi) \tag{2.30}$$

Where n, l, m_l are the quantum numbers, N is the normalization constant, Y_{lm_l} is the spherical harmonic and $\rho = r/a_0$. n_{eff} is the effective principal quantum number which is related to the true principal quantum number n by the following map [41].

$$n \rightarrow n_{eff}: \quad 1 \rightarrow 1 \quad 2 \rightarrow 2 \quad 3 \rightarrow 3 \quad 4 \rightarrow 3.7 \quad 5 \rightarrow 4.0 \quad 6 \rightarrow 4.2 \tag{2.31}$$

Orbitals with different values of quantum number n but same values of quantum numbers l and m_l are not orthonormal to each other. Moreover, s-orbitals with $n > 1$ have zero amplitude at the nucleus in the case of Slater-type orbitals (STOs) [41].

Slater-type orbitals are mathematical functions to define the wave function of an electron in an atom, however they are not suitable for many electron atoms. [43] They are generally used in atomic or diatomic system calculations if high accuracy is required and also in semiemprical methods in which three and four centre integrals are not taken into account [44].

Although STOs have a number of attractive features, in ab initio HF theory they are limited. If the basis functions are chosen as STOs, there would be no analytical solution for the four index integral [21]. In 1950 Boys suggested an alternative to the usage of STOs that uses e^{-r^2} instead of e^{-r} where the AO-like functions have the form of a Gaussian function [45]. This AO-like functions are called Gaussian type orbitals (GTO) which are mathematical functions to define the wave function [48, 49].

16

The normalized GTO in atom-centered Cartesian coordinate is

$$\phi(x, y, z: \alpha, i, j, k) = \left(\frac{2\alpha}{\pi}\right)^{3/4} \left[\frac{(8\alpha)^{i+j+k} \, i! \, j! \, k!}{(2i)! \, (2j)! \, (2k)!}\right]^2 x^i y^j z^k e^{-\alpha(x^2+y^2+z^2)} \qquad (2.32)$$

where α is the exponent that controlls the width of GTO and i, j, k are non-negative integers that order the nature of the orbital in a Cartesian sense.

GTO has a spherical symmetry when all of these integers are zero and it is referred as s-type GTO. If one of the indices is equal to one the function is called p-type GTO where it has an axial symmetry about a single axis. Moreover, if the sum of the indices is equal to two, it is called d-type GTO [21].

On the other hand STO calculations require less primitives than GTO basis sets to define the wave function which is also seen in Figure 2.1 [43].
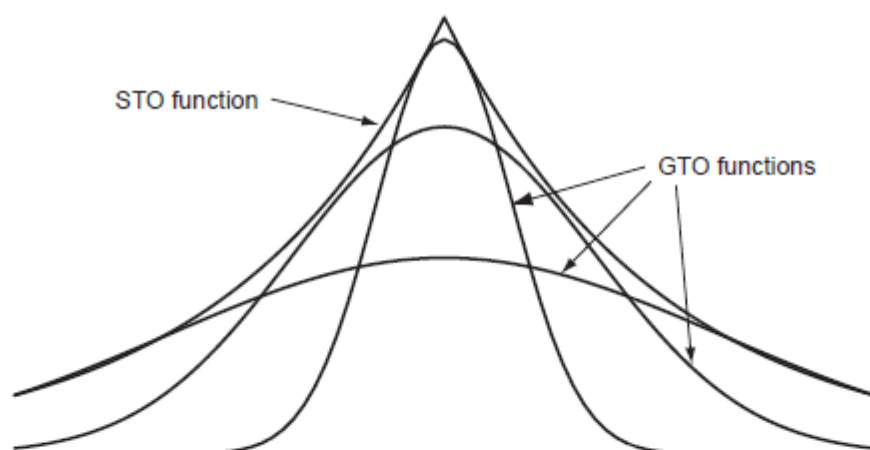
Figure 2.1 : Approximating of several Gaussian-type orbitals with a Slater-type orbital [43]

The wave functions are defined by a finite number of functions by choosing a standard GTO basis set. Thus, the calculation approximates that an infinite number of GTO functions would be needed to define an exact wave function [43]. Although the real hydrogenic atomic orbitals have a cusp, GTOs are smooth and differentiable at the nucleus. Moreover, the GTOs is exponential in r^2, which results a rapid reduction in amplitude with distance for the GTOs, while the hydrogenic atomic orbitals are exponential in r [21].

2.5 Semi-Empirical Methods

In an ab initio calculation the core integral H_{rs}^{core}, density matrix elements P_{tu}, and the electronic repulsion integrals (rs/tu), (ru/ts) are used to calculate the Fock matrix element

$$F_{rs} = H_{rs}^{core}(1) + \sum_{t=1}^{m} \sum_{u=1}^{m} P_{tu} \left[(rs|tu) - \frac{1}{2}(ru|ts) \right] \tag{2.33}$$

where density matrix is given as

$$P_{tu} = 2 \sum_{i=1}^{n/2} c_{ti} c_{ui} \tag{2.34}$$

and core integral is given as

$$H_{rs}^{core} = \int ds_1 \phi_r(1) \left[-\frac{1}{2}\nabla^2 - \sum_{i=1}^{k} \frac{Z_i}{|r_1 - R_i|} \right] \phi_s(1) \tag{2.35}$$

An initial guess of the coefficients to calculate the density matrix values P_{tu} is necessary where it would be calculated by a simple Hückel calculation or extended Hückel calculation. To improve the energy levels and coefficients the Fock matrix of F_{rs} elements is diagonalized continually.

In an ab initio calculation much numbers of basis functions could be used. On the other hand semi-empiric methods use the basis functions which correspond to the atomic orbitals and Slater functions are used in SCF-type semi-empirical methods instead of the approximating them as sum of Gaussian functions. Moreover, semi-empirical calculations taken into account only the valance or the π electrons, thus the elements of core turn out an atomic nucleus plus its core electrons [19].

The cost of HF calculations is arise from the two-electron integrals which are necessary to construct the Fock matrix. Semi-empirical methods reduce the number of these integrals by taking them as zero to reduce the computational cost [44]. The integrals that are ignored are one-electron integrals involving three centers which are neglected by differential overlap [19, 44].

Furthermore, in SCF-type semi-empirical methods the overlap matrix is taken as a unit matrix (S=1). Therefore the Roothaan-Hall equations $FC = SCE$ are clear away

without using orthogonalizing matrix to transform this equations into standard eigenvalue form $FC = CE$ [19].

2.5.1 Zero Differential Overlap (ZDO) Approximation

Zero Differential Overlap approximation is the center of semi-empirical methods. The approximation neglects all products of basis functions that depend of the same electron coordinates on different atoms [44]. The basis functions are taken to be orthonormal according to the equation (2.36) and the ZDO expands this idea to the two-electron integrals [46].

$$\int \chi_i(r)\chi_j(r)d\tau = \begin{cases} 1 & \text{if i} = 0 \\ 0 & \text{otherwise} \end{cases} \tag{2.36}$$

$$\frac{e^2}{4\pi\epsilon_0} \int \cdots \frac{1}{r_{12}} \chi_i(r_1)\chi_j(r_1)d\tau_1 \tag{2.37}$$

If i and equals to each other (i=j) the integral is set to zero and the two-electron integrals have the form of

$$\frac{e^2}{4\pi\epsilon_0} \int \chi_i(r_1)\chi_j(r_1)\frac{1}{r_{12}} \chi_k(r_2)\chi_l(r_2)d\tau_1 d\tau_2 \tag{2.38}$$

are set to zero unless i=j and k=l.

2.5.2 PM3

Parametrized Model 3 was reported by Stewart at 1999 which is his third parameter set [47]. In this parameter set he adopted an NDDO functional, which is also identical to the AM1, and he used two Gaussian functions rather than four for per atom to employ a larger data set in evaluating the penalty function [21].

The Hamiltonian in PM3 contains the same elements as AM1 but the parameters in PM3 were derived using an automated parametrization procedure which was also devised by Stewart [20]. On the contrary the chemical knowledge and the intuition is the source to obtain the parameters in AM1. Thus, AM1 and PM3 have different values for some parameters. However, there are also some problems in PM3 model. One of them is the bonds where they are taken too short in the case of hydrogens and they are underestimated when they are between Si, Cl, Br, I. Additionally the amide

bond's rotational barrier is too low and in some cases it is almost not exists, but it could be corrected by the usage of an empirical torsional potential.

2.6 Density Functional Theory (DFT)

The energy of a molecule could be determined by the molecule's electron density instead of a wave function and density functional theory is based on both the wave function and the electron density [19, 43, 48]. The function of an external potential energy which is acting on the density of the ground state energy of an inhomogeneous interacting many particle system is the main subject of density functional theory [49].

The earliest model for density functional was suggested by Thomas (1927) and Fermi (1927, 1928). In 1920 Dirac and in 1935 von Weizsacker suggested the extensions of the model [48]. However the theory was firstly proposed by Kohn and Sham in 1965, but it was started to use as a computational tool for chemical problems in 1980s [50a]. In their formulation, Kohn and Sham express the electron density as a linear combination of basis functions and from these functions a determinant is formed which is called Kohn-Sham orbitals [43]. Energy is computed by using electron density from this determinant [43]. Moreover the function of electron density depends on three variables (x, y, z), but the wave function of an n-electron molecule depends on 4n variables (three spatial coordinates and one spin coordinate) [19]. Thus the most important advantage of the DFT calculations is based on its simplicity according to the ab initio methods and the calculation time while it gives the same quality [19, 50a].

The Kohn-Sham equations are similar to the standard HF equation. However the exchange term in HF is changed to the exchange-correlation potential.

The defined electronic energy of a molecule in conjuction with Konh-Sham studies is given by the equation

$$E_e = E_v + E_T + E_J + E_{XC} \tag{2.39}$$

The first term on the right hand side of the equation (2.39) is the potential energy term while the second term defines the kinetic energy due to the electron motion. E_J term is the Coulomb repulsion between the electrons and E_{XC} term is the exchange – correlation energy [51].

Calculating the Coulomb energy of the electrons which are on their own field is hard, but assuming that they move independently and each electron experiences the field because of all electrons [50b] it could be calculated by

$$E_J = \frac{1}{2} \iint \frac{\rho(\vec{r}_1)\rho(\vec{r}_2)}{r_{12}} \, d\vec{r}_1 d\vec{r}_2 \tag{2.40}$$

where the r_{12} is the distance between two electrons.

The exchange correlation functionals involves the difference between classical and quantum mechanical electron-electron repulsion. In addition to the repulsion, it also contains the difference in kinetic energy between the non-interaction system and the real system [21]. Therefore, exchange – correlation energy is defined by the following equation where E_{T_s} refers the interacting system

$$E_{XC}(\rho) = \left[E_T(\rho) - E_{T_s}(\rho)\right] + \left[E_{ee}(\rho) - E_J(\rho)\right] \tag{2.41}$$

Exchange – correlation functional is composed of two parts, the exchange part and the correlation part, hence the traditional definition of the exchange – correlational energy could be written as

$$E_{XC} = E_X + E_C \tag{2.42}$$

Due to the α and β spin densities are contribute to give the exchange energy, exchange energy involves only the electrons of the same spin [44].

$$E_X = E_X^\alpha[\rho_\alpha] + E_X^\beta[\rho_\beta] \tag{2.43}$$

$$E_C = E_C^{\alpha\alpha}[\rho_\alpha] + E_C^{\beta\beta}[\rho_\beta] + E_C^{\alpha\beta}[\rho_\alpha, \rho_\beta] \tag{2.44}$$

where the total density is the sum of the α and β, $\rho = \rho_\alpha + \rho_\beta$, and for a closed shell singlet those are same.

Both of the exchange and correlation energies could be written in terms of energy per particle (ε_X and ε_C) as

$$E_{XC} = \int \rho(r)\varepsilon_{XC}[\rho(r)]dr$$

$$E_{XC} = \int \rho(r)\varepsilon_X[\rho(r)]dr + \int \rho(r)\varepsilon_c[\rho(r)]dr \tag{2.45}$$

This formulation is defined as local density approximation (LDA) [52]. The exchange part of the energy density was given by Dirac exchange energy functional which is defined as

$$\varepsilon_X(\rho) = -C_X \rho(r)^{1/3}$$

$$C_X = \frac{3}{4}\left(\frac{3}{\pi}\right)^{1/3}$$

(2.46)

LDA indicates that the values of ε_{XC} at some position r could be calculated with ρ. Therefore, there is only one requirement for solution, a single-valued ρ at every position [21].

Constructing a gradient-corrected exchange functional to calculate accurate exchange energy was the main objective and Becke in 1988 reported a gradient corrected exchange functional as

$$E_X^{Becke}(\rho) = E_X^{LDA} - b \int \rho^{4/3} \frac{x^2}{1 + 6\beta \sinh^{-1} x} \, dr$$

(2.47)

$$x = \frac{|\nabla \rho|}{\rho^{4/3}}$$

(2.48)

where Becke defined $b = 0.0042$ [53].

2.6.1 Hybrid Functionals

One of the key features of DFT is the incorporation of correlation effects from the beginning unlike HF theory. Furthermore, if the correlation is incorporated into the HF formalism, it causes computational overhead [20]. On the other hand, HF theory provides exact means of treating exchange contribution. Thus adding a correlation energy to the HF energy which is derived from DFT could be an attractive option [20]. However this approach did not work well.

According to the Becke's strategy the exchange correlation energy could be written as

$$E_{XC} = \int_0^1 U_{XC}^\lambda \, d\lambda$$

(2.49)

The coupling parameter λ takes the values from 0 to 1. If it takes the value of 0, it corresponds to a system where there is no Coulomb repulsion between the electrons. Interelectronic Coulomb repulsion is involved if the value of the parameter λ is chosen as 1, which is also corresponds to a real system. Solving this integral could be performed by approximation by using linear interpolation

$$E_{XC} = \frac{1}{2} (U_{XC}^0 + U_{XC}^1) \tag{2.50}$$

Becke's proposition to calculate the exchange correlation energy U_{XC}^1 of a fully interacting real system is the usage of local spin-density approximation.

$$E_{XC}^1 \approx E_{XC}^{LSDA} = \int u_{XC} \, [\rho_\alpha(r), \rho_\beta(r)] dr \tag{2.51}$$

where u_{XC} is the exchange correlation potential density. However Becke recognised that there were some problems when the parameter λ is chosen 0 and according to the Becke's solution the U_{XC}^0 term is removed. As a result HF/DFT exchange correlation functional could be represented by involving an LSDA gradient corrected DFT expression, which is also called hybrid DFT functional [19].

Becke in 1993 developed a hybrid functional based on exchange energy functional which is called Becke3LYP or B3LYP functional [19, 54]. This functional is written as

$$\begin{aligned} E_{XC}^{B3LYP} = (1 - a_0 - a_X)E_X^{LSDA} + a_0 E_X^{HF} + a_X E_X^{Becke} \\ + (1 - a_c)E_C^{VWN} + a_c E_C^{LYP} \end{aligned} \tag{2.52}$$

Where E_X^{LSDA} is the pure DFT LSDA non-gradient corrected exchange functional, E_X^{HF} is the KS-orbital based HF exchange energy functional, E_X^{Becke} is the Becke's exchange functional that developed at 1988, E_C^{VWN} is Vosko, Wilk, Nusair function and E_C^{LYP} is the LYP correlational functional. The a_0, a_X and a_c parameters (typical values are $a_0 = 0.7$, $a_X = 0.2$, $a_c = 0.8$) are those which give the best fit of the calculated energy to molecular atomization energies [19, 44]. This functional is called gradient corrected hybrid functional.

2.6.2 Basis Set

Atomic orbital wave functions which are based on the solution of Schrödinger equation for hydrogen atom could be used in atomic calculations. Due to the absence of a prototype species that occupies a place which is analogous to hydrogen atom, this is not convenient for molecules [19]. Solution to this problem comes from Roothaan's and Hall's studies, which points that MOs could be represented as a linear combination of basis functions [19]. The most popular way is writing each spin orbital as a linear combination of single electron orbitals [20].

$$\psi_1 = c_{11}\phi_1 + c_{21}\phi_2 + \ldots + c_{m1}\phi_m$$
$$\psi_2 = c_{12}\phi_1 + c_{22}\phi_2 + \ldots + c_{m2}\phi_m$$

$$\vdots$$

$$\psi_m = c_{1m}\phi_1 + c_{2m}\phi_2 + \ldots + c_{mm}\phi_m$$

(2.53)

which is also written as

$$\psi_i = \sum_{s=1}^{m} c_{si}\phi_s \qquad i = 1,2,3,\cdots,m \tag{2.54}$$

where ϕ_s represents the basis functions, c_{si} is the coefficient of the sth basis function of corresponding i^{th} MO. The numbers of basis functions are represented by m.

Gaussian functions do not have a cusp at the origin and also they diminish to zero more rapidly according to the Slater functions. However unacceptable errors occur if the Slater type orbital is changed with a single Gaussian function. On the other hand, if linear combinations of Gaussian functions are used to represent the atomic orbitals, the problem would be solved [19, 20]. Therefore the linear combination has the form of

$$\phi_s = \sum_{i=1}^{N} d_{si}\phi_i(\alpha_{si}) \tag{2.55}$$

where d_{is} represents the coefficient of the primitive Gaussian function $\phi_i(\alpha_{is})$ and N is the number of functions.

Thus substitution of equations (2.52) and (2.53) gives

$$\psi_i = \sum_{s=1}^{m} c_{si} \sum_{j=1}^{N} d_{sj} \phi_j(\alpha_{sj}) \qquad i = 1,2,3,\cdots,m \qquad (2.56)$$

2.7 Solvation Effect

Due to the energy interactions between the solute and the solvent, the solute properties depend on vibrational frequencies, total energy and electronic spectrum which depends on the solvent. Moreover the charge seperation within the molecule could be stabilized by solvent. As a result, the solvent could change the not only the energy but also electron density [43]. Solvation effects to a structure or reaction could be visualized by adding the free energy of solvation point to point to the gas-phase PES and define another PES.

Methods to describe the effects of solvent are divided into two types. One of them describes the individual solvent molecules and the other kind treats the solvent as a continuum medium. Moreover, combinations of these kinds are also possible. These kinds could be also divided according to the usage of the classical or the quantum mechanical description. On the other hand, solvent effects could be divided into two parts as specific solvation and short-range effects.

Cavitation energy, which is one of the effects that occurs where the molecule meets the solvent shell, is the required energy to push aside the solvent molecules. Force attraction is another solvent effect which occurs due to the van der Waals, dispersion and hydrogen bonding interactions [43].
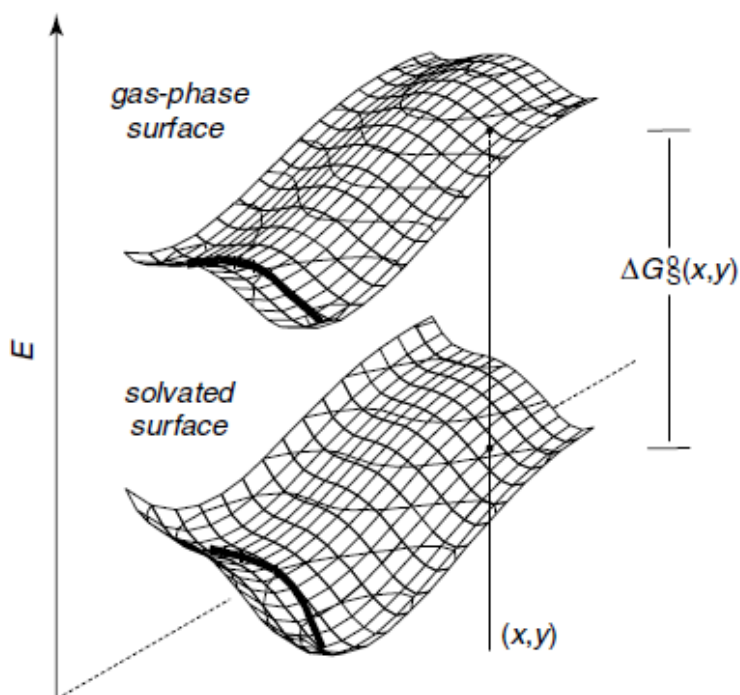
Figure 2.2 : A two dimensional gas-phase PES and the PES that derived from addition of solvation. Thick lines show a chemical reaction [43].

2.7.1 Polarized Continuum Models

Surface boundary approach is a kind of implementation of Poisson equation which was first formalized by Miertus, Scrocco and Tomassi in 1981. This formalization is called polarized continuum model (PCM) [21].

PCM manage the van der Waals surface type cavity and parametrizes the cavity/dispersion contributions based on the area of the surface.

The non-linear Schrödinger equation according to the quantum mechanical continuum models have the formulation of

$$\left(H - \frac{1}{2}V\right)\Psi = E\Psi \qquad (2.57)$$

where V is the general reaction field inside the cavity which depends on wave function. If wave function is expressed as a Slater determinant the orbitals that minimizes the Schrödinger equation could be derived from [21].

$$(F_i - V)\, \psi_i = e_i \psi_i \tag{2.58}$$

where F is the Fock operator.

The difference between the energy in gas phase and the energy in solution gives the electrostatic component of the solvation

$$\Delta G_{ENP} = \left[\langle \Psi^{sol} | H | \Psi^{sol} \rangle + \langle \Psi^{sol} | G_P | \Psi^{sol} \rangle \right] - \langle \Psi^{gas} | H | \Psi^{gas} \rangle \tag{2.59}$$

$$\Delta G_{ENP} = \Delta E_{EN} + G_P \tag{2.60}$$

where ΔE_{EN} is the distortion energy and EN term is associated with the electronic and nuclear components of the total energy [21].

According to PCM model cavity creation in the medium needs energy and electric charge distribution polarize the medium. Therefore the free energy of the solvation is calculated by [44]

$$\Delta G_{solvation} = \Delta G_{cavity} + \Delta G_{dispertion}\, \Delta G_{electrostatic} \tag{2.61}$$

Choosing the cavity as spherical is the simplest reaction field model where only the dipole moment and the net charge are considered while the cavity/dispersion effects are ignored. Thus Born model is given by [44]

$$\Delta G_{el}(q) = -\left(1 - \frac{1}{\varepsilon}\right) \frac{q^2}{2a} \tag{2.62}$$

where q is the net charge, a is the radius of cavity, ε is the dielectric constant.

2.8 Population Analysis

Partitioning the wave function or the electron density into charges on the nuclei and bond orders are performed by a mathematical way which is called population analysis. The results that are obtained from population analysis are those which can not be observed by experiments. For example due to the lack of physical property, atomic charges could not be observed experimentally. On the other hand abstraction of electron density and the nuclear charges on each atom to partial charges is helpful to understand electron density distribution [43]. Thus, predicting the sites where nucleophilic or electrophilic attack could occur would be easy to predict.

2.8.1 Natural Bond Order (NBO) Analysis

Natural bond order analysis involves a set of analysis techniques. Natural population analysis is one of them and it is performed to obtain occupancies and charges NBO uses natural orbitals instead of molecular orbital [43]. The eigenfunctions of first order which reduces density matrix are the natural orbitals [43]. Natural orbitals could be used to derive atomic charges and molecular bonds by distribute the electrons into atomic and molecular orbitals. The shape of the atomic orbitals is defined by the one electron density matrix by performing Natural Atomic Orbital and Natural Bond Orbital analysis [44].

The electron density is calculated from the wave function by

$$|\Psi|^2 = \Psi * \Psi \tag{2.63}$$

Therefore the reduced density matrix of order k, γ_k, is defined by

$$\gamma_k(r_1', r_2', \dots, r_k', r_1, r_2, \dots, r_k)$$

$$= \binom{N}{k} \int \Psi^*(r_1, r_2, \dots, r_k, r_{k+1}, \dots, r_N) \, \Psi(r_1, r_2, \dots, r_k, r_{k+1}, \dots, r_N) dr_{k+1} \dots dr_N \tag{2.64}$$

The integration of first order density matrix over the coordinate 1, yields the number of electrons. The first order density matrix could be diagonalized and Natural Orbitals and Occupation Numbers could be found [43]. The occupation number of the natural orbitals could be eighter 0 or 2.

The first step in NBO analysis is localization of natural atomic orbitals which are associated almost entirely with a single atom [21]. The second step involves the localization of orbitals that contains bonding/antibonding between pairs by the usage of the basis set AOs of the corresponding atoms [21, 43]. The last step in analysis is, identification of Rydberg-like orbitals and orhogonalization of orbitals with each other [21, 43]. Therefore, all of the NAOs (and also Rydberg orbitals) are described by the basis set AOs of a single atom and all of the NBOs are described by the basis set AOs of two atoms [21]. Moreover, characterization of three center bonds would be performed by decomposition into three body orbitals.

2.9 Potential Energy Surface (PES) and Conformational Analysis

Potential energy surface (PES) is a kind of graphical representation of the Born-Openheimer (BO) potential energy function that links key chemical concepts and basic geometrical features of any given molecule, molecular complex or a chemical reaction [50c]. The minima of a potential energy surface is the minimum energy conformations and the saddle points are the transition state. For this reason both of the minima and the saddle points are really important. The local minimum which represents the minimum energy conformation is defined by the atomic arrangements where the gradient of potential energy function vanishes [50c]. On the other hand saddle points are like the top of a mountain that would be passed from one valley to another [50c].

Small distortions not only in bond angles but also in the bond lengths cause the interconvertion of the arrays of the atoms of a molecule which determines the conformations of that molecule [20, 50d]. Furthermore three dimensional structures of a molecule, define the physical, chemical and also biological properties of a molecule [50d]. In biochemical researches determining a protein structure is important, thus finding the lowest energy conformer, which is the most stable conformer, is also important. In order to find the lower energy shape of geometry a local minimum of the conformer should be found [43, 50e]. Besides the conformational differences are really important drug chemistry due to the importance of using the lowest energy conformer to prevent the deformations from the conformations [50d].

Determining the most stable conformations and transition states between the conformers could be analyzed by conformational search [50e]. The aim of a conformational analysis is identifying the dynamics of atomic motion characteristic of the conformational behavior of a molecule [50c]. Conformations of a molecule involve all of the low energy minimas on the PES. Therefore the conformational search could be referred as searching the local minimas or the low energy saddle points on the PES [50c]. Moreover the conformational analysis could be referred as the study about the conformations which affect a molecule's properties [20, 50d]. Although the earliest and the simplest conformational ideas have been performed by

Sachse and Bischoff in 1890, the modern conformational analysis has been developed by D. H. R. Barton at 1950 [20, 50d, 55].

Energy minimizations have a big role in conformational analysis. That's why having a seperate algorithm is necessary to find the minimas on energy surface [20]. The energy of conformations could be calculated by ab initio, semiemprical and also MM methods. The method that is chosen to calculate the conformational energy is depends on not only the size of the molecule but also the required accuracy of the energies according to the availability of parameters [50e]. On the other hand, there could be lots of minimas on a energy surface while the Boltzmann function (K= exp($\Delta G/RT$) controls the distribution of the conformers of a conformational space [20, 50d]. In that case it is preferred to find all the accessible minimas [20].

2.10 Computational Details

The conformer analysis for the PLP – 5-amino-2 fluorocyclohex-3-enecarboxylic acid complex model structure was performed at PM3 level of theory using Spartan 04 programme [47, 56]. The first five lowest energy structures were chosen for further optimization. All of the structures; reactants, intermediates, transition states and products along the reaction path were optimized at the B3LYP/6-31+G(d,p) using Gaussian 03 programme [57]. The model compound and the intermediates formed along the reaction coordinate are changed species. Therefore, diffused functions are added to the basis set. Since the path is included proton transfers, addition of one set of p primitives to hydrogen atoms is inevitable. Once the lowest energy conformer for PLP – 5-amino-2 fluorocyclohex-3-enecarboxylic acid complex is determined, the proposed reaction mechanisms were modeled. To observe the charge distribution of the conformers and also the structures on the mechanism NBO analysis was performed. The single point energy calculations were carried out in order to determine the solvent effect with Integral Equation Formalism PCM (IEFPCM) methodology as implemented in G03 at 6-31+g(d,p) level of theory [58]. Both water (ε=78.39) and diethylether (ε =4.335) were used as a solvent in order to mimic the highly and moderately polar types of surroundings of the active site. The molecular cavity is build up with UFF radii which uses UFF force field. By choosing this model, a sphere around each solute atom with the radii scaled by a factor of 1.1 is placed where the explicit hydrogens have individual spheres.

3. RESULTS AND DISCUSSION

The two proposed mechanism for inactivation of GABA-AT; namely Michael addition and Aromatization mechanisms have common steps at the beginning where the PLP-substrate complex is formed, proton abstraction occurs and fluorine is eliminated. These steps are grouped under the heading of Fluorine Elimination (**Figure 3.1**, Mechanism 1). Once the fluorine is eliminated, the inactivation mechanism either follows Michael addition or Aromatization paths. Michael Addition path have several alternatives regarding the native of the assistant molecules used in the addition mechanism (**Figure 3.1**, Mechanism 2). In conjunction with the literature, two different types of aromatization mechanisms can be proposed for the carbinolamine formation step. In the first one, the proton abstraction from structure **15** occurs which is followed by the proton transfer to quinonoid (structure **17**) to form carbinolamine (**Figure 3.1**, Mechanism 3a) [13, 59]. The second one differs in the sequence of the steps where the proton abstraction from structure **15** involves the carbinolamine formation via proton transfer to structure **15** and proceeds with a proton abstraction from structure **21** (**Figure 3.1**, Mechanism 3b) [14].
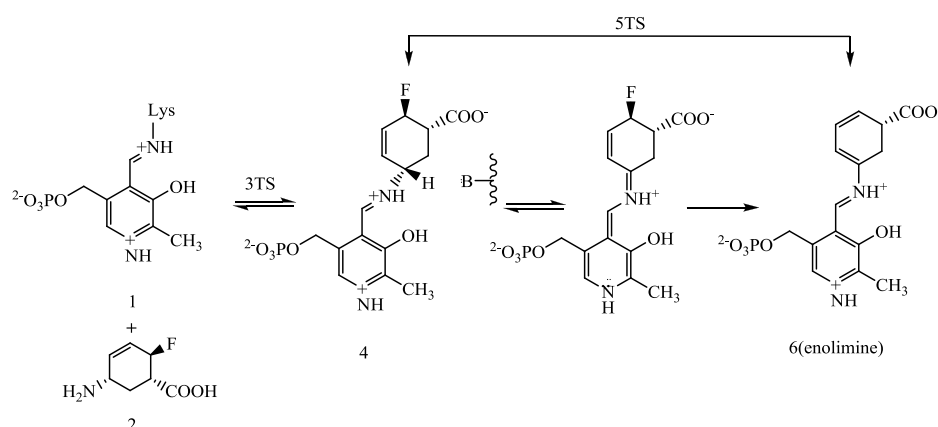
Mechanism 1

Figure 3.1 : Schematic representation of inactivation mechanisms of GABA-AT with 5-amino-2 fluorocyclohex-3-enecarboxylic acid. **Mechanism 1.** Fluorine elimination from PLP-5-amino-2 fluorocyclohex-3-enecarboxylic acid complex.

32

Mechanism 2

6(enolimine)   15(quinonoid)   17(quinonoid)   19(carbinolamine)

Mechanism 3a

6(enolimine)   15(quinonoid)   21(carbinolamine)   19(carbinolamine)
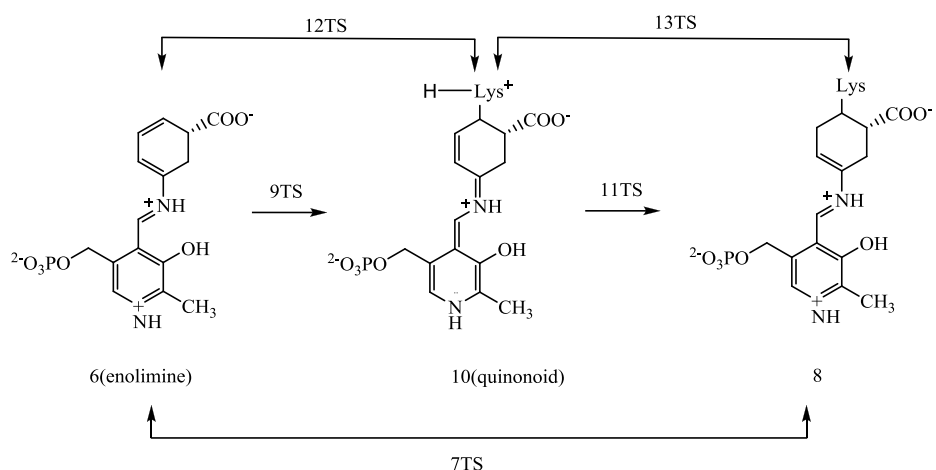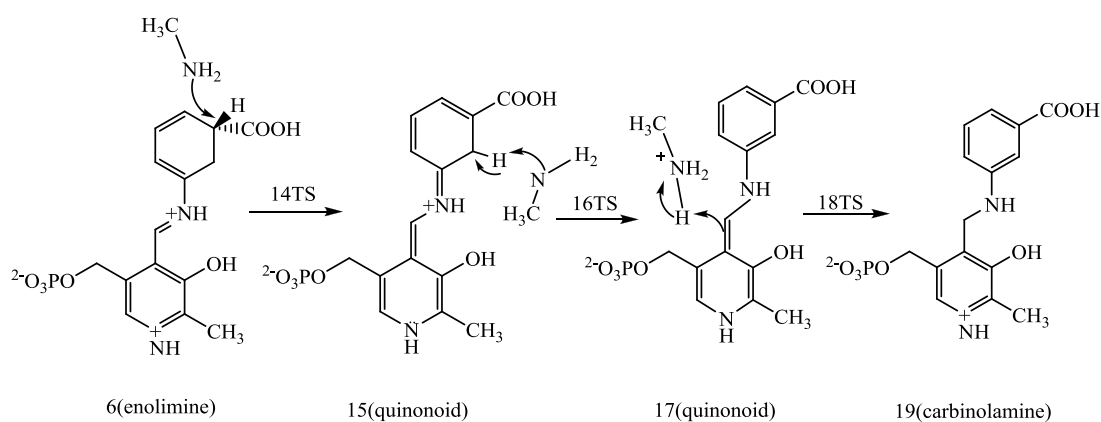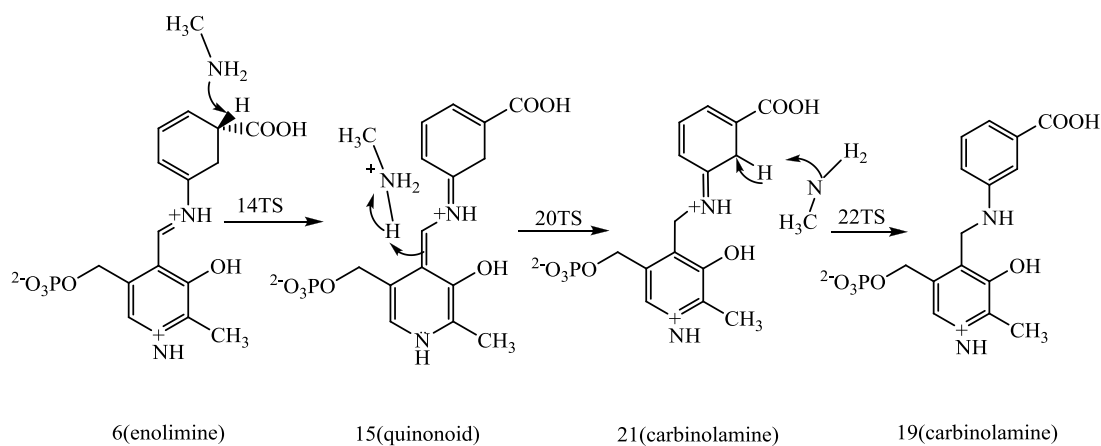
Mechanism 3b

Figure 3.1 : (continued) Schematic representation of inactivation mechanisms of GABA-AT with 5-amino-2 fluorocyclohex-3-enecarboxylic acid. **Mechanism 2.** Inactivation via Michael Addition Meachanism **Mechanism 3a.** Inactivation via Aromatization Mechanism − 1. **Mechanism 3b.** Inactivation via Aromatization Mechanism − 2.

3.1 Model Structures

In order to mimic the inactivation mechanism of GABA – AT with 5-amino-2 fluorocyclohex-3-enecarboxylic acid, model structures are used. In this study Lysine329 (Lys329), attached to PLP, has been represented as a methylamine (**Figure 3.2a**) . This method of representing PLP dependent enzymes is common and widely accepted in literature [60]. Also, the phosphate group on PLP was replaced with a methyl group which is also widely used application (**Figure 3.2b**) [8,10,60]. Moreover, to model the threonine assisted stepwise Michael Addition mechanism 2-propyl alcohol is used to mimic Threonine353 (Thr353) (**Figure 3.2c**). Although being in the sequence of the other monomer, Thr353 is close to the active site based on the crystal structure (**PDB code: 1OHV**). The distance between the nitrogen at the side chain of Lys329 and the oxygen at the side chain of Thr353 is 3.791 Å (**Figure 1.2**). It was also suggested that the hydroxyl group of Thr353 could be a candidate for deprotonation of the substrate ammonium ion due to its closeness to the phosphate group of PLP [18].


(a) (b) (c)
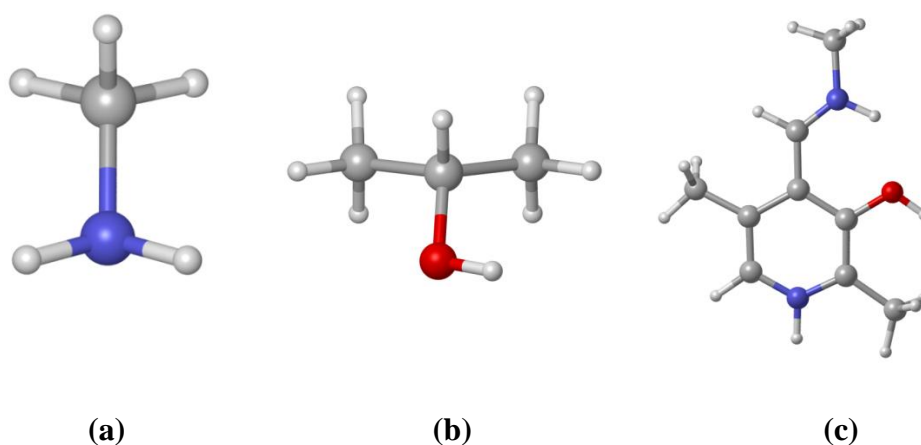
Figure 3.2 : Three dimensional geometries of model structures. **a)** Methylamine as Lys329. **b)** 2-propyl alcohol as Thr353. **c)** PLP-methylamine complex as PLP-Lys329 complex.

3.2. Conformational Analysis

Conformational analysis was performed for the PLP-5-amino-2-florocyclohex-3-enecarboxylic acid complex (**4**) using semiemprical method PM3 implemented in the Spartan 04 programme. The first five lowest energy conformers were chosen for further optimization at high level of theory. The frequency and energy calculations

for these conformers has been performed with B3LYP/6-31+G(d,p) level. The two lowest energy conformers are depicted in **Figure 3.3**. The energy difference between the two lowest energy conformers is found to be 5.71 kcal/mol. The main structural difference between these conformers is the position of carboxyl hydrogen. The dihedral angle H20 – O19 – C17 – O18 has a value of 0.4^0 in the lowest energy conformer, where it changes to -176.4^0 in the second lowest energy conformer.


(a)

(b)
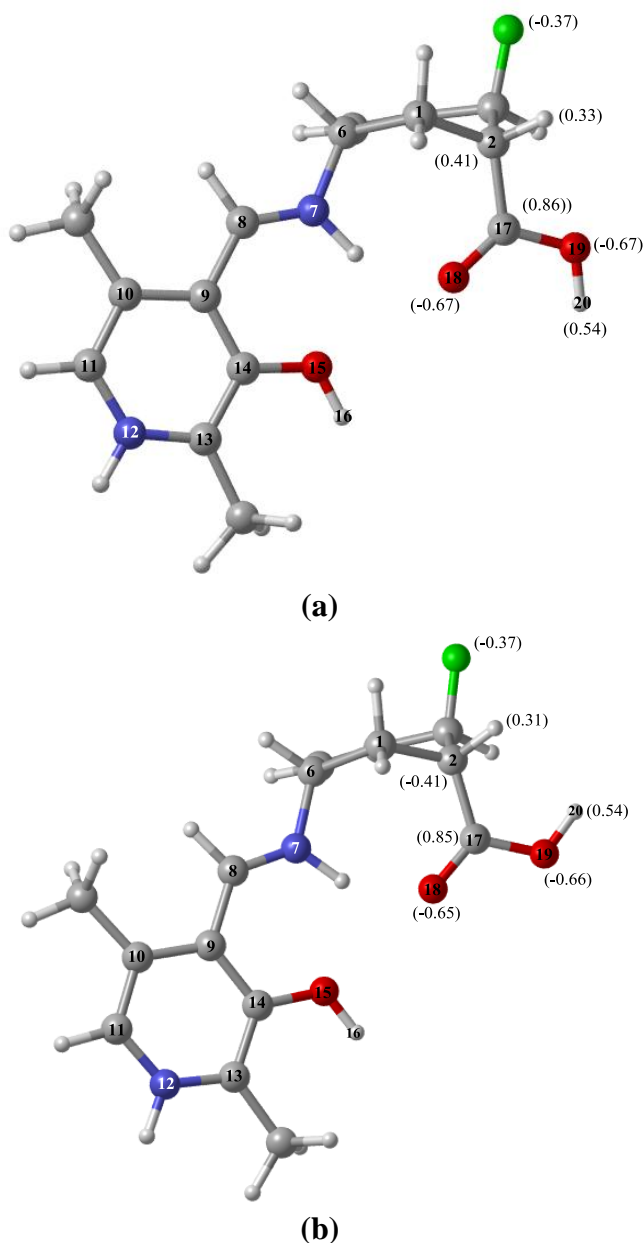
Figure 3.3 : Three dimensional geometries of optimized (B3LYP/6-31+G(d,p)) geometries of PLP-5-amino-2 fluorocyclohex-3-enecarboxylic acid complex **(4) a)** The lowest energy conformer. **b)** The second lowest energy conformer. NBO charges are shown in parenthesis.

3.3 Fluorine Elimination

Fluorine elimination mechanism starts with the formation of PLP – substrate complex as Lys – 329 leaves the PLP. In this step N7 of substrate **(2)** attacks nucleophilically to the C8 of methylamine – PLP complex **(1)** (**Figure 3.4a**). The formation of a bond between N7 and C8 and a proton transfer from N7 to N25 on methylamine occurs simultaneously. In the transition state, **3TS**, the N7 – C8 – N25 is 94.8^0 and the N7 – C8 distance is 1.503 Å (**Figure 3.4c**). In addition, the N7 – H27 and N25 – H27 distances are 1.309 Å, 1.353 Å respectively. The transition state structure (**3TS**) is determined with one imaginary frequency having a value of -1603.92. The relative free energy barrier for the transition state (**3TS**) is found to be 23.7 kcal/mol. The transition state (**3TS**) was also validated with intrinsic reaction coordinate (IRC) calculations. The reverse IRC calculation produced an intermediate structure namely methylamine – PLP – substrate complex instead of the two reactants (**Figure 3.4a**). The forward IRC calculations pointed out a different PLP – substrate conformer (**Figure 3.4b**) then the conformational analysis results. However, further optimization after the removal of methylamine produced a compatible geometry.

(a)   **(b)**
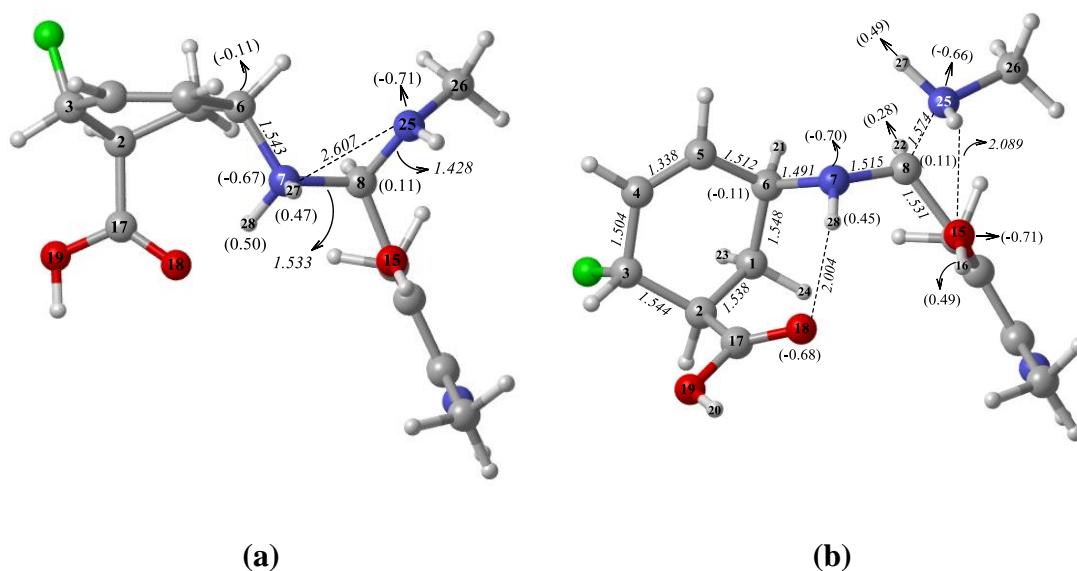
Figure 3.4 : Three dimensional geometries of formation of PLP-5-amino-2-fluorocyclohex-3-enecarboxylic acid complex (structure **4**). **a)** Structure 1-2 Complex before transition state formation. **b)** Geometry optimization result from forward IRC calculation. NBO charges are shown in parenthesis.
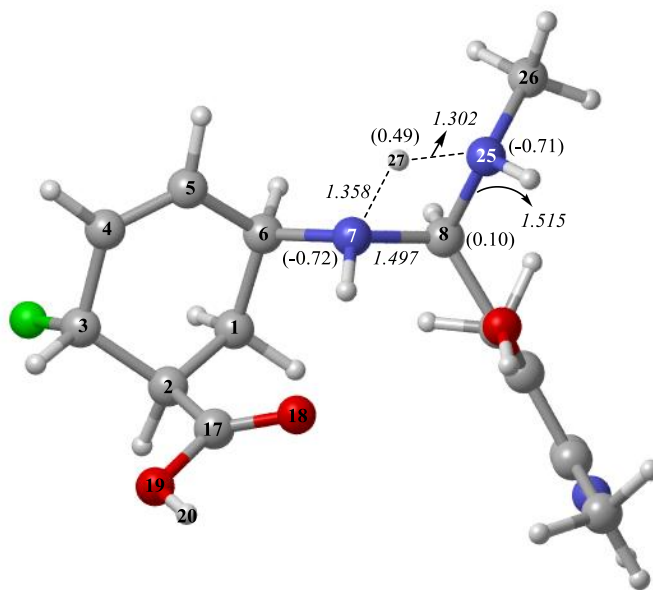
(c)

Figure 3.4 : (continued) Three dimensional geometries of formation of PLP-5-amino-2-fluorocyclohex-3-enecarboxylic acid complex (structure **4**). **c)** Transition state (**3TS**) of fluorine containing PLP – 5 – amino – 2 – florocyclohex complex. NBO charges are shown in parenthesis.

In literature stepwise mechanism is proposed for the HF elimination step. However, calculations have revealed that a water assisted concerted mechanism (**Figure 3.5a**) is the most probable path. In transition state (**5TS**), the oxygen of water (**O30**) is found at to be at a distance of 1.155 Å from H21 of C6 with an angle O30 – H21 – C6 of 159.8^0.   While the proton is transferred to the water, the single bond between fluorine atom and C3 breaks, and the lone pairs of fluorine atom interacts with the O30 – H31 antibonding orbital via O30 – H31 – F angle of 153.3^0. The NBO second order stabilization energy is found to be 22.35 kcal/mol for this interaction. Due to the HF elimination, C3 – C4 and C5 – C6 single bonds (1.507 Å and 1.515 Å respectively) turn to double bonds (1.368 Å and 1.380 Å respectively) while the C4 – C5 double bond with the distance of 1.338 Å lengthens to single bond with the distance of 1.427 Å. Moreover, the C8 – N7 – C6 – C5 dihedral angle alters to -10.4^0 in structure **6** (**Figure 3.5b**) **,** from -105.5^0 in structure **4**. The relative free energy barrier for this transition state (**5TS**) was calculated as 27.8 kcal/mol. The reaction is highly exergonic. The energy profile for fluorine elimination mechanism is depicted in **Figure 3.6**.
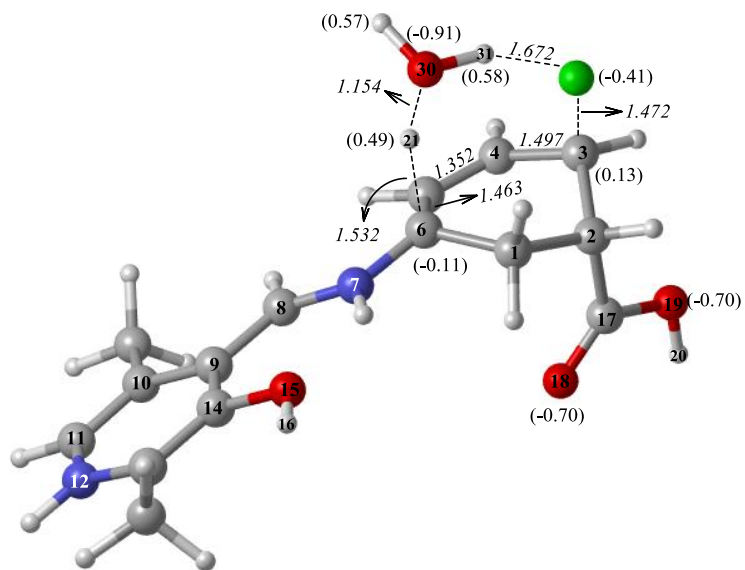
(a)
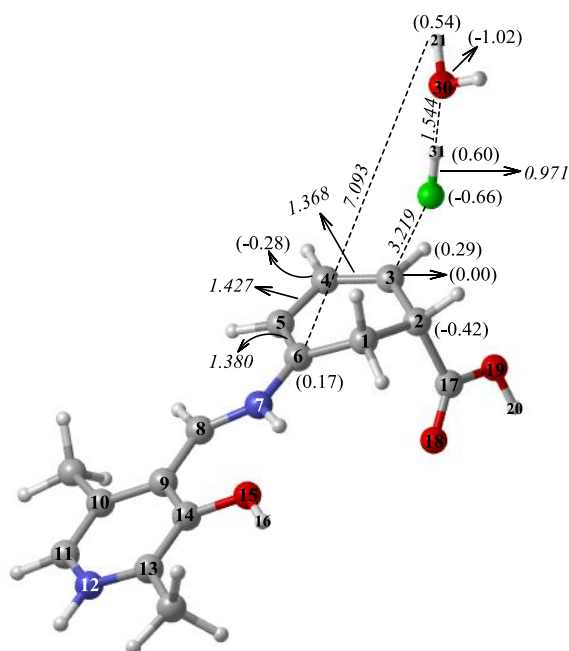
(b)

Figure 3.5 : Three dimensional geometries of fluorine elimination in a concerted way. **a.** Transition state (**5TS**) with water assistance. **b.** Geometry optimization result from forward IRC calculation of 5TS. NBO charges are shown in parenthesis.
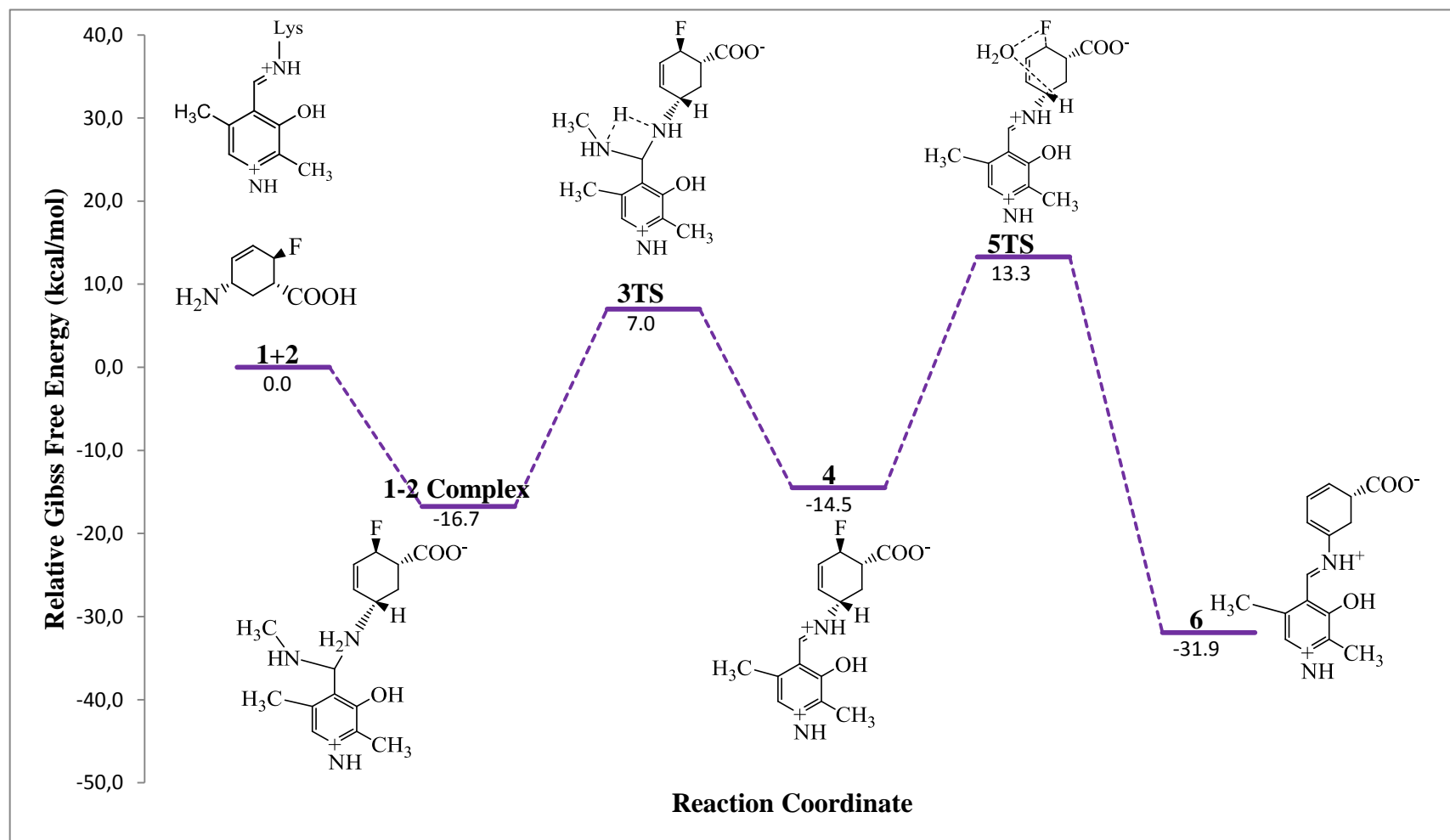
Figure 3.6 : Energy profile for fluorine elimination mechanism. Relative Gibbs free energies are given as kcal/mol.

3.4. Michael Addition

Based on the experimental findings, formation of amine bond between enolamine (**6**) and proton transfer in the presence of Lys329 via Michael addition is proposed as stepwise mechanism. [14] On the other hand, the mechanism is modeled not only as stepwise but also concerted path. The concerted mechanism is modeled using only the side chain of Lys329 which is methylamine in the model structure. The stepwise mechanism is modeled with the assistance of either water or Threonine (Thr353) which is represented as 2-propyl alcohol in the model structure. Thr353 is chosen due to its closeness to the active site although it is in the sequence of the other monomer.

In the case of concerted mechanism, the N25 of methylamine attacks nucleophilically to C3 of structure **6** while one of the protons of amino group transfers to the C4. The bond formation between the N25 and C3 was seen at a distance of 1.518 Å with an angle N25 – C3 – C4 of 96.8^0 (**Figure 3.7a**). The proton transfer was achieved with the N25 – H27 distance of 1.461 Å and the H27 – C4 distance of 1.344 Å while the N25 – H27 – C3 angle is 108.9^0. Formation of enolimine (structure **8a**, **Figure 3.7b**) while methylamine forms a secondary amine via Michael addition with concerted mechanism has an energy barrier of   32.0 kcal/mol. The energy profile of both the concerted, water and Threonine assisted mechanisms are shown in Figure **3.8**.

| (a) | (b) |
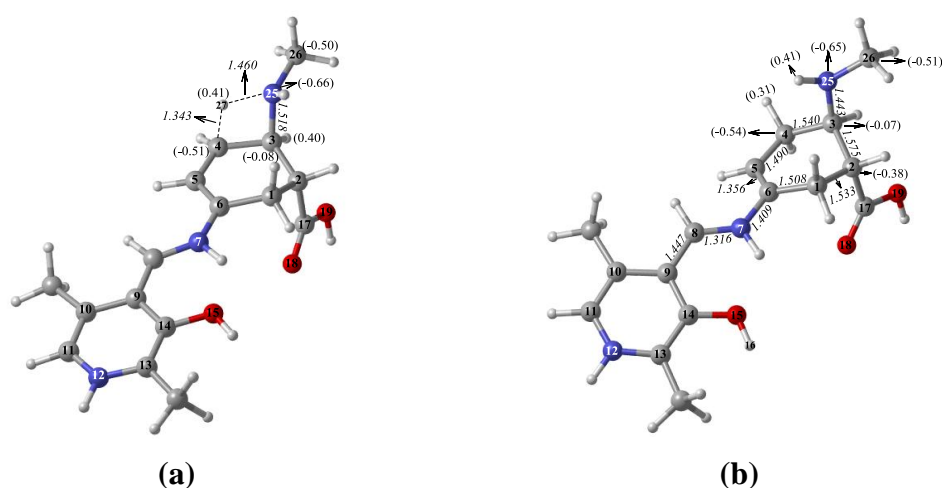
Figure 3.7 : Three dimensional geometries of Michael Addition mechanism via concerted mechanism. **a.** Transition state of N25-C3 bond formation and the proton transfer (**7TS**). **b.** Structure **8a**. NBO charges are shown in parenthesis.
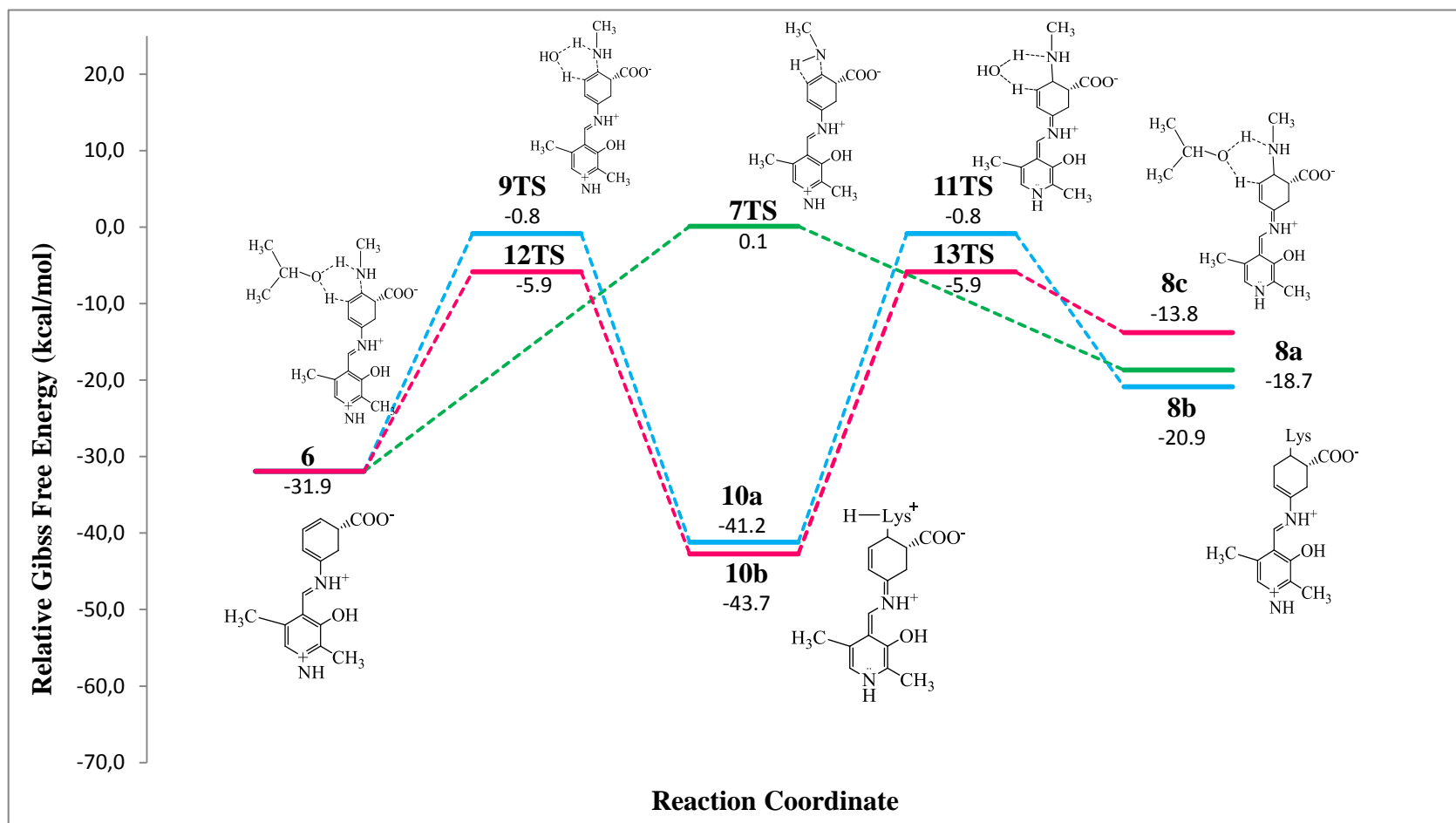
Figure 3.8 : Energy profile of inhibition via Michael Addition mechanism in gas phase. ─ : Water assisted stepwise mechanism. ─ : Thr353 assisted stepwise mechanism. ─ : Concerted mechanism

In the water assisted stepwise mechanism, first the N25 of methylamine forms a single bond with C3 of structure **6**. Incorporation of water was performed with an angle C3 – N25 – O30 of 92.9^0 and the bond formation is achieved at a C3 – N25 distance of 1.505 Å. Furthermore, lone pairs of O30 interact with H27 of methylamine at a distance of 1.051 Å with an NBO second order stabilizing energy of 322.74 kcal/mol. Although the distance of O30 – H31 is 1.278 Å and H31 – C4 is 1.360 Å, the [1,3] proton transfer is not seen during this step (**9TS**, **Figure 3.9a**). The results are validated with IRC calculations. The energy barrier of this transition state which leads the formation of structure **10** (**Figure 3.9b**) was calculated as 31.1 kcal/mol.

(a) **(b)**
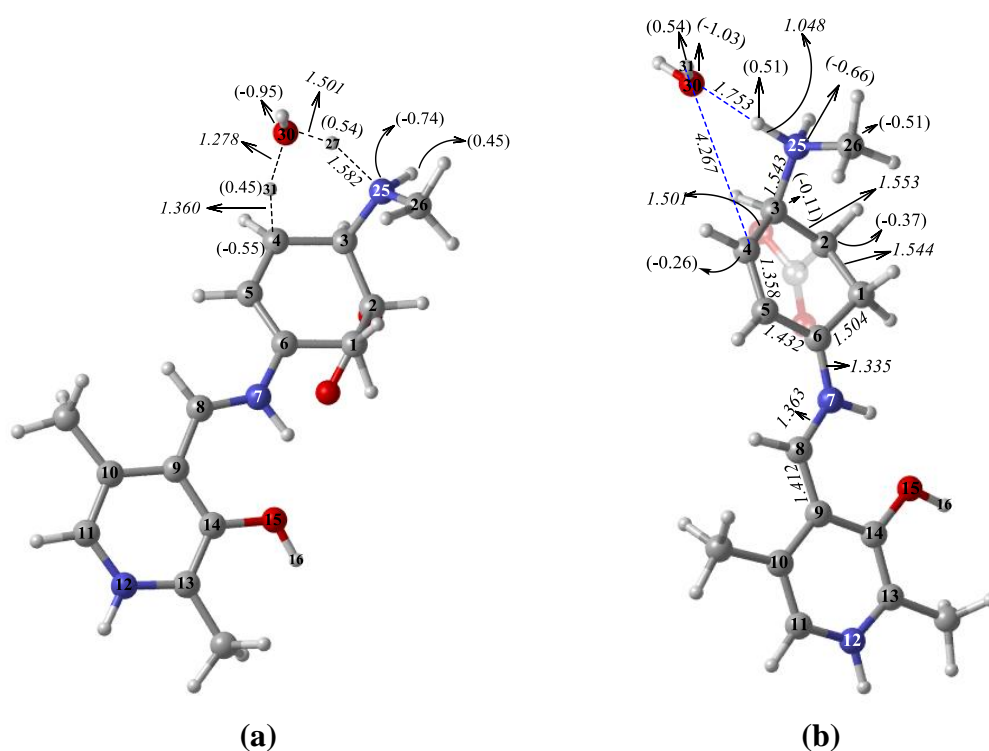
Figure 3.9 : Three dimensional geometries of water assisted Michael addition mechanism. **a.** Water assisted bond formation between N25 and C3 (**9TS**). **b.** Quinonoid (structure **10a**) from geometry optimization of forward IRC calculation of **9TS**. NBO charges are shown in parenthesis.

In the second step of water assisted Michael addition mechanism, [1,3] proton transfer is achieved. The geometrical parameters for the elimination of one proton from N25 and transfer of proton from water to C4 can be seen in **Figure 3.10**. Both of the bonding and antibonding orbitals of C4 – C5 interact with the transferring proton (H31). The NBO second order stabilizing energies of the corresponding

interactions are found to be 281.25 kcal/mol and 200.24 kcal/mol respectively. Moreover the NBO second order stabilizing energy of the interaction between lone pairs of O30 and H31 is found to be 200.24 kcal/mol. The transition state (**11TS**)(**Figure 3.10a**) which has an energy barrier of 40.4 kcal/mol, results the transformation of the C4 – C5 double bond with the distance of 1.353 Å to single bond with the distance of 1.473 Å and C5 – C6 single bond with the distance of 1.439 Å to double bond with the distance of 1.362 Å. Thus the double bond between C6 – N7 (1.335 Å changes to 1.396 Å) shifts to N7 – C8 (1.363 Å changes to 1.318 Å). The transition state for this step yields structure **8b** (**Figure 3.10b**), which is also validated with geometry optimization of forward IRC result of **11TS**.


(a)　　　　　　　　　　　　　**(b)**
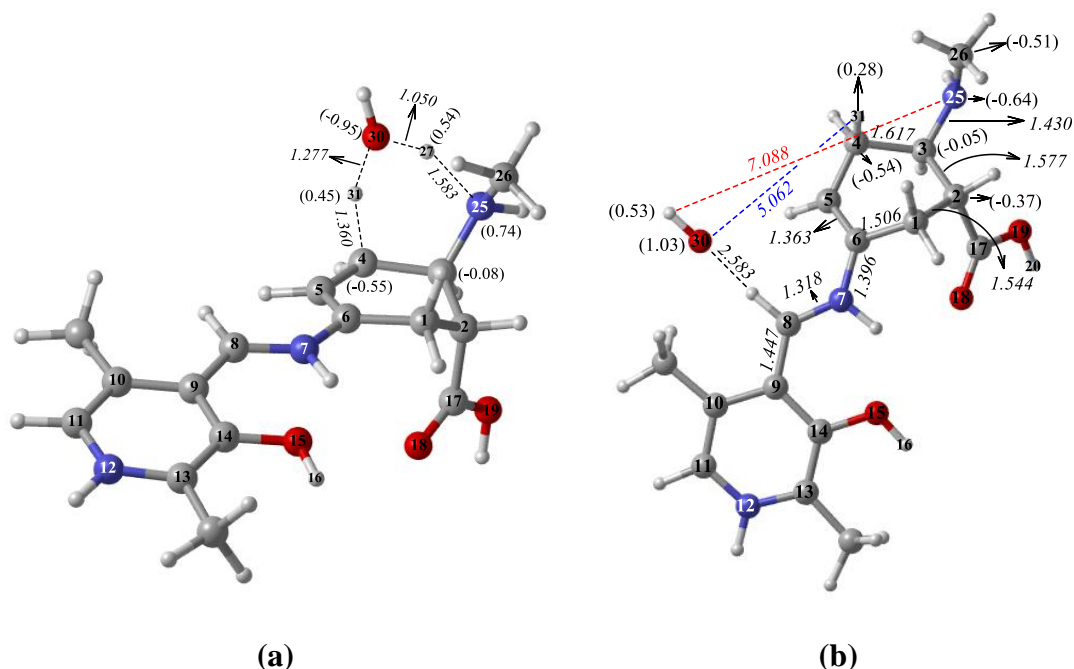
Figure 3.10 : Three dimensional geometries of water assisted Michael addition mechanism. **a.** Water assisted [1,3] proton transfer (**11TS**). **b.** Structure **8b** from geometry optimization of forward IRC calculation of **11TS**. NBO charges are shown in parenthesis.

The stepwise mechanism was also studied with the assistance of Thr353 (2-propyl alcohol). The first step of Thr353 assisted mechanism resembles the water assisted one. Instead of using water, N25 – C3 bond formation is achieved via the usage of 2-propyl alcohol (**12TS**, **Figure 3.11a**). The achievement of bond formation with an angle C3 – N25 – O32 of 92.0^0 and the distance C3 – N25 of 1.490 Å that yields transformations of C3 – C4 and C5 – C6 double bonds (1.368 Å and 1.380 Å respectively) to single bonds (1.509 Å and 1.439 Å respectively) and C4 – C5 single

bond with the distance of 1.426 Å to double bond with the distance of 1.352 Å. Moreover, lone pairs of O33 interacts with H27 of methylamine with an NBO second order stabilizing energy of 391.09 kcal/mol. Transition state of N25 – C3 bond formation via threonine assisted mechanism has a free energy barrier of 26.1 kcal/mol which is smaller than both the concerted and water assisted mechanisms. The result is validated with IRC calculations where the geometry optimization of forward IRC calculation of **12TS** yields structure **10** and 2-propyl alcohol (**Figure 3.11b**).

(a)   (b)
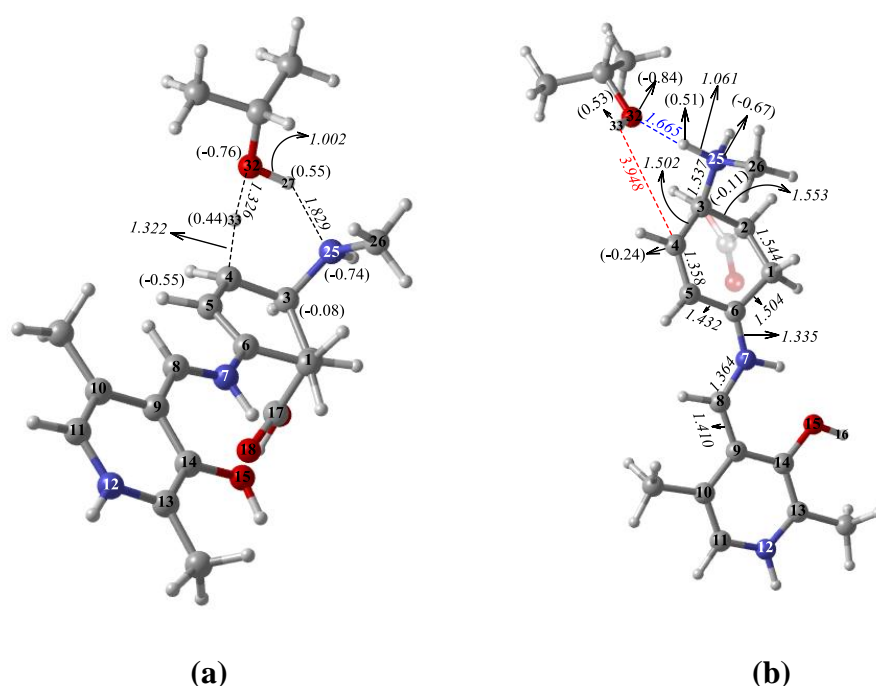
Figure 3.11 : Three dimensional geometries of Threonine assisted Michael addition mechanism **a.** 2-propyl alcohol assisted bond formation between N25 and C3 (**12TS**). **b. S**tructure **10b** from geometry optimization of forward IRC calculation of **12TS**. NBO charges are shown in parenthesis.

The last step of threonine assisted mechanism, [1, 3] proton transfer step (**13TS, Figure 3.12a**), is achieved with an approximation of 2-propyl alcohol where the O32 – H27, H33 – O32 and H33 – C4 distances being 1.829 Å, 1.327 Å, 1.323 Å respectively. H27 of N25 in methylamine transfers to the O32 with an angle N25 – H27 – O32 of 141.3^0 and the H33 of O32 transfers to C4 with an angle O32 – H33 – C4 of 152.4^0. These proton transfers at the dihedral angle C3 – N25 – O32 – C4 of 10.4^0 results the transformation of the C4 – C5 double bond (1.358 Å) to single bond (1.481 Å) and the C5 – C6 single bond (1.432 Å) to double bond (1.359 Å).

Moreover, the bonding and antibonding orbitals of C4 – C5 interact with the transferring proton (H33) with the NBO second order stabilizing energies of 179.47 kcal/mol and 251.78 kcal/mol respectively. Also it is found that the lone pairs of O33 interacts with the H33 with an NBO second order stabilizing energy of 162.43 kcal/mol. Formation of structure **8c** (**Figure 3.12b**) via threonine assisted transition state requires a free energy of 37.8 kcal/mol which is smaller than the water assisted mechanism.

<center>(a)   (b)</center>
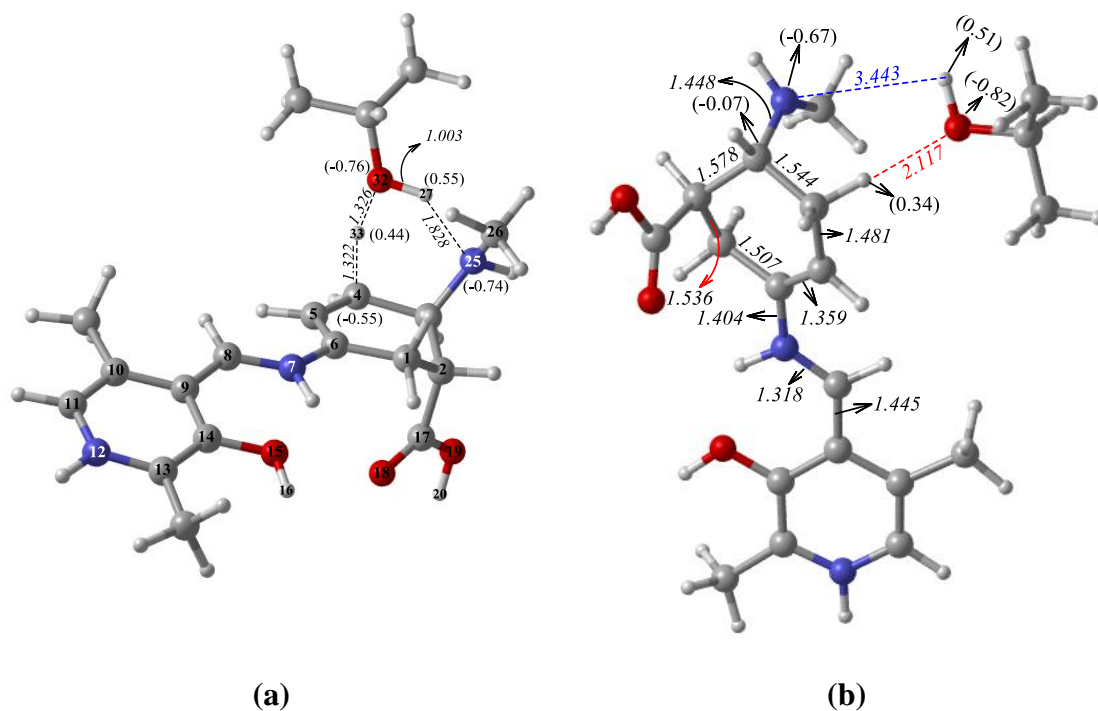
Figure 3.12 : Three dimensional geometries of threonine assisted Michael addition mechanism **a.** 2-propyl alcohol assisted [1,3] proton transfer (**13TS**). **b.** Structure **8c** from geometry optimization of forward IRC calculation of **13TS**. NBO charges are shown in parenthesis.

According to the gas phase calculations, the threonine assisted Michael addition mechanism has lower relative Gibbs free energy barriers than the water assisted mechanism. When the reaction free energy profile is analyzed in detail, it is seen that the activation energy barrier of concerted mechanism is lower than the activation energy barriers of second step of Threonine assisted mechanism. However the gained energy from the previous step is sufficient to overcome the barrier of later step. Incorporation of one water molecule does not lower the energy barrier relative to the concerted one. Moreover, water assisted mechanism proceeds to the structure **10a** with almost the same energy barrier as in the concerted mechanism which produces

the final product **8a**. On the contrary threonine assistance lowers the energy barrier by 5.1 kcal/mol according to the water assisted mechanism while it proceeds to structure **10b.** As a result of gas phase calculations, the threonine assisted mechanism is found to be the most plausible mechanism for the inactivation of GABA-AT with 5-amino-2-fluorocyclohex-3-enecarboxylic acid.

3.5. Aromatization Mechanisms

Aromatization mechanism may proceed via two different paths where the sequence of formation of carbinolamine is the main difference between those paths. There are two proton abstraction and one proton transfer steps in both paths. Although the first proton elimination is common, the second proton elimination and proton transfer steps are switched in the alternative path. Methylamine is used as the proton acceptor in proton elimination steps while protonated methylamine is used as proton donor in both of the paths.

Aromatization mechanisms start with the proton elimination from α carbon (C2) of the substrate. In this step methylamine is used as the proton acceptor where the H22 is transferred to N25 at a C2 − H22 distance of 1.286 Å and H22 − N25 distance of 1.498 Å (**14TS, Figure 3.13a**). While the proton is transferred to N25, the double bond with a distance of 1.368 Å between C3 − C4 turns to the single bond having a value of 1.444 Å. Moreover, the double bond between C5 − C6 shifts to C6 − N7 where C5 − C6 bond length changes from 1.380 Å to 1.425 Å. This double bond shift leads to the formation of quinonoid intermediate **15** (**Figure 3.13b**). Additionally due to the charge delocalization alterations within the ring, C2 − C3 single bond (1.500 Å) to shortens to double bond (1.354 Å). Relative Gibbs free energy barrier for this transition state is found to be 8.0 kcal/mol.
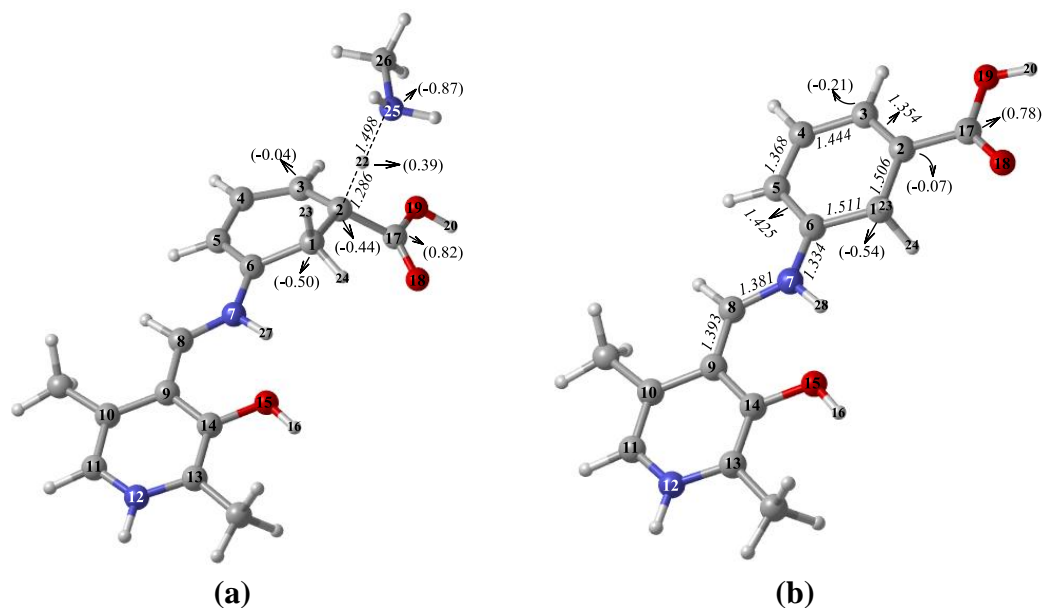
Figure 3.13 : Three dimensional geometries of proton abstraction as the first step of Aromatization mechanisms **a.** Transition state of proton transfer to Lys329 (**14TS**). **b.** Optimized geometry of structure **15**. NBO charges are shown in parenthesis

3.5.1. Aromatization via Mechanism 3a

After formation of structure **15**, the next step in Mechanism 3a is the proton abstraction from the structure **15**. Methylamine is used as a proton acceptor in this step. Surprisingly, two different transition state structures is found relative to the position of methylamine. The energy profile of Aromatization path via the Mechanism 3a is shown in **Figure 3.14**.

In the first transition state structure, (**16TSa**, **Figure 3.15a**) methylamine is approaching to structure **15** with C1 − H23 and H23 − N25 distances having values 1.359 Å and 1.388 Å respectively. In addition the C1 − H23 − N25 − C29 dihedral angle and C1 − H23 − N25 angle having values -101.3^0 and 168.7^{0}respectively determines the position of methylamine in Cartesian space. The transition state is determined with one imaginary frequency having a value of -1156.97 and has a relative energy barrier of 9.4 kcal/mol. The accuracy of this step is validated with the IRC calculations where the transition state produces protonated methylamine and structure **17** with a relative energy of -87.4 kcal/mol (**Figure 3.15b**). The C1 − H23 distance is 2.908 Å, the dihedral angle C1 − H23 − N25 − C29 is -113.3^0 and the angle C1 − N25 − C29 is 121.1^0.
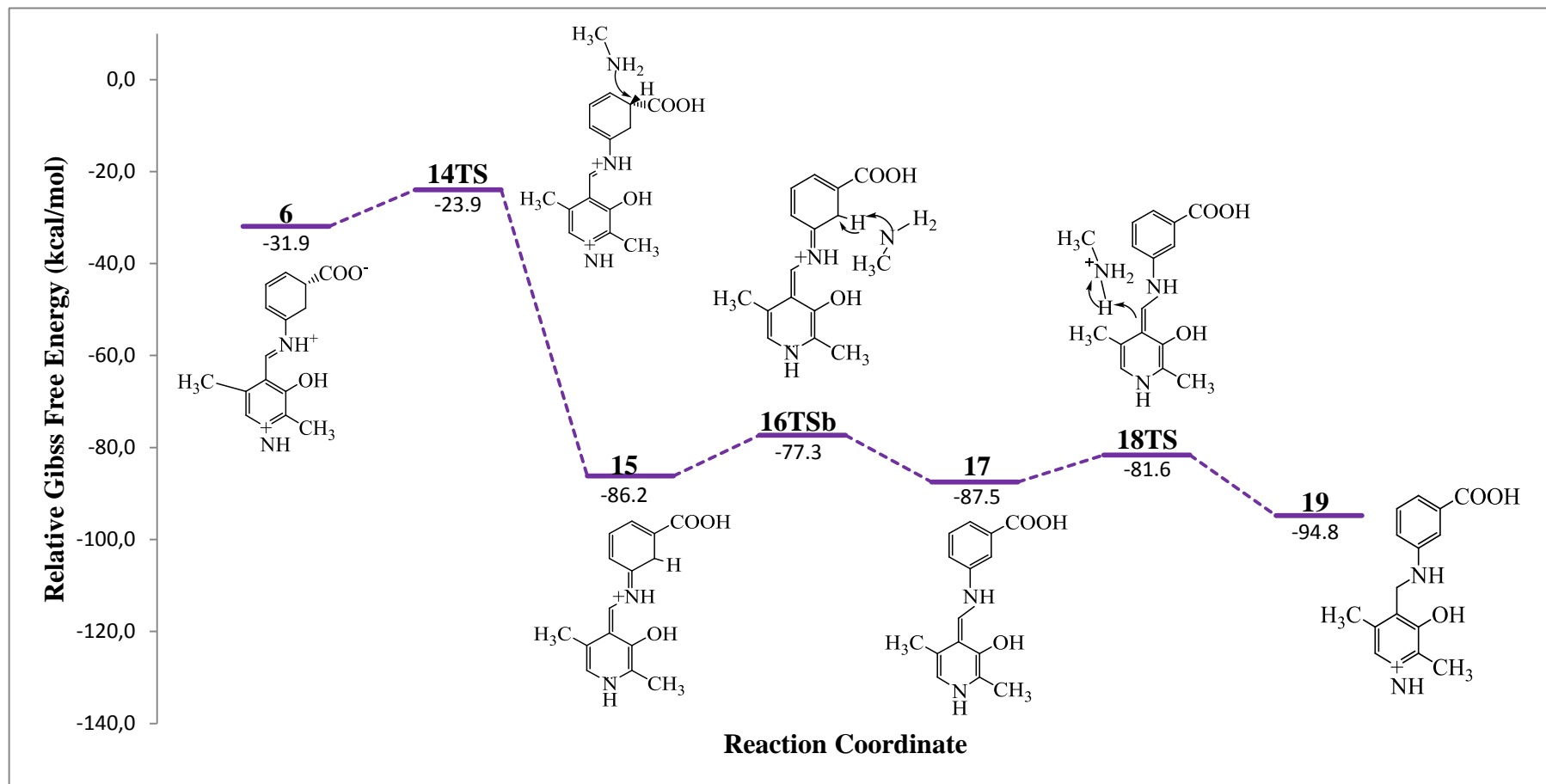
Figure 3.14 : Energy profile of Mechanism 3a in gas phase. Relative Gibbs free energies are given as kcal/mol.

**(a)**   **(b)**
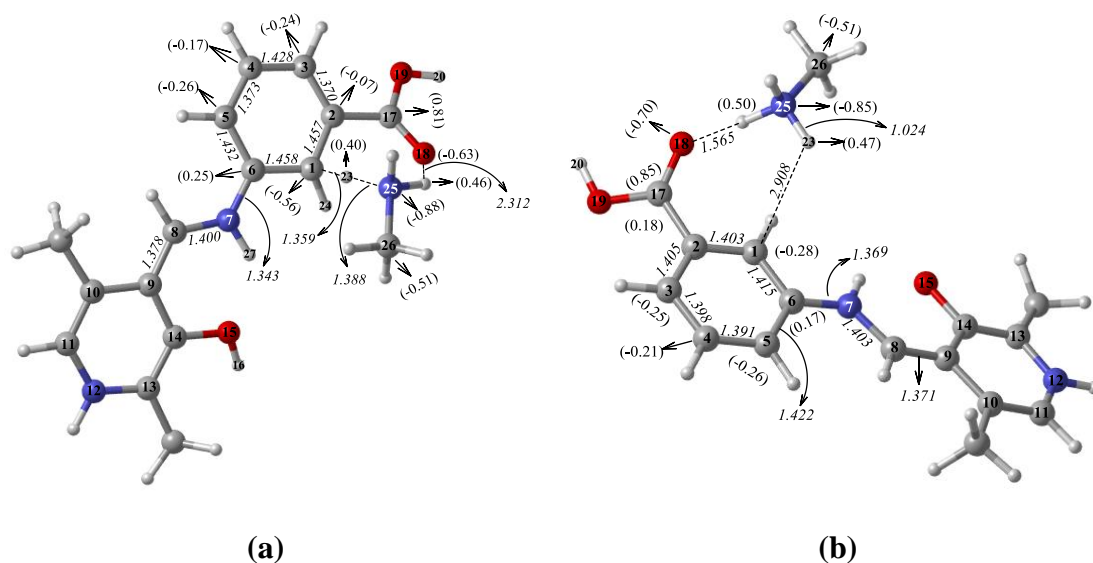
Figure 3.15 : Proton elimination from structure **15** as the first step of Mechanism 3b.
a. Proton transfer from structure **15** to methylamine (**16TSa**). **b.**
Optimized geometry from forward IRC calculation of **16TSa**. NBO
charges are shown in parenthesis

In the second transition state structure (**16TSb**, **Figure 3.16a**) of proton abstraction
from structure **15**, the C1 – H23 distance is found to be 1.358 Å while the H23 – N25
distance is 1.386 Å. These distances are relative with the distances in **16TSa**. On the
other hand the dihedral angle C1 – H23 – N25 – C26 is found to be 136.3^0 where the
CH$_3$ of methylamine is placed towards the substrate ring. Moreover, the C1 – H23 –
N25 angle is 169.2^0 which is also similar to the C1 – H23 – N25 angle in **16TSa**. The
IRC calculations are also performed to validate the accuracy and it is found to be that
the this transition state, with one imaginary frequency having a value of 1152.00,
produces the protonated methylamine and structure **17** with a relative free energy of
-87.5 kcal/mol, where it differs only by the final position of protonated methylamine
in optimized geometry of the result from **16TSa** (**Figure 3.16b**). The C1 – H23
distance in structure **17** is found to be 2.908 Å just like in optimized structure of
forward IRC calculation of **16TSa**. On the other hand, the dihedral angle C1 – H23 –
N25 – C29 is found to be 139.0^0 and the C1 – N25 – C29 is 141.8^0 which are also
different from optimized structure of forward IRC result of **16TSa**. The relative
Gibbs free energy barrier is found to be 8.9 kcal/mol for this transition state and it is
0.5 kcal/mol lower than the barrier of **16TSa** where the optimized geometries from
IRC results have the same energies.

49

(a)   **(b)**
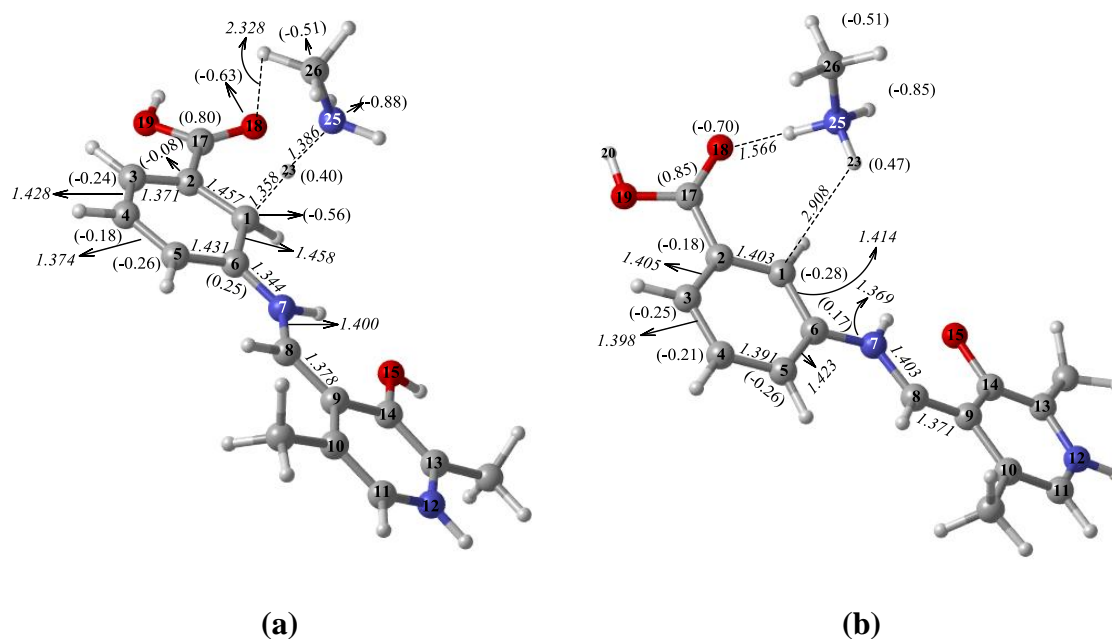
Figure 3.16 :   Proton elimination from structure **15** as the first step of Mechanism 3b. **a.** Proton transfer from structure **15** to methylamine (16TSb). **b.** Optimized geometry from forward IRC calculation of 16TSb. NBO charges are shown in parenthesis

The proton transfer from protonated methylamine to C8 is achieved in such a way that the distance between N12 and H is 1.282 Å where it is 1.472 Å between C8 and H. The C8 – H – N25 angle is 163.7^0 where the C9 – C8 – H – N25 dihedral angle is 144.1^0 and the N7 – C8 – H – N25 dihedral angle is 17.0^0. The transition state (**18TS**, **Figure 3.17a**) leads the change of double bond with the distance of 1.370 Å between C8 – C9 to single bond while the distance turns to 1.517 Å. Proton transfer leads aromatic compound **19** (**Figure 3.17b**) where the uncharged N12 gains a positive charge. The transition state (**18TS**) is determined with one imaginary frequency having a value of -1143.34 and has a free energy barrier of 5.8 kcal/mol when the structure **17** is taken as optimized geometry of forward IRC result of 16TSa and 5.9 kcal/mol when the structure 17 is taken as optimized geometry of forward IRC result of 16TSb.

50
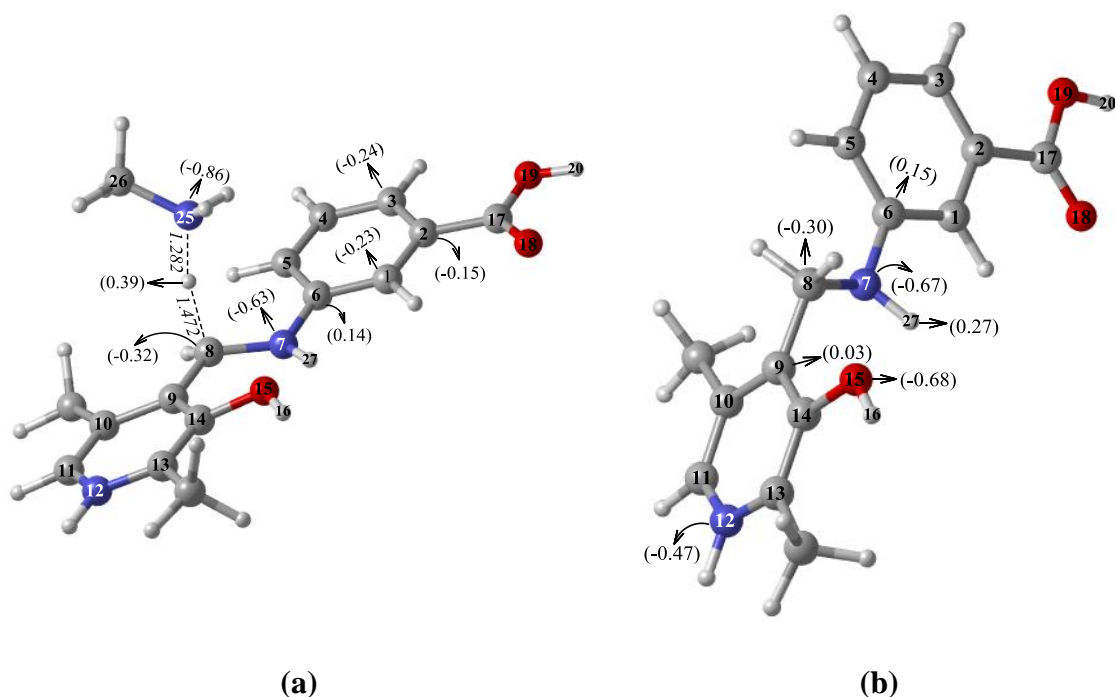
Figure 3.17 : Proton transfer to structure **17**. **a)** The last step of Mechanism 3a, (**18TS**). **b)** The final product (**19**). NBO charges are shown in parenthesis.

3.5.1. Aromatization via Mechanism 3b

After proton abstraction from structure **6** in Mechanism 3b, the next step is the proton transfer to C8. The proton donor for this step is chosen as protonated methylamine to represent the positively charged lysine. In the transition structure **20TS**, N25 – H and C8 – H distances are 1.278 Å and 1.493 Å respectively. The N25 – H – C8 and C9 – C8 – N7 angles are 176.6 and 118.0^{0} respectively. The transition state (**20TS**, **Figure 3.18a**) yields the structure **21** (**Figure 3.18b**). The double bond between C8 – C9 turns to single bond while the distance changes from 1.393 Å to 1.524 Å. Moreover, the C9 – C8 – N7 – C6 dihedral angle is 180.0^{0} in structure **15** while it changes to 144.6^{0} in structure **21**. The relative energy barrier for this transition state is calculated as 53.1 kcal/mol. The energy profile for aromatization via Mechanism 3b is given in **Figure 19**.

51

(a)   **(b)**
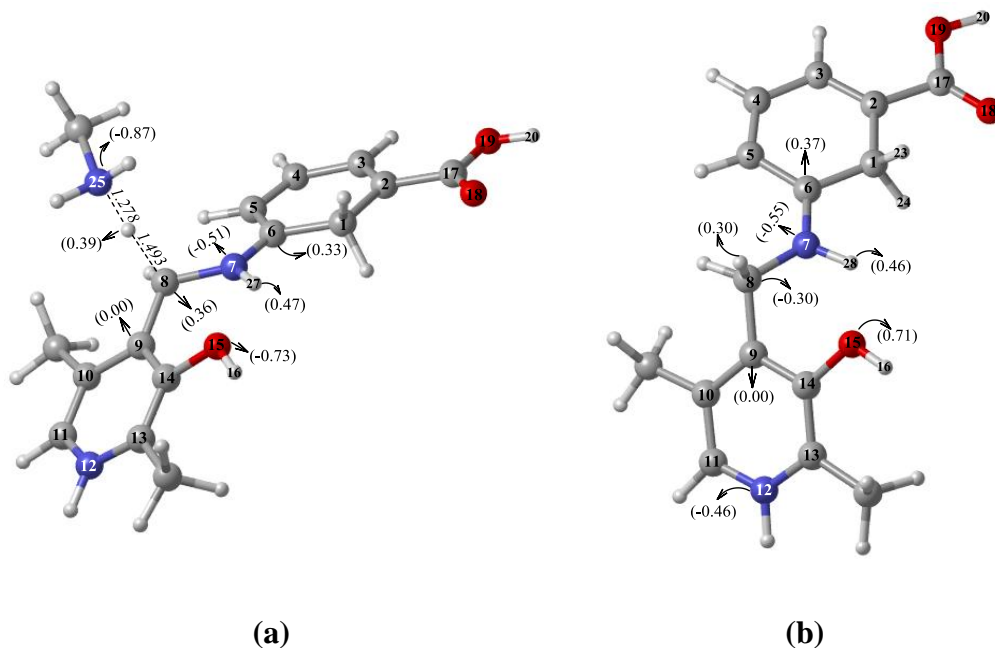
Figure 3.18 : Proton transfer step of Mechanism 3a and the associated product.
a. Proton transfer from protonated Lys329 to structure **15** (**20TS**).
b. Optimized geometry of structure **21**. NBO charges are shown in parenthesis.

The next step in Mechanism 3b is the proton transfer from structure 21. However, no transition structure can be modeled up to now. All of the attempts failed where the approximations of methylamine are relative to the **14TS** and especially in **16TS**. The reason for inability to find a transition state structure could be the steric effects due to the geometry.

As a result of the gas phase calculations for aromatization mechanisms, the Mechanism 3a has lower energy barrier than Mechanism 3b at their second steps (**16TS** and **20TS**). The Gibbs free energy barrier gap between **16TS** and the **20TS** is 44.2 kcal/mol. Moreover, the relative Gibbs free energy of **16TS** (-77.3 kcal/mol) is lower than the relative Gibbs free energy of **20TS** (-33.1 kcal/mol). Although there is no comparable result for **22TS** with **18TS**, it could be said that aromatization mechanism via Mechanism 3a is more preferable than the Mechanism 3b.
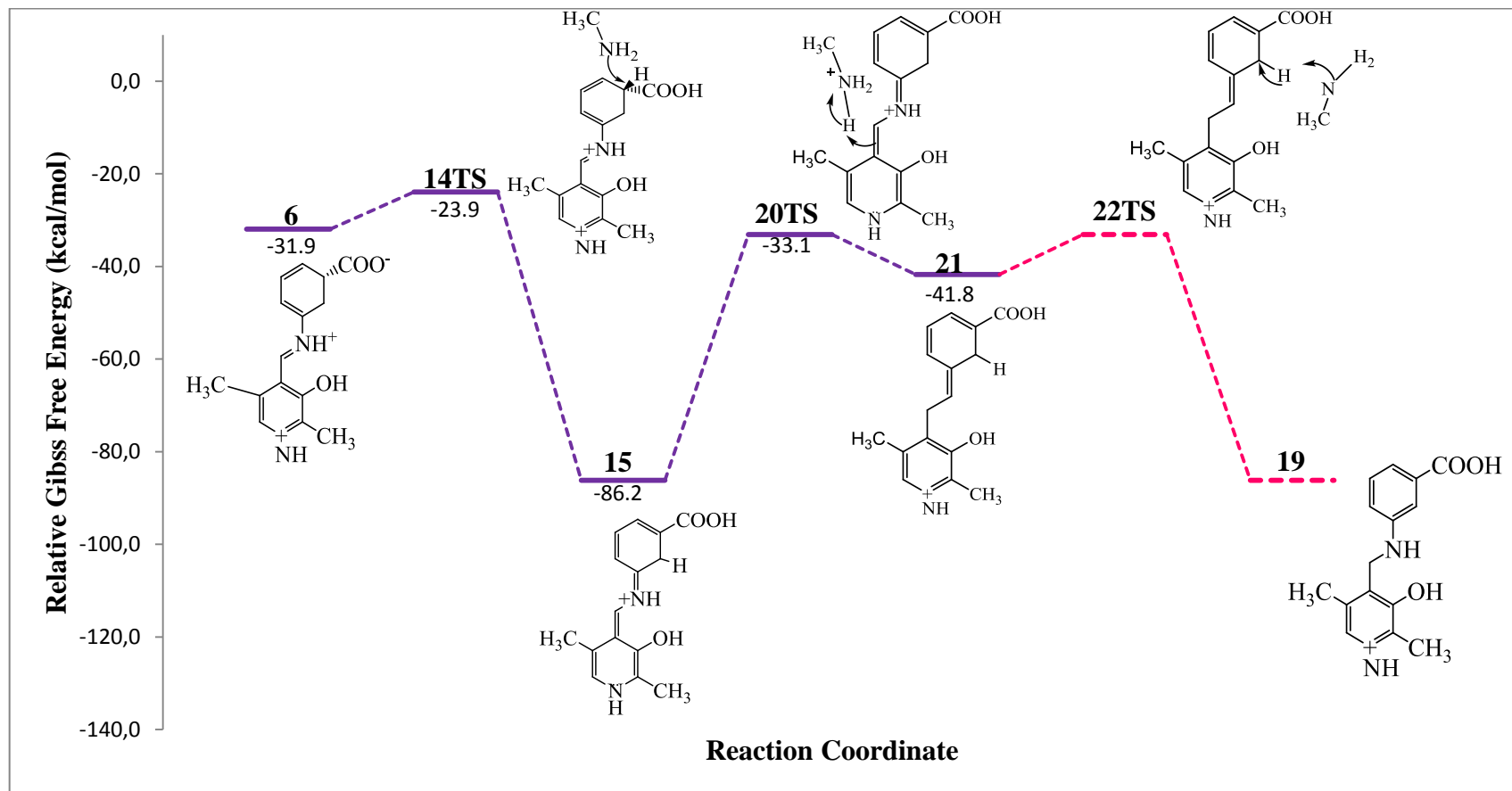
Figure 3.19 : Energy profile of Mechanism 3b in gas phase. Relative Gibbs free energies are given as kcal/mol.

Furthermore, the relative Gibbs free energy of the final product of Mechanism 3a (-94.8 kcal/mol) is smaller than the relative Gibbs free energy of the final product of threonine assisted Michael addition mechanism (-13.8 kcal/mol) which is the more preferable Michael addition path. Thus the final product of Mechanism 3a (**19**) is more stable than the structure **8c**. Additionally, the relative Gibbs free energy of rate determining step of Mechanism 3a (**14TS**, -23.9kcal/mol) is lower than the relative Gibbs free energy of rate determining step of threonine assisted Michael addition mechanism (**13TS**, -5.9 kcal/mol). Moreover the activation free energy barrier for **13TS** is bigger than the **14TS** and also bigger than the remaining steps of Mechanism 3a (**16TS** and **18TS**). As a result, Mechanism 3a is found to be more plausible inactivation mechanism of GABA-AT with 5-amino-2-fluorocyclohex-3-enecarboxylic acid.

In conclusion, the rate determining step for threonine assisted Michael addition mechanism is **13TS** and it is **14TS** in Mechanism 3a. On the other hand, it is found to be that the rate determining step for overall reaction coordinate is the fluorine elimination step (**5TS**) which has a relative Gibbs free energy of 13.3 kcal/mol (**Figure 3.20**). Threonine assisted Michael addition have less free Gibbs energy barriers relative to the water assisted and concerted ones. However, inactivation via Aromatization mechanism is found to be the more plausible path while the Mechanism 3a is the most preferable path due to the reasons that are mentioned above.

3.6 Solvent Effect

The effect of the solvent on modeled mechanisms was studied with IEFPCM method. Two types of solvent environments was chosen; water (ε=78.39) and diethylether (ε =4.335). It was found that almost all the barriers are fall off while relative free energies that define the potential surface increased. In the case of the diethylether, the relative energies are smaller than the case of the water as the solvent. Moreover, the smaller energy barriers are seen when the diethylether is chosen as the solvent type.
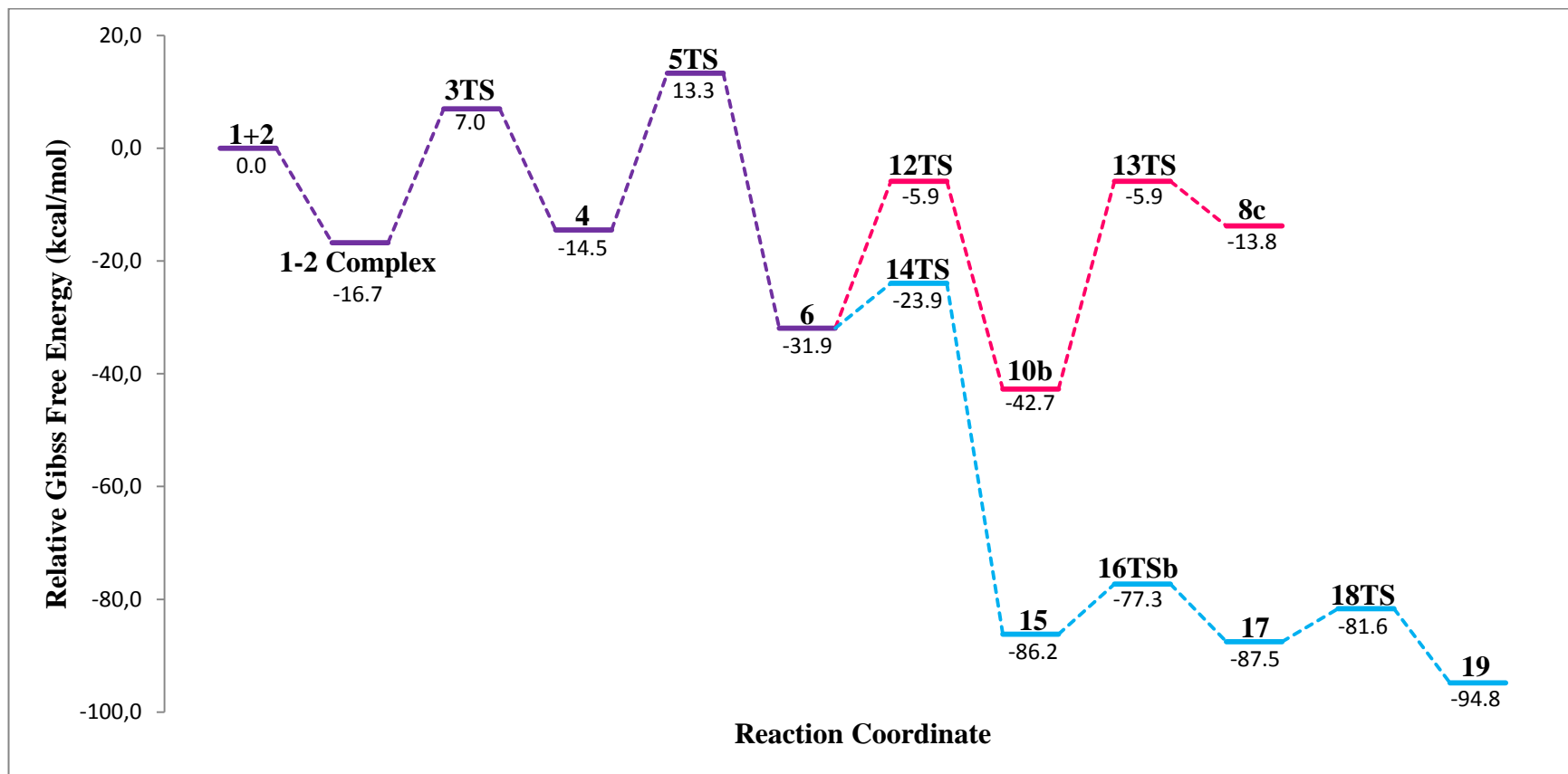
Figure 3.20 : Energy profile of inactivation of GABA-AT via threonine assisted Michael addition mechanism and aromatization mechanism via Mechanism 3a. Fluorine elimination is shown in **purple**, threonine assisted Michael addition is shown in **pink** and Mechanism 3a shown in **blue**. Relative Gibbs free energies are given in kcal/mol.

3.6.1. Solvent Effect on Fluorine Elimination

The first step in fluorine elimination mechanism is the formation of substrate – PLP complex. The methylamine – PLP – substrate complex has a relative energy as -16.7 kcal/mol in the gas phase while it increases to -9.7 kcal/mol in diethylether and -4.0 in the water cases. Moreover the relative energy for transition state structure is increased to 15.7 kcal/mol in the diethylether and 21.2 kcal/mol in the water from -16.7 kcal/mol. The required energy barrier for this step is increased to 25.2 kcal/mol when the solvent is water. On the other hand, the required energy is increased to 25.4 kcal/mol in the diethylether case. Therefore, the energy barrier increases for water and diethylether are 1.5 kcal/mol and 1.7 kcal/mol respectively. Thus, it could be said that the increases in the energy barrier are almost same. The energy profile for both the gas phase, water as the solvent and diethylether as the solvent is given in **Figure 3.21**.

The step where the fluorine is eliminated via water assistance has an energy barrier of 27.8 kcal/mol in the gas phase. The energy increase is also seen in this step where the barriers are increased to 30.5 kcal/mol for water and 27.7 kcal/mol for diethylether. There is an energy gap as 2.8 kcal/mol between the water and the diethylether cases where the diethylether as the solvent gives the smaller barrier.,

3.6.2. Solvent Effect on Michael Addition Mechanism

There are three types of Michael Addition mechanisms which are investigated. The first one is the concerted Michael addition which is calculated with methylamine. The second one is the water assisted Michael Addition where the water is used to assist bond formation between methylamine and structure **6**, and [1,3] proton transfer. The last one is the Threonine assisted Michael Addition which resembles the water assisted one.
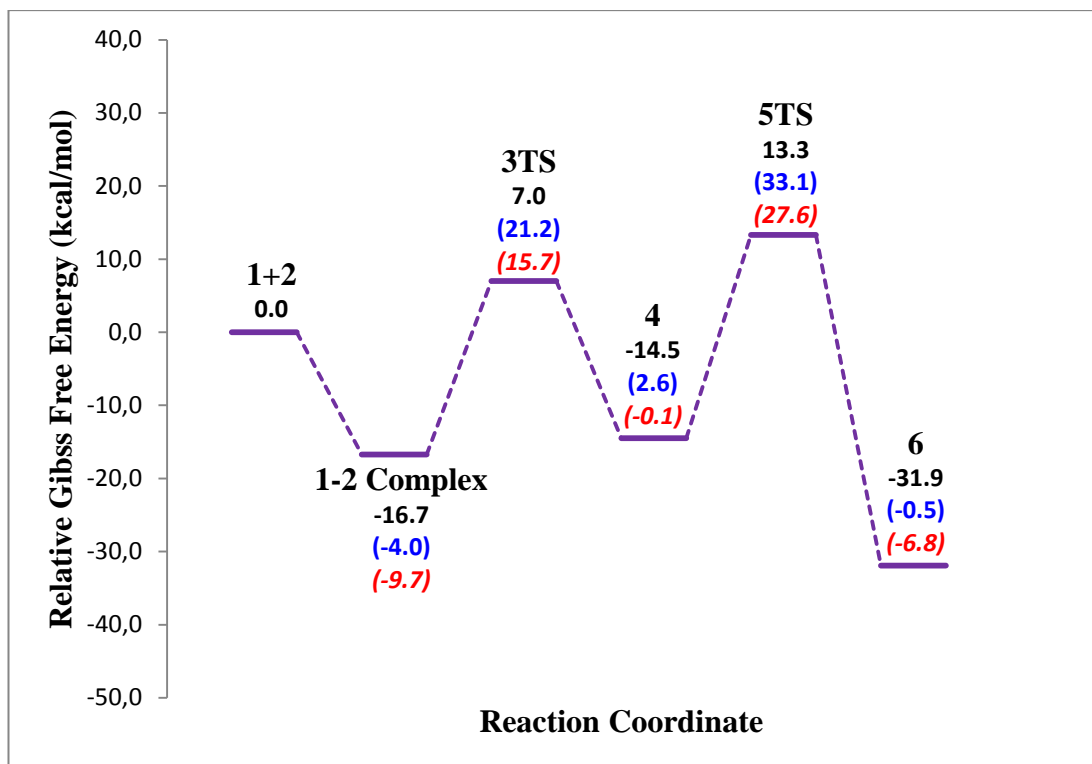
Figure 3.21 : Solvent effect on Fluorine elimination. Gas phase energies are written in **black**, the energies when the solvent is water is written in **blue** and the energies when the solvent is diethylether is written in *red*. All of the relative Gibbs free energies are given in kcal/mol.

The increase in relative free energy barriers along the reaction coordinate of the concerted mechanism 3 kcal/mol. The barrier for this step (**7TS**) in gas phase is 32.0 kcal/mol while it increases to 35.4 kcal/mol in water and 34.7 kcal/mol in diethylether. The energy gap between water and the diethylether cases is 0.7 kcal/mol thus the barrier increments are almost same. The energy profile for both of the cases is shown in **Figure 3.22**.

In water assisted Michael addition the first step has an energy barrier of 31.1 kcal/mol in gas phase. In this step, the water is selected as the solvent, the barrier decreases to 26.0 kcal/mol where it decreases to 23.6 kcal/mol when the diethylether is used as solvent. The energy gap between the barriers of the solvents is 2.4 kcal/mol where the diethylether gives the better result.

The second step (**11TS**) in water assisted Michael Addition Mechanism is the [1,3] proton transfer. This step has an energy barrier as 40.4 kcal/mol in the gas phase. However, the energy barrier for this step decreases when the water is used as solvent. The required relative free energy for this step (**11TS**) is found to be 35.1 kcal/mol with a decrease of 5.3 kcal/mol and it is compatible with the activation free energy barrier of concerted one (**7TS**). Additionally, diethylether is also decreases the energy barrier to 36.2 kcal/mol. Those results indicate that the water assisted mechanism in the presence of water as the solvent for this step (**11TS**) have almost the same energy relative to the concerted manner. Thus, the relative free energy gain from the previous step (35.1 kcal/mol and 36.6 kcal/mol for water and diethylether as solvents respectively), the relative free energy of the **11TS** (25.4 kcal/mol for water as solvent and 16.4 kcal/mol for diethylether as solvent) and also having lower relative energies of the product compared to the concerted mechanism makes water assisted mechanism more preferable than the concerted one.

The threonine assisted Michael addition mechanism starts with bond formation between methylamine and PLP – substrate complex (**12TS**) as in the water assisted manner (**9TS**). It is mentioned before that the relative energy for this step is smaller than both of the water assisted and the concerted Michael Addition mechanisms in gas phase. The usage of water as the solvent does not make too much difference in energy barrier where it is 25.9 kcal/mol and which is almost same as in the gas phase. However, it was found that the usage of diethylether as the solvent decreases the Gibbs free energy barrier by 2.9 kcal/mol where the required energy is 23.1 kcal/mol. This energy barrier is similar to the water assisted manner.

The required energy for the last step of the threonine assisted mechanism (**13TS**) is 26.0 kcal/mol in gas phase calculations. However the Gibbs free energy barrier increases to 48.1 kcal/mol when the water is used as the solvent. Although the required energy of the threonine assisted manner is smaller than the water assisted manner in gas phase, the presence of the water as the solvent makes threonine assisted mechanism less preferable than the water assisted manner. On the other hand, the usage of diethylether decreases required energy where the decrement is 3.4 kcal/mol. Despite the fact that the required energy is smaller than the water when

diethylether is the solvent, the final product of threonine is less stable than the water assisted mechanisms where the transition structures have almost the same energy.

As a result, the usage of water as the solvent lowers the required energy for the first step in water assisted mechanism while the energy barrier for threonine assisted mechanism increases. Although the water assisted Michael Addition at the step of **9TS** has almost same energy barrier relative to the concerted manner in the gas phase, it is found that in the case of the water as the solvent, it become almost same as the concerted mechanism. When the diethylether is used as the solvent at step where the [1,3] proton transfer occurs, the required energy for threonine assisted mechanism is decreased while it increases for water assisted mechanism. In other words, threonine assisted manner has smaller energy barrier than water assisted one both in the gas phase and in diethylether. However, it is found that the water assisted Michael Addition is much more exothermic than the threonine assisted one. Due to the same relative energies of transition structures, the energy gain from the last step of the water assisted manner is much bigger than the threonine assisted manner. Thus, according to the SCRF calculations, the most preferable mechanism is not the threonine assisted mechanism, it is water assisted Michael Addition.

3.6.3. Solvent Effect on Aromatization Mechanisms

The first step in both of the aromatization mechanisms is the proton transfer to methylamine and formation of structure 15 and protonated methylamine. In this step the required energy barrier in gas phase is 8.0 kcal/mol as mentioned above. It was found that the usage of solvent increases the required Gibbs free energy. When the water is used as solvent, the relative Gibbs free energy barrier increases to 16.2 kcal/mol. On the other hand, when the diethylether is the solvent, the relative energy of the transition structure (**14TS**) increases to 8.8 kcal/mol. In spite of the differences in relative energies of the transition structure, the required energies are not that much different. The required energy in the solvents as water and diethylether are 16.8 kcal/mol and 15.6 kcal/mol respectively.
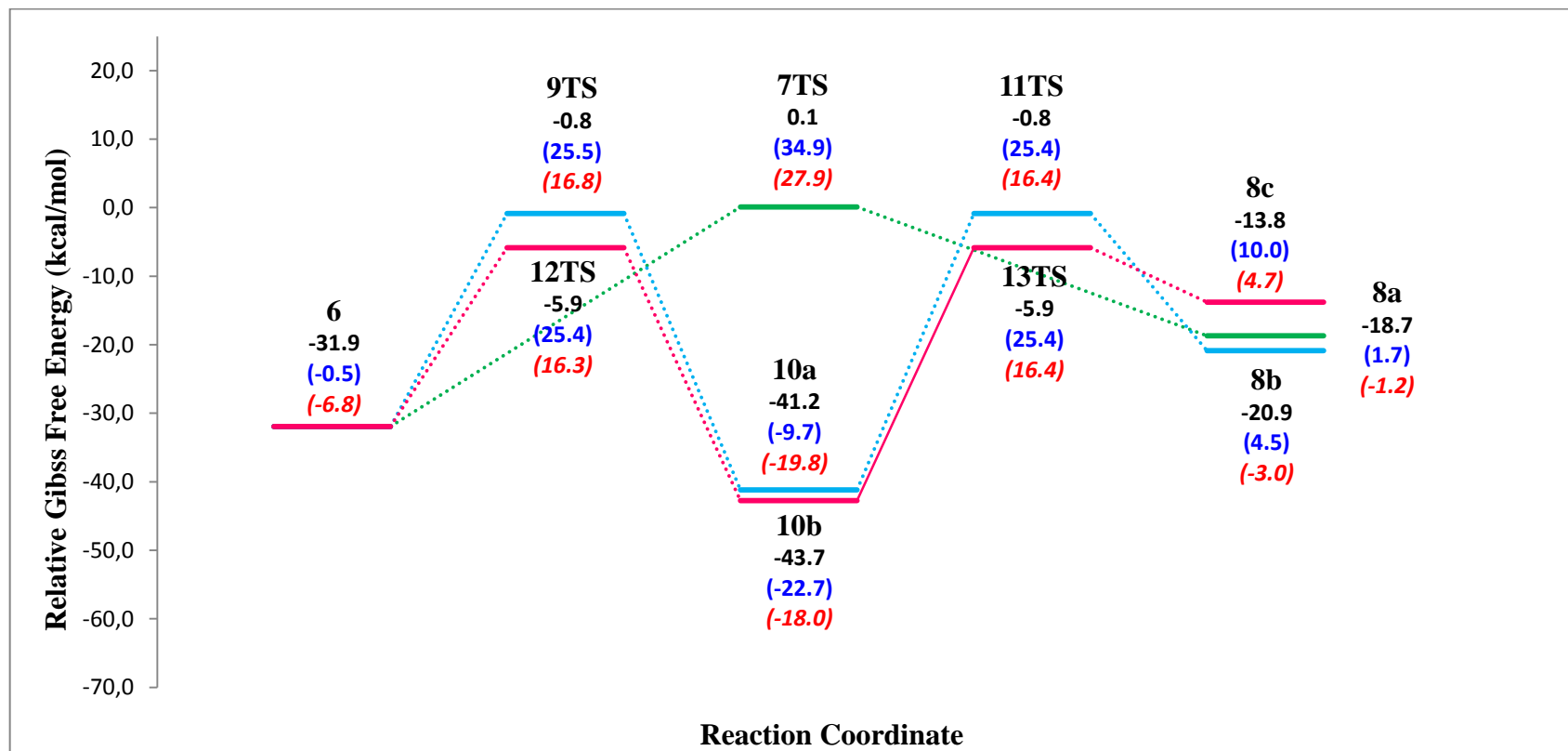
Figure 3.22 : Solvent effect on Michael Addition mechanism. — : Water assisted stepwise mechanism. — : Thr353 assisted stepwise mechanism. — : Concerted mechanism. Gas phase energies are written in **black**, the energies when the solvent is water is written in **blue** and the energies when the solvent is diethylether is written in *red*. All of the relative Gibbs free energies are given in kcal/mol.

3.6.3.1 Mechanism 3a

After proton abstraction from structure **6**, the second step in the Mechanism 3a is proton elimination from structure **15** (**16TSb**). The required energy for this step is 8.9 kcal/mol in the gas phase. When the calculations are performed in water, the energy barrier decreases to 8.0 kcal/mol, but it is only 0.9 kcal/mol lower than the gas phase (8.4 kcal/mol for **16TSa**). On the contrary, when the diethylether is used as the solvent, the required energy for this step decreases to 5.8 kcal/mol where the decrement is 3.1 kcal/mol (6.1 kcal/mol for **16TSa**). The required energy differences according to the solvent types and gas phase could be seen in energy profile for both of the situations of aromatization via Mechanism 3a (**Figure 3.23**).
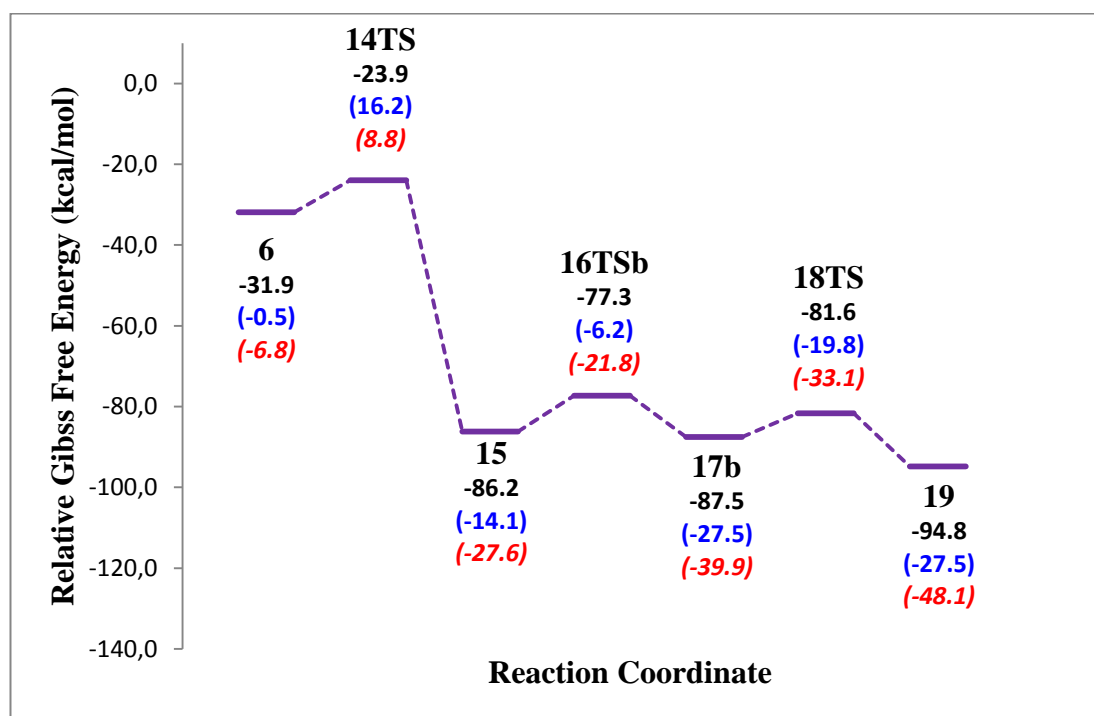
Figure 3.23 : Solvent effect on Aromatization via Mechanism 3a. Gas phase energies are written in **black**, the energies when the solvent is water is written in **blue** and the energies when the solvent is diethylether is written in *red*. All of the relative Gibbs free energies are given in kcal/mol.

The last step in Mechanism 3a is the proton transfer to structure **17** where the protonated methylamine is chosen as the proton donor. In the gas phase, the required energy for this step is 5.9 kcal/mol. This energy barrier increases to 7.6 kcal/mol with

an increment of 1.7 kcal/mol when the water is used as the solvent. In the case of the diethylether, the increment is 0.9 kcal/mol where the barrier is 6.8 kcal/mol. Hence, the usage of diethylether gives better result than the water as the solvent.

3.6.3.2. Mechanism 3b

The second step in Mechanism 3b is the proton transfer to structure **15** where the proton donor is chosen as the protonated methylamine (**20TS**). This step requires an energy of 53.1 kcal/mol in the gas phase. The usage of solvent sharply decreases the energy barrier. The required free Gibbs energies for **20TS** in water and diethylether are 17.3 kcal/mol and the 24.9 kcal/mol respectively. The largest improvement is seen in the usage of water as the solvent for this step. The decrement in the water as the solvent is 36.4 kcal/mol while it is 28.2 kcal/mol when the diethylether is the solvent. The energy profile that involves both of the solvents and the gas phase is depicted in **Figure 3.24**.
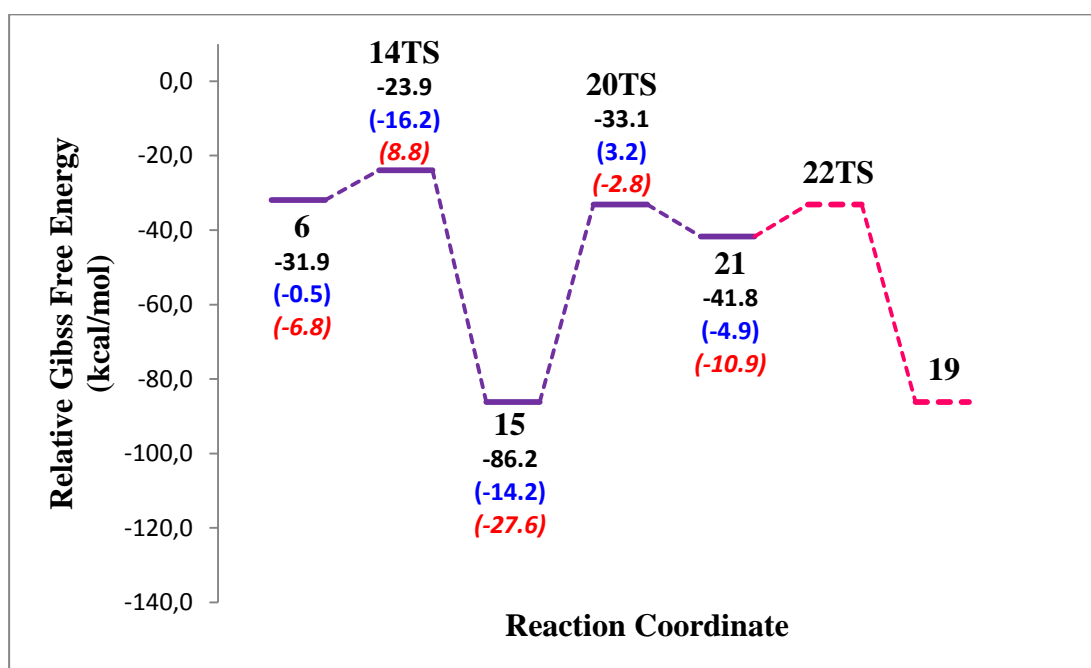
Figure 3.24 : Solvent effect on Aromatization via Mechanism 3b. Gas phase energies are written in **black**, the energies when the solvent is water is written in **blue** and the energies when the solvent is diethylether is written in *red*. All of the relative Gibbs free energies are given in kcal/mol.

In conclusion, according to the gas phase calculations and the calculations to investigate effect of solvent, Mechanism 3a have the lowest energy barriers. Also the relative energies of transition structures in Mechanism 3a have the lowest values relative to the whole mechanisms according to the SCRF calculations. Moreover, the final product of Mechanism 3a has a relative free energy of -27.5 kcal/mol in water and -48.12 kcal/mol in diethylether which are smaller than all of the Michael Addition mechanisms. As a result of having the lowest energy barriers and relative energies, the most preferable mechanism for inactivation of GABA-AT with -amino-2 fluorocyclohex-3-enecarboxylic acid is found to be the aromatization via Mechanism 3a which is also the more plausible one in gas phase calculations.

4. CONCLUSION

Inactivation mechanism occurs either via Michael Addition or Aromatization mechanism. Both mechanisms have common step at the beginning where fluorine is eliminated. Although it has been suggested that the fluorine elimination occurs via stepwise mechanism, it has been found that fluorine is eliminated via concerted mechanism in the presence of water assistance. The rate determining step has been found to be the fluorine elimination with a relative free energy value of 13.3 kcal/mol.

It has been proposed that the Michael Addition proceeds via concerted or stepwise mechanisms. However, it has been found that assistance of water or threonine leads the formation of stepwise mechanism. According to gas phase calculations, threonine assistance decreases relative free energies. It is also noticable that the second step of threonine assisted mechanism has a higher free energy barrier than concerted step, but the energy gain from previous step facilitates to overcome this free energy barrier. Based on the gas phase calculations, it can be deduced that stepwise threonine assisted Michael Addition is more prone to occur.

In aromatization mechanism two paths, namely Mechanism 3a and Mechanism 3b, were proposed. The only difference between two paths is the order of proton transfer. Unfortunately, one of the transition states of the Mechanism 3b cannot be modeled. It is noteworthy to state that, when the second steps of two paths are compared both the activation energy barriers and relative free energies indicate that path 3a is more preferred relative to the path 3b.

The product of aromatization mechanism is more stable than the one obtained from Michael Addition. Having the information provided from gas phase calculations, it can be deduced that Aromatization is the preferred mechanism. Our results are in harmony both with the calculations on the PLP – dependent enzymes and experimental evidence.

The solvent effect has been also taken into consideration. The Michael Addition mechanisms have been severely affected by the addition of water where the water assisted mechanism became more plausible than threonine assisted one. However, this does not affect the overall conclusion. Both gas phase and solvent calculations pointed out that the inactivation of GABA – AT with 5-amino-2 fluorocyclohex-3-enecarboxylic acid occurs via Aromatization mechanism.

REFERENCES

[1]   **Alberts, B., Bray, D., Hopkin, K., Johnson, A., Lewis, J., Raff, M., Roberts, K., Walter, P.**, (2004), *Essential Cell Biology Second Edition*, Garland Science, Taylor and Francis Group, New York, USA, pp. 92, 93

[2]   **Silverman, R. B.**, 2002, *The Organic Chemistry of Enzyme-Catalyzed Reactions*, Academic Press, London, UK, pp. 2, 4, 6

[3]   **Lodish, H., Berk, A., Matsudaria, P., Kaiser, C. A., Krieger, C. A., Scott, M. P., Zipursky, S. Lawrance, Darnell, J.**, (2004), *Molecular Cell Biology Fifth Edition*, W. H. Freeman and Company, New York, pp. 73,74,75

[4]   **Nelson, D. L., Cox, M. M.**, (2000), *Lehninger Principles of Biochemistry*, W. H. Freeman & Co., New York, pp. 244, 245

[5]   **Gramatikova, S., Mouratou, B., Stetefeld, J., Mehta, P. K., Christen**, P., 2002, *Journal of Immunological Methods*, 269, 99–110

[6]   **Ondrechen, M. J. , Briggs, J. M. , McCammon, J. A.** , 2001, *J. Am. Chem. Soc.*, 123, 2830-2834

[7]   **Snell, E. E., in Dolphin, D., Poulson, R., Avramovic, O. (Eds.)**, (1986), *Vitamin B6 Pyridoxal Phosphate, Chemical, Biochemical and Medical Aspects*, Part A, Wiley-Interscience, New York, USA, pp. 1 – 12

[8]   **Salva, S., Donoso, J., Frau, J., Munoz, F.**, 2002, *Journal of Molecular Structure (Theochem)*, 577, 229-238

[9]   **Casasnovas, R., Salva, A., Frau, J., Donoso, J., Munoz, F.**, 2009, *Chemical Physics*, 355, 149-156

[10]   **Salva, A., Donoso, J., Frau, J., Munoz, F.**, 2002, *International Journal of Quantum Chemistry*, 89, 48-56

[11]   **Rando, R. R., Bangerter, F. W.**, 1977, *Journal of the American Chemical Society*, 99, 15, 5141-5145

[12]   **Silverman, R. B., George, C.,** 1988, *Biochemistry*, 27, 3285-3289

[13]   **Fu, M., Silverman, R. B.,** 1999, *Bioorganic & Medicinal Chemistry*, 7, 1581-1590

[14]   **Wang, Z., Yuan, H., Nikolic, D., Van Breemen, R. B. and Silverman, R. B.,** 2006, *Biochemistry*, 45, 14513-14522.

[15]   **Storici, P., De Biase, D., Bossa, F., Bruno, S., Mozzarelli, A., Peneff, C., Silverman, R. B. and Schirmer, T.,** 2004, *The Journal Of Biological Chemistry*, 279, 1, 363–373

[16]   **Storici, P., De Biase, D., Bossa, F., Bruno, S., Mozzarelli, A., Peneff, C., Silverman, R., Schirmer, T.,** *2004, J.Biol.Chem.,* **279,** 363-373

[17]   **Choi, S., Storici, P., Schirmer, T. and Silverman, R. B.,** 2002, *J. Am. Chem. Soc.,* 124, 1620

[18]   **Clift, M. D., Ji, H., Deniau, G. P., O'Hagan, D., Silverman, R. B.,** 2007, *Biochemistry*, 46, 13819-13828

[19]   **Lewars, E.,** (2003), *Computational chemistry - Introduction to the Theory and Applications of Molecular and Quantum Mechanics*, Kluwer Academic Publishers, Dordrecht, pp. 5, 160,162-163, 339-343, 383-386, 398-399, 178, 212

[20]   **Leach, A., R.,** (2001), *Molecular modelling - Principles and applications Second Edition*, Pearson Education Limited, Harlow, England, pp. 640, 51-53, 135, 56, 67

[21]   **Cramer, C. J.,** (2004), *Essentials of Computational Chemistry-Theories and Models Second Edition*, John Wiley & Sons Ltd, Chichester, England, pp. 62,120,129,167,172-180, 257-259, 397,399-401, 578, 457

[22]   **Solomon, E. P., Berg, L. R., Martin, D. W.,** (1999), *Biology Fifth Edition*, Saunders Collage Publishing, Orlando, FL, pp. 149-150

[23]   **Storici, P., Qiu, J., Schirmer T. and Silverman, R. B.,** 2004, *Biochemistry,* 43, 14057

[24]   **Fu, M. and Silverman, R. B.,** 2004, *Bioorganic & Medicinal Chemistry Letters*, 14, 203–206

[25]   **Clift, M. D. and Silverman, R. B.,** 2008, *Bioorganic & Medicinal Chemistry Letters*, 18, 3122–3125

[26]   **Silverman, R. B., Durkee, S. C. and Invergo B. J.,** 1986, *J. Med. Chem.*, 29, 764-770

[27]   **Lu, H. and Silverman, R.B.,** 2006, *J. Med. Chem.*, 49, 7404-7412

[28]   **Johnston, G. A. R., Curtis, D. R., Beart, P. M., Game, C. J. A., McColloch, R. M., Twichin, B. J.,** 1975, *Neurochem.*, 24, 157-160

[29]   **Brehm, L., Hjeds, H., Krogsgarrd-Larsen, P.,** 1972, *Acta Chem. Scand.*, 26, 1298-1299

[30]   **Choi, S. and Silverman, R. B.,** 2002, *J. Med. Chem.,* 45, 4531-4539

[31]   **Qiu, J., Pingsterhaus, J. M. and Silverman, R. B.,** 1999, *J. Med. Chem.,* 42, 4725-4728

[32]   **Wade, L. G. Jr.,** (2003), *Organic Chemistry Fifth Edition*, Pearson Education Inc. New Jersey, 1042, 1043

[33]   **Jing-ping, K., Yu-juan, L., Xu-yang, L. and Ji-zhen, L.,** 2009, *Chem. Res. Chinese Universities*, 25(4), 461- 464

[34]   **Ivanetich, K. M; Santi, D. V.,** 1992, *Prog. Nucleic Acid Res. Mol. Biol.*, 42, 127

[35]   **March, J.,** 1985, *Advanced Organic Chemistry,* 3rd ed., John Wiley & Sons, Inc., New York, 657-666, pp. 711-712

[36]   **House, H.O.,** 1972, *Modern Synthetic Reactions,* 2nd ed.; W. A. Benjamin, Inc.: Menlo Park, CA, pp 595-628

[37]   **Pardo, L., Osman, R., Weinstein, H., Rabinowitz, J. R.,** 1993, *J. Am. Chem. Soc.*, 115,8 263

[38]   **Kamimura, A., Sasatani, H., Hashimoto, T., Kawai, T., Hori, K., Ono, N.,** 1990, *J. Org. Chem.*, 55, 2437

[39]   **Miyata, O., Shinada, T., Ninomiya, I., Naito, T., Date, T., Okamura, K., Inagaki, S.,** 1991, *J. Org.Chem*, 56, 6556

[40]   **Thomas IV, B. E. and Kollman, P. A.,** 1995, *J. Org. Chem.*, 60**,** 8375-8381

[41]   **Fitts**, **D. D.,** (1999), *Principles of Quantum Mechanics as Applied to Chemistry and Chemical Physics***,** Cambridge University Press, New York, USA, p. 46

[42]   **Atkins, P., Friedman, R. S.,** (2005), *Molecular quantum mechanics 4ed*, Oxford University Press, USA , pp. 24, 249, 233

[43]   **Young, D. C.**, (2001), *Computational Chemistry: A Practical Guide for Applying Techniques to Real-World Problems*, John Wiley & Sons Inc., ISBN: 0-471-33368-9, pp. 42, 81-82, 100-101, 159-160, 173-174, 179, 369, 364, 79, 80, 206-207, 389-390, 100-101, 513-514, 520, 531-533, 521, 529

[44]   **Jensen,** F., (1999), *Introduction to Computational Chemistry*, John Wiley & Sons Ltd., Chischester, England, pp. 150-151, 81-82, 182, 187-188, 392-393, 395, 230-231, 229

[45]   **Boys, S. F.**, 1950, *Proc. R. Soc. (London) A*, 200, 542

[46]   **Hinchliffer, A.**, (2003), *Molecular Modelling for Beginners*, John Wiley and Sons Ltd., Chichester, England, p. 325

[47]   **Stewart, J. J. P.,** 1989. *J. Comput. Chem.*, 10, 209, 221

[48]   **Dreizler, R. M., Gross, E. K. U., (1990),** *DFT - An Approach to the Quantum Many-Body Problem* , Springer – Verlag Berlin Heidelberg, Germany, pp. 66 – 68

[49]   **Eschrig, H.**, 1996, *The Fundamentals of DFT*, B. G. Teubner Verlagsgesellschaft Leipzig, Germany, p. 176

[50]   **von Rague Schlenyer, P.,** (1998), *Encyclopedia of Computational Chemistry*, *Vol 1 A-D*, John Wiley & Sons Ltd., Chichester, UK

    a.   **Hu, C.-H. and Chong**, D. P., *Density Functional Applications*, p. 664

    b.   **Gill**, P. M. W., *Densit Functional Theory (DFT), Hartree-Fock (HF), and Self-Consistent Field*, 683

    c.   **Istvan Kolossvary, Wayne C. Guida**, *Conformational Analysis: 1*, pp. 513-520

    d.   **Ernest L. Eliel**, *Conformational Analysis: 3*, pp. 531-533

    e.   **Sandor Vajda**, *Conformational Analysis: 2*, pp. 521-529

[51]   **Hinchliffe, A.,** *Modelling molecular structures 2ed*, (2000), John Wiley & Sons Ltd., Chichester, England, pp. 224-225

[52]   **Koch, W., Holthausen, M. C.,** (2001), *A Chemists Guide to DFT 2ed*, Wiley-VCH Verlag GmbH, Weinheim, Federal Republic of Germany, p. 71

[53]   **Becke, D.,** 1993, *Physical Rev. A140*, pp. 1133-1138

[54]   **Stephens, P. J., Devlin, F. J., Chablowski, C. F. and Frisch**, M. J., 1994, *J. Phys. Chem.*, 98, 11623

[55] **Barton, D. H. R.,** 1950, *Experientia*, 6, 316-329, reprinted in *Top. Stereochem*, 1971, 6, 1-10

[56] Spartan '04, Wavefunction Inc., 18401 Von Karman Ave., Suite 370, Irvine, CA 92612

[57] Gaussian 03, Revision D.01, M. J. Frisch, G. W. Trucks, H. B. Schlegel, G. E. Scuseria, M. A. Robb, J. R. Cheeseman, J. A. Montgomery, Jr., T. Vreven, K. N. Kudin, J. C. Burant, J. M. Millam, S. S. Iyengar, J. Tomasi, V. Barone, B. Mennucci, M. Cossi, G. Scalmani, N. Rega, G. A. Petersson, H. Nakatsuji, M. Hada, M. Ehara, K. Toyota, R. Fukuda, J. Hasegawa, M. Ishida, T. Nakajima, Y. Honda, O. Kitao, H. Nakai, M. Klene, X. Li, J. E. Knox, H. P. Hratchian, J. B. Cross, V. Bakken, C. Adamo, J. Jaramillo, R. Gomperts, R. E. Stratmann, O. Yazyev, A. J. Austin, R. Cammi, C. Pomelli, J. W. Ochterski, P. Y. Ayala, K. Morokuma, G. A. Voth, P. Salvador, J. J. Dannenberg, V. G. Zakrzewski, S. Dapprich, A. D. Daniels, M. C. Strain, O. Farkas, D. K. Malick, A. D. Rabuck, K. Raghavachari, J. B. Foresman, J. V. Ortiz, Q. Cui, A. G. Baboul, S. Clifford, J. Cioslowski, B. B. Stefanov, G. Liu, A. Liashenko, P. Piskorz, I. Komaromi, R. L. Martin, D. J. Fox, T. Keith, M. A. Al-Laham, C. Y. Peng, A. Nanayakkara, M. Challacombe, P. M. W. Gill, B. Johnson, W. Chen, M. W. Wong, C. Gonzalez, and J. A. Pople, Gaussian, Inc., Wallingford CT, 2004

[58] **Becke, A. D.,** 1993, *J.Chem.Phys.*, 98, 5648-5652

[59] **Fu, M., Nikolic, D., Van Breemen, R. B., Silverman, R. B.,** 1999, *J. Am. Chem. Soc.*, 121, 7751-7759

[60] **Liao, R., Ding, W., Yu, J., Fang, W., Liu, R.,** 2008, *J. Comput. Chem.*, 29, 1919

APPENDICES

Appendix A : Gibbs free energies and relative Gibss free energies of molecules in gas phase. PCM energies and relative PCM energies of molecules in water as the solvent and diethylether as the solvent.

Appendix B : Gaussian03 input file samples.

APPENDIX A

Gas Phase Gibbs Free Energies

	Gas phase free energy (Hartree)	Gas phase relative free energy (Hartree)	Gas phase relative free energy (kcal/mol)
1	-535.383505	0.000000	0.0
2	-577.706662	0.000000	0.0
3TS_rev	-1113.116851	-0.026684	-16.7
3TS	-1113.079022	0.011145	7.0
4	-1017.282531	-0.023106	-14.5
5TS	-1093.668645	0.021189	13.3
6	-1093.740703	-0.050869	-31.9
7TS	-1012.631493	0.000153	0.1
8a	-1012.661427	-0.029781	-18.7
9TS	-1089.063397	-0.001342	-0.8
10	-1012.682426	-0.050780	-31.9
11TS	-1089.063400	-0.001345	-0.8
8b	-1089.095309	-0.033254	-20.9
12TS	-1206.941270	-0.009345	-5.9
13TS	-1206.941266	-0.009341	-5.9
8c	-1206.953924	-0.021999	-13.8
14TS	-1012.669796	-0.038150	-23.9
15	-916.597003	-0.137331	-86.2
16TSa	-1012.412773	-0.122359	-76.8
16TSa_fwd	-1012.429685	-0.139271	-87.4
16TSb	-1285.474520	-0.123202	-77.3
16TSb_fwd	-1285.490795	-0.139477	-87.5
18TS	-1012.420523	-0.130109	-81.6
18TS_fwd	-1012.441497	-0.151083	-94.8
20TS	-1285.404110	-0.052792	-33.1
20TS_fwd	-1285.417845	-0.066527	-41.8

PCM Energies (solvent=water)

	PCM Energy (Hartree)	Relative PCM Energy (Hartree)	PCM Energy (kcal/mol)
1	-535.826343	0.000000	0.0
2	-577.841069	0.000000	0.0
3TS_rev	-1113.673841	-0.006429	-4.0
3TS	-1113.633591	0.033821	21.2
4	-1017.791619	0.004104	2.6
5TS	-1094.183543	0.052712	33.1
6	-1094.237082	-0.000827	-0.5
7TS	-1013.156113	0.055567	34.9
8a	-1013.208910	0.002770	1.7
9TS	-1089.611575	0.040637	25.5
10	-1013.242617	-0.030937	-19.4
11TS	-1089.611693	0.040519	25.4
8b	-1089.644970	0.007242	4.5
12TS	-1207.548452	0.040536	25.4
13TS	-1207.548452	0.040536	25.4
8c	-1207.573038	0.015950	10.0
14TS	-1013.185801	0.025879	16.2
15	-916.900528	-0.017583	-11.0
16TSa	-1012.758878	-0.009194	-5.8
16TSa_fwd	-1012.792933	-0.043249	-27.4
16TSb	-1285.989453	-0.009820	-6.7
16TSb_fwd	-1286.023409	-0.043776	-27.5
18TS	-1012.781300	-0.031616	-19.8
18TS_fwd	-1012.793460	-0.043776	-27.5
20TS	-1013.206610	0.005070	3.2
20TS_fwd	-1013.219547	-0.007867	-4.9

PCM Energies (solvent=diethylether)

	PCM Energy (Hartree)	Relative PCM Energy (Hartree)	PCM Energy (kcal/mol)
1	-535.766423	0.000000	0.0
2	-577.838899	0.000000	0.0
3TS_rev	-1113.620744	-0.015422	-9.7
3TS	-1113.580283	0.025039	15.7
4	-1017.734617	-0.000148	-0.1
5TS	-1094.128577	0.044002	27.6
6	-1094.183468	-0.010889	-6.8
7TS	-1013.106761	0.044393	27.9
8a	-1013.152994	-0.001840	-1.2
9TS	-1089.562546	0.026718	16.77
10	-1013.187280	-0.036126	-22.67
11TS	-1089.562659	0.026605	16.69
8b	-1089.594073	-0.004809	-3.02
12TS	-1207.502108	0.026032	16.34
13TS	-1207.502087	0.026053	16.35
8c	-1207.520712	0.007428	4.66
14TS	-1013.137144	0.014010	8.79
15	-916.886305	-0.044023	-27.62
16TSa	-1012.747425	-0.034290	-21.52
16TSa_fwd	-1012.776270	-0.063135	-39.62
16TSb	-1285.949037	-0.034752	-21.81
16TSb_fwd	-1285.977878	-0.063593	-39.91
18TS	-1012.765954	-0.052819	-33.14
18TS_fwd	-1012.789816	-0.076681	-48.12
20TS	-1013.155562	-0.004408	-2.77
20TS_fwd	-1013.168469	-0.017315	-10.87

Gas Phase and PCM Energies of Used Molecules

(solvent = water and solvent=diethylether)

Molecule	Gas Phase Energy (Hartree)	PCM (solvent=water) Energy (hartree)	PCM (solvent=diethylether) Energy (Hartree)
H_2O	-76.430409	-76.440532	-76.438110
H_3O	-76.690755	-76.833563	-76.804967
CH_3NH_2	-95.830742	-95.871689	-95.870853
CH_3NH_3	-96.171974	-96.333685	-96.308872
HF	-100.458521	-100.455732	-100.454168
2-propyl-alcohol	-194.300279	-194.377308	-194.376986

APPENDIX B

Gas Phase Stationary Point Geometry Optimization Input Sample:

```
%chk=1.chk
%mem=240MW
%nproc=4
# opt freq b3lyp/6-31+g(d,p)

Title Card Required

2 1
 N
 C                    1          B1
 C                    2          B2     1          A1
 C                    2          B3     1          A2    3          D1
 O                    4          B4     2          A3    1          D2
 C                    4          B5     2          A4    1          D3
 C                    6          B6     4          A5    2          D4
 C                    6          B7     4          A6    2          D5
 C                    8          B8     6          A7    4          D6
 C                    1          B9     2          A8    4          D7
 N                    7          B10    6          A9    4          D8
 H                    3          B11    2          A10   1          D9
 H                    3          B12    2          A11   1          D10
 H                    3          B13    2          A12   1          D11
 H                    5          B14    4          A13   2          D12
 H                    7          B15    6          A14   4          D13
 H                    9          B16    8          A15   6          D14
 H                    9          B17    8          A16   6          D15
 H                    10         B18    1          A17   2          D16
 H                    9          B19    8          A18   6          D17
 H                    1          B20    2          A19   4          D18
 H                    11         B21    7          A20   6          D19
 C                    11         B22    7          A21   6          D20
 H                    23         B23    11         A22   7          D21
 H                    23         B24    11         A23   7          D22
 H                    23         B25    11         A24   7          D23

   B1          1.34771600
   B2          1.49703824
   B3          1.41077929
   B4          1.34485694
   B5          1.41626641
   B6          1.46591555
   B7          1.42559552
   B8          1.50813084
   B9          1.35166662
   B10         1.29228843
   B11         1.09263498
   B12         1.09732843
   B13         1.09731795
   B14         0.97175218
   B15         1.08654193
   B16         1.09109964
   B17         1.09542747
   B18         1.08344312
   B19         1.09542314
   B20         1.02090056
   B21         1.02259541
   B22         1.47375381
```

```
B23             1.09367807
B24             1.09369013
B25             1.08970379
A1            120.20585136
A2            115.90137905
A3            121.20162221
A4            121.03746105
A5            122.51216012
A6            119.60154300
A7            124.08938407
A8            125.77600522
A9            127.06117970
A10           111.55122922
A11           111.13177868
A12           111.14060188
A13           114.60993382
A14           117.16941780
A15           110.54036897
A16           111.67482578
A17           116.40040397
A18           111.68031160
A19           117.04963900
A20           117.94179026
A21           125.36291061
A22           108.44270536
A23           108.44334658
A24           109.94794525
D1            179.98883307
D2           -179.99184209
D3             0.00000000
D4           -179.99623697
D5             0.00000000
D6            179.99694143
D7            -0.00282566
D8             0.00371623
D9            -0.08779981
D10           119.29646056
D11          -119.46115537
D12           -0.02953526
D13          -180.00000000
D14          -179.96598516
D15           -60.89011010
D16          -180.00000000
D17            60.95419484
D18           180.00000000
D19             0.00000000
D20           179.99499645
D21           120.82825740
D22          -120.77892995
D23             0.02141975
```

Gas Phase TS Optimization Input File Sample:

```
%chk=3TS.chk
%mem=240MW
%nproclinda=2
%nprocshared=8
# opt=(calcfc,ts,noeigen) freq rb3lyp/6-31+g(d,p)

Title Card Required

2 1
 N
 C                    1              B1
 C                    2              B2     1              A1
 C                    2              B3     1              A2     3              D1
 O                    4              B4     2              A3     1              D2
 C                    4              B5     2              A4     1              D3
 C                    6              B6     4              A5     2              D4
 C                    6              B7     4              A6     2              D5
 C                    8              B8     6              A7     4              D6
 C                    1              B9     2              A8     4              D7
 N                    7              B10    6              A9     4              D8
 H                    3              B11    2              A10    1              D9
 H                    3              B12    2              A11    1              D10
 H                    3              B13    2              A12    1              D11
 H                    5              B14    4              A13    2              D12
 H                    7              B15    6              A14    4              D13
 H                    9              B16    8              A15    6              D14
 H                    9              B17    8              A16    6              D15
 H                   10              B18    1              A17    2              D16
 H                    9              B19    8              A18    6              D17
 H                    1              B20   10              A19    8              D18
 H                   11              B21    7              A20    6              D19
 C                   11              B22    7              A21    6              D20
 C                   23              B23   11              A22    7              D21
 C                   23              B24   11              A23    7              D22
 C                   24              B25   23              A24   11              D23
 H                   24              B26   23              A25   11              D24
 C                   25              B27   23              A26   11              D25
 H                   25              B28   23              A27   11              D26
 C                   28              B29   25              A28   23              D27
 H                   28              B30   25              A29   23              D28
 H                   23              B31   11              A30    7              D29
 H                   30              B32   28              A31   25              D30
 F                   30              B33   28              A32   25              D31
 H                   24              B34   23              A33   11              D32
 H                   26              B35   24              A34   23              D33
 C                   26              B36   24              A35   23              D34
 O                   37              B37   26              A36   24              D35
 O                   37              B38   26              A37   24              D36
 H                   39              B39   37              A38   26              D37
 N                    7              B40    6              A39    4              D38
 H                   41              B41    7              A40    6              D39
 H                   41              B42    7              A41    6              D40
 C                   41              B43    7              A42    6              D41
 H                   44              B44   41              A43    7              D42
 H                   44              B45   41              A44    7              D43
 H                   44              B46   41              A45    7              D44

   B1         1.35151289
   B2         1.49725237
   B3         1.40309418
   B4         1.35284982
   B5         1.40865546
   B6         1.51841126
   B7         1.41522730
   B8         1.51009794
   B9         1.35033582
   B10        1.50258739
   B11        1.09258660
   B12        1.09650954
```

```
B13         1.09701788
B14         0.96943815
B15         1.08908335
B16         1.09135862
B17         1.09487604
B18         1.08327614
B19         1.09484056
B20         1.01880745
B21         1.03002382
B22         1.50723036
B23         1.54390280
B24         1.51109512
B25         1.53782989
B26         1.09497418
B27         1.33751247
B28         1.08779823
B29         1.50508780
B30         1.08639877
B31         1.09760403
B32         1.09238389
B33         1.40703285
B34         1.09402238
B35         1.09709239
B36         1.52077831
B37         1.22872599
B38         1.33055899
B39         0.97402101
B40         1.51191919
B41         1.02146635
B42         1.30876368
B43         1.48586898
B44         1.09105428
B45         1.09336572
B46         1.09157806
A1        119.92572164
A2        116.02963659
A3        121.91412663
A4        121.51358507
A5        119.62401378
A6        119.34777295
A7        123.80560225
A8        125.04388220
A9        117.35205747
A10       111.62355246
A11       111.01993449
A12       111.08027960
A13       113.94071597
A14       110.21944263
A15       110.76832591
A16       111.69135338
A17       116.33652697
A18       111.64590004
A19       117.59300717
A20       112.04860127
A21       119.65574576
A22       113.61286117
A23       107.71472250
A24       114.53428288
A25       110.69046183
A26       123.91749645
A27       116.18481823
A28       123.21394041
A29       119.90062526
A30       105.43377261
A31       111.45472789
A32       108.25491218
A33       107.43732614
A34       109.06899263
A35       114.32511036
A36       125.48558753
A37       111.85458646
A38       110.39283437
```

```
A39           117.16323917
A40           111.97193999
A41            76.05183095
A42           118.84183451
A43           108.03161049
A44           111.50202434
A45           109.35308910
D1            179.93365993
D2           -177.99879815
D3              0.49865443
D4            177.78423259
D5             -1.28769569
D6           -179.22345101
D7              0.50628787
D8            -56.75248068
D9              0.85633135
D10           120.54076232
D11          -118.68202798
D12           -13.40691106
D13           178.33246538
D14           179.53451513
D15           -61.05299624
D16           179.32416764
D17            60.18620090
D18           179.93777328
D19            20.52940988
D20          -107.28744909
D21            80.27954478
D22          -153.62133473
D23            90.75326547
D24           -34.90560985
D25          -122.78097517
D26            59.99722498
D27             2.04857807
D28          -175.56974906
D29           -38.66900630
D30           145.98550391
D31           -97.20669904
D32          -151.15091106
D33           169.81099599
D34           -72.17736847
D35             4.77587549
D36          -174.10773465
D37          -179.77721904
D38            55.17062205
D39           -25.37551363
D40          -130.56209959
D41           106.78987004
D42           172.99426053
D43           -67.06582313
D44            54.74775313
```

IRC Calculation Input File Sample:

```
%chk=3TS_irc_rev.chk
%mem=240MW
%nproclinda=2
%nprocshared=8
# b3lyp/6-31+g(d,p) geom=connectivity irc=(reverse,calcfc)

Title Card Required

2 1
 N
 C                  1        B1
 C                  2        B2    1         A1
 C                  2        B3    1         A2    3         D1
 O                  4        B4    2         A3    1         D2
 C                  4        B5    2         A4    1         D3
 C                  6        B6    4         A5    2         D4
 C                  6        B7    4         A6    2         D5
 C                  8        B8    6         A7    4         D6
 C                  1        B9    2         A8    4         D7
 N                  7        B10   6         A9    4         D8
 H                  3        B11   2         A10   1         D9
 H                  3        B12   2         A11   1         D10
 H                  3        B13   2         A12   1         D11
 H                  5        B14   4         A13   2         D12
 H                  7        B15   6         A14   4         D13
 H                  9        B16   8         A15   6         D14
 H                  9        B17   8         A16   6         D15
 H                 10        B18   1         A17   2         D16
 H                  9        B19   8         A18   6         D17
 H                  1        B20   10        A19   8         D18
 H                 11        B21   7         A20   6         D19
 C                 11        B22   7         A21   6         D20
 C                 23        B23   11        A22   7         D21
 C                 23        B24   11        A23   7         D22
 C                 24        B25   23        A24   11        D23
 H                 24        B26   23        A25   11        D24
 C                 25        B27   23        A26   11        D25
 H                 25        B28   23        A27   11        D26
 C                 28        B29   25        A28   23        D27
 H                 28        B30   25        A29   23        D28
 H                 23        B31   11        A30   7         D29
 H                 30        B32   28        A31   25        D30
 F                 30        B33   28        A32   25        D31
 H                 24        B34   23        A33   11        D32
 H                 26        B35   24        A34   23        D33
 C                 26        B36   24        A35   23        D34
 O                 37        B37   26        A36   24        D35
 O                 37        B38   26        A37   24        D36
 H                 39        B39   37        A38   26        D37
 N                  7        B40   6         A39   4         D38
 H                 41        B41   7         A40   6         D39
 H                 41        B42   7         A41   6         D40
 C                 41        B43   7         A42   6         D41
 H                 44        B44   41        A43   7         D42
 H                 44        B45   41        A44   7         D43
 H                 44        B46   41        A45   7         D44

   B1          1.35151289
   B2          1.49725237
   B3          1.40309418
   B4          1.35284982
   B5          1.40865546
   B6          1.51841126
   B7          1.41522730
   B8          1.51009794
   B9          1.35033582
   B10         1.50258739
   B11         1.09258660
   B12         1.09650954
```

B13	1.09701788
B14	0.96943815
B15	1.08908335
B16	1.09135862
B17	1.09487604
B18	1.08327614
B19	1.09484056
B20	1.01880745
B21	1.03002382
B22	1.50723036
B23	1.54390280
B24	1.51109512
B25	1.53782989
B26	1.09497418
B27	1.33751247
B28	1.08779823
B29	1.50508780
B30	1.08639877
B31	1.09760403
B32	1.09238389
B33	1.40703285
B34	1.09402238
B35	1.09709239
B36	1.52077831
B37	1.22872599
B38	1.33055899
B39	0.97402101
B40	1.51191919
B41	1.02146635
B42	1.30876368
B43	1.48586898
B44	1.09105428
B45	1.09336572
B46	1.09157806
A1	119.92572164
A2	116.02963659
A3	121.91412663
A4	121.51358507
A5	119.62401378
A6	119.34777295
A7	123.80560225
A8	125.04388220
A9	117.35205747
A10	111.62355246
A11	111.01993449
A12	111.08027960
A13	113.94071597
A14	110.21944263
A15	110.76832591
A16	111.69135338
A17	116.33652697
A18	111.64590004
A19	117.59300717
A20	112.04860127
A21	119.65574576
A22	113.61286117
A23	107.71472250
A24	114.53428288
A25	110.69046183
A26	123.91749645
A27	116.18481823
A28	123.21394041
A29	119.90062526
A30	105.43377261
A31	111.45472789
A32	108.25491218
A33	107.43732614
A34	109.06899263
A35	114.32511036
A36	125.48558753
A37	111.85458646
A38	110.39283437

```
A39          117.16323917
A40          111.97193999
A41           76.05183095
A42          118.84183451
A43          108.03161049
A44          111.50202434
A45          109.35308910
D1           179.93365993
D2          -177.99879815
D3            0.49865443
D4           177.78423259
D5           -1.28769569
D6          -179.22345101
D7            0.50628787
D8          -56.75248068
D9            0.85633135
D10          120.54076232
D11         -118.68202798
D12          -13.40691106
D13          178.33246538
D14          179.53451513
D15          -61.05299624
D16          179.32416764
D17           60.18620090
D18          179.93777328
D19           20.52940988
D20         -107.28744909
D21           80.27954478
D22         -153.62133473
D23           90.75326547
D24          -34.90560985
D25         -122.78097517
D26           59.99722498
D27            2.04857807
D28         -175.56974906
D29          -38.66900630
D30          145.98550391
D31          -97.20669904
D32         -151.15091106
D33          169.81099599
D34          -72.17736847
D35            4.77587549
D36         -174.10773465
D37         -179.77721904
D38           55.17062205
D39          -25.37551363
D40         -130.56209959
D41          106.78987004
D42          172.99426053
D43          -67.06582313
D44           54.74775313

1 2 1.5 10 1.5 21 1.0
2 3 1.0 4 1.5
3 12 1.0 13 1.0 14 1.0
4 5 1.0 6 1.5
5 15 1.0
6 7 1.0 8 1.5
7 11 1.0 16 1.0 41 1.0
8 9 1.0 10 1.5
9 17 1.0 18 1.0 20 1.0
10 19 1.0
11 22 1.0 23 1.0
12
13
14
15
16
17
18
19
20
```

```
21
22
23 24 1.0 25 1.0 32 1.0
24 26 1.0 27 1.0 35 1.0
25 28 2.0 29 1.0
26 30 1.0 36 1.0 37 1.0
27
28 30 1.0 31 1.0
29
30 33 1.0 34 1.0
31
32
33
34
35
36
37 38 2.0 39 1.5
38
39 40 1.0
40
41 42 1.0 44 1.0
42
43
44 45 1.0 46 1.0 47 1.0
45
46
47
```

NBO Calculation Input File Sample:

```
%chk=3TS_fwd.chk
%mem=240MW
%nproclinda=2
%nprocshared=8
# b3lyp/6-31+g(d,p) pop=(nbo)

Title Card Required

2 1
 N
 C                   1          B1
 C                   2          B2    1           A1
 C                   2          B3    1           A2    3           D1
 O                   4          B4    2           A3    1           D2
 C                   4          B5    2           A4    1           D3
 C                   6          B6    4           A5    2           D4
 C                   6          B7    4           A6    2           D5
 C                   8          B8    6           A7    4           D6
 C                   1          B9    2           A8    4           D7
 N                   7          B10   6           A9    4           D8
 H                   3          B11   2           A10   1           D9
 H                   3          B12   2           A11   1           D10
 H                   3          B13   2           A12   1           D11
 H                   5          B14   4           A13   2           D12
 H                   7          B15   6           A14   4           D13
 H                   9          B16   8           A15   6           D14
 H                   9          B17   8           A16   6           D15
 H                   10         B18   1           A17   2           D16
 H                   9          B19   8           A18   6           D17
 H                   1          B20   10          A19   8           D18
 H                   11         B21   7           A20   6           D19
 C                   11         B22   7           A21   6           D20
 C                   23         B23   11          A22   7           D21
 C                   23         B24   11          A23   7           D22
 C                   24         B25   23          A24   11          D23
 H                   24         B26   23          A25   11          D24
 C                   25         B27   23          A26   11          D25
 H                   25         B28   23          A27   11          D26
 C                   28         B29   25          A28   23          D27
 H                   28         B30   25          A29   23          D28
 H                   23         B31   11          A30   7           D29
 H                   30         B32   28          A31   25          D30
 F                   30         B33   28          A32   25          D31
 H                   24         B34   23          A33   11          D32
 H                   26         B35   24          A34   23          D33
 C                   26         B36   24          A35   23          D34
 O                   37         B37   26          A36   24          D35
 O                   37         B38   26          A37   24          D36
 H                   39         B39   37          A38   26          D37
 N                   7          B40   6           A39   4           D38
 H                   41         B41   7           A40   6           D39
 H                   11         B42   7           A41   6           D40
 C                   41         B43   7           A42   6           D41
 H                   44         B44   41          A43   7           D42
 H                   44         B45   41          A44   7           D43
 H                   44         B46   41          A45   7           D44

    B1           1.35305824
    B2           1.49858194
    B3           1.40109598
    B4           1.36048213
    B5           1.40920230
    B6           1.53683190
    B7           1.41469210
    B8           1.50984878
    B9           1.34978137
    B10          1.53271442
    B11          1.09261716
    B12          1.09696806
```

```
B13              1.09673756
B14              0.96951740
B15              1.08948265
B16              1.09141527
B17              1.09495571
B18              1.08337563
B19              1.09442878
B20              1.01846540
B21              1.05248028
B22              1.54300275
B23              1.53740505
B24              1.50705388
B25              1.53912282
B26              1.09522826
B27              1.33807742
B28              1.08899707
B29              1.50624318
B30              1.08655735
B31              1.09375602
B32              1.09334388
B33              1.40390474
B34              1.09388340
B35              1.09615609
B36              1.51980562
B37              1.23299026
B38              1.32407922
B39              0.97514286
B40              1.42828043
B41              1.01452567
B42              1.02442778
B43              1.47222851
B44              1.09139679
B45              1.09803011
B46              1.09351405
A1             119.71339319
A2             115.97279615
A3             121.58897052
A4             121.81056565
A5             119.67028337
A6             119.04412553
A7             123.67559142
A8             124.90666541
A9             109.67821448
A10            111.53529419
A11            111.24805830
A12            111.22913216
A13            113.63633943
A14            108.65128745
A15            110.78077010
A16            111.29339096
A17            116.28919422
A18            111.70038205
A19            117.67288250
A20            111.03600162
A21            115.25326814
A22            111.19454376
A23            108.15283590
A24            114.61842903
A25            111.48463208
A26            123.60136797
A27            116.58072992
A28            123.61025434
A29            119.86734370
A30            104.07323827
A31            111.33131603
A32            107.57952163
A33            106.65376766
A34            109.04382658
A35            114.14854561
A36            125.30298868
A37            112.35503625
A38            110.65996092
```

```
A39           115.34065284
A40           113.84371922
A41           107.68665158
A42           118.33797002
A43           108.15925657
A44           113.86069654
A45           109.62712067
D1            179.80975126
D2           -179.49843136
D3             0.14858440
D4           -175.77506017
D5             0.08444984
D6            179.43501306
D7            -0.20054208
D8            -61.93286695
D9            -0.54178479
D10           118.86402955
D11          -120.00515767
D12            1.25004329
D13          -176.15257318
D14           179.79623098
D15           -60.95278093
D16          -179.76675787
D17            60.29695374
D18           179.98257466
D19           -50.01128166
D20          -169.67573420
D21            82.28073537
D22          -152.69710762
D23            87.04161819
D24           -39.56742499
D25          -116.66328427
D26            67.21328638
D27             1.33796998
D28          -175.17829274
D29           -36.51510171
D30           143.42034823
D31          -100.14171450
D32          -154.82628858
D33           168.84762346
D34           -73.05966905
D35            13.03111061
D36          -166.47593478
D37          -179.77767643
D38            62.24490978
D39           -42.22802410
D40            68.51955780
D41            93.91058677
D42           172.87480673
D43           -66.72538223
D44            55.79495126
```

SCRF Calculation Input File Sample:

```
%chk=1.chk
%mem=240MW
%nproclinda=2
%nprocshared=8
# b3lyp/6-31+g** scf=tight nosym scrf=(solvent=water,iefpcm,read)

Title Card Required

2 1
 N
 C                    1         B1
 C                    2         B2    1         A1
 C                    2         B3    1         A2    3         D1
 O                    4         B4    2         A3    1         D2
 C                    4         B5    2         A4    1         D3
 C                    6         B6    4         A5    2         D4
 C                    6         B7    4         A6    2         D5
 C                    8         B8    6         A7    4         D6
 C                    1         B9    2         A8    4         D7
 N                    7         B10   6         A9    4         D8
 H                    3         B11   2         A10   1         D9
 H                    3         B12   2         A11   1         D10
 H                    3         B13   2         A12   1         D11
 H                    5         B14   4         A13   2         D12
 H                    7         B15   6         A14   4         D13
 H                    9         B16   8         A15   6         D14
 H                    9         B17   8         A16   6         D15
 H                    10        B18   1         A17   2         D16
 H                    9         B19   8         A18   6         D17
 H                    1         B20   2         A19   4         D18
 H                    11        B21   7         A20   6         D19
 C                    11        B22   7         A21   6         D20
 H                    23        B23   11        A22   7         D21
 H                    23        B24   11        A23   7         D22
 H                    23        B25   11        A24   7         D23

    B1           1.34771600
    B2           1.49703824
    B3           1.41077929
    B4           1.34485694
    B5           1.41626641
    B6           1.46591555
    B7           1.42559552
    B8           1.50813084
    B9           1.35166662
    B10          1.29228843
    B11          1.09263498
    B12          1.09732843
    B13          1.09731795
    B14          0.97175218
    B15          1.08654193
    B16          1.09109964
    B17          1.09542747
    B18          1.08344312
    B19          1.09542314
    B20          1.02090056
    B21          1.02259541
    B22          1.47375381
    B23          1.09367807
    B24          1.09369013
    B25          1.08970379
    A1         120.20585136
    A2         115.90137905
    A3         121.20162221
    A4         121.03746105
    A5         122.51216012
    A6         119.60154300
    A7         124.08938407
    A8         125.77600522
```

```
A9              127.06117970
A10             111.55122922
A11             111.13177868
A12             111.14060188
A13             114.60993382
A14             117.16941780
A15             110.54036897
A16             111.67482578
A17             116.40040397
A18             111.68031160
A19             117.04963900
A20             117.94179026
A21             125.36291061
A22             108.44270536
A23             108.44334658
A24             109.94794525
D1              179.98883307
D2             -179.99184209
D3                0.00000000
D4             -179.99623697
D5                0.00000000
D6              179.99694143
D7               -0.00282566
D8                0.00371623
D9               -0.08779981
D10             119.29646056
D11            -119.46115537
D12              -0.02953526
D13            -180.00000000
D14            -179.96598516
D15             -60.89011010
D16            -180.00000000
D17              60.95419484
D18             180.00000000
D19               0.00000000
D20             179.99499645
D21             120.82825740
D22            -120.77892995
D23               0.02141975

radii=UFF
```

CIRRICULUM VITAE

Full name **:** Hatice GÖKCAN

Place of birth **:** Etimesgut

Date of birth **:** 14.08.1984

High school **:** 19 Mayıs Anatolian High School, 19 Mayıs, Samsun

University   **: B. Sc.** **:** (2002 – 2007) ITU Molecular Biology and Genetics

        : M. Sc. **:** (20 08 - 2010) ITU Informatic Institute,
               Computational Science and Engineering

Publications **: Gökcan**, **H**., Konuklar, F. A., 2009, Inactivation Mechanism of GABA-AT by 5-amino-2 fluorocyclohex-3-enecarboxylic acid: A Computational Study**,** *DFT09 **International Conference on the Applications of Density Functional Theory in Chemistry and Physics**,* **August 31 – September 4,** Lyon, France

         Gökcan, **H**., Konuklar, F. A., 2010, Computational Study on Two Competing Mechanisms of Inactivation of GABA-AT, *7th Congress on Electronic Structure: Principles and Applications (ESPA)*, June 29 – July 2, Oviedo, Spain